DESIGN AND ANALYSIS OF ROBOTIC EXOSKELETON FOR HUMAN UPPER LIMB REHABILITATION

A thesis submitted to the
University of Petroleum and Energy Studies

For the award of
Doctor of Philosophy
in
Mechanical Engineering

BY
Akash Gupta

October 2020

SUPERVISOR (s)
Dr. Mukul Kumar Gupta
Dr. Amit Kumar Mondal

UPES
UNIVERSITY WITH A PURPOSE

Department of Mechanical Engineering
School of Engineering
University of Petroleum &Energy Studies,
Dehradun – 248007: Uttarakhand

DESIGN AND ANALYSIS OF ROBOTIC EXOSKELETON FOR HUMAN UPPER LIMB REHABILITATION

A thesis submitted to the
University of Petroleum and Energy Studies

For the award of
Doctor of Philosophy
in
Mechanical Engineering

BY
Akash Gupta
(SAP ID- 500056854)

October 2020

Internal Supervisor

Dr. Mukul Kumar Gupta
Assistant Professor – Selection Grade
Department of Electrical and Electronics Engineering
University of Petroleum and Energy Studies

External Supervisor

Dr. Amit Kumar Mondal
Assistant Professor
Department of Mechatronics Engineering
Manipal Academy of Higher Education, Dubai

Department of Mechanical Engineering
School of Engineering
University of Petroleum &Energy Studies,
Dehradun – 248007: Uttarakhand

DECLARATION

I declare that the thesis entitled "**Design and Analysis of Robotic Exoskeleton for Human Upper Limb Rehabilitation"** has been prepared by me under the guidance of **Dr. Mukul Kumar Gupta**, Assistant Professor of Electrical and Electronics Engineering Department, University of Petroleum & Energy Studies, and **Dr. Amit Kumar Mondal**, Assistant Professor of Department of Mechatronics Engineering, Manipal Academy of Higher Education

No part of this thesis has formed the basis for the award of any degree or fellowship previously.

Akash Gupta

Department of Mechanical Engineering,
School of Engineering
University of Petroleum & Energy Studies
Dehradun-248007: Uttarakhand

Date: 18/10/2020

UPES
UNIVERSITY WITH A PURPOSE

Great Place To Work. Certified APR 2019-MAR 2020 INDIA

CERTIFICATE

I certify that **Akash Gupta** has prepared his thesis entitled "**Design and Analysis of Robotic Exoskeleton for Human Upper Limb Rehabilitation**," for the award of PhD degree of the University of Petroleum & Energy Studies, under my guidance. He has carried out the work at the Department of Mechanical Engineering, University of Petroleum & Energy Studies, Dehradun.

Supervisor

Dr. Mukul Kumar Gupta
Assistant Professor – Selection Grade
Department of Electrical and Electronics Engineering
University of Petroleum and Energy Studies

Date: 22/10/2020

CORPORATE OFFICE: 210, 2nd Floor, Okhla Industrial Estate, Phase III, New Delhi - 110 020, India.
T: +91 11 41730151/53, 46022691/5
F: +91 11 41730154

ENERGY ACRES: Bidholi Via Prem Nagar, Dehradun - 248 007 (Uttarakhand), India.
T: +91 135 2770137, 2776053/54/91, 2776201
F: +91 135 2776090/95

KNOWLEDGE ACRES: Kandoli Via Prem Nagar, Dehradun - 248 007 (Uttarakhand), India.
T: +91 8171979021/2/3, 7060111775

MANIPAL
ACADEMY *of* HIGHER EDUCATION
DUBAI CAMPUS
(Deemed to be University under Section 3 of the UGC Act, 1956)
INSPIRED BY LIFE

CERTIFICATE

I certify that **Akash Gupta** has prepared his thesis entitled **"Design and Analysis of Robotic Exoskeleton for Human Upper Limb Rehabilitation"**, for the award of PhD degree of the University of Petroleum & Energy Studies, under my guidance. He has carried out the work at the Department of Mechanical Engineering, University of Petroleum & Energy Studies, Dehradun.

External Supervisor

Dr. Amit Kumar Mondal
Assistant Professor
Department of Mechatronics Engineering,
School of Engineering and Information Technology,
Manipal Academy of Higher Education.
Dubai, UAE

Date: Oct 18th, 2020

P.O. Box 345050, DIAC-G-008, Dubai International Academic City, U.A.E. ◆ Tel: +971 4 429 0777 ◆ Fax: +971 4 369 4541 ◆ Website: www.manipaldubai.com
MAHE in Manipal - India was established under Section 3 of the UGC Act 1956 vide notification no. F.9-8/89-U.3 dated 1st June 1993 of the Govt. of India)

ABSTRACT

The development of upper limb and lower extremity robotic exoskeletons has emerged as a way to improve the quality of life as well as act as a primary rehabilitation device for individuals suffering from stroke or spinal cord injury. This work contains extractions from the database of robotic exoskeleton for human upper limb rehabilitation and prime factors behind the burden of stroke. Various studies on stroke-induced deficiency from different countries were included. The data were extracted from both clinical tests and surveys. Though there have been splendid advancements in this field, they still present enormous challenges. Through literature, Robot-assisted training (RT) was found to be more effective than conventional training (CT) sessions. Complete kinematics and dynamics, along with the joint position analysis of a 3 DOF upper-limb robotic exoskeleton has been conducted in this work. This research investigates the feasibility of computed torque control for an exoskeleton device. After studying the biomechanics of the human upper-limb, a 3 DOF exoskeleton has been designed. The present research work in this field has many weaknesses as they do not cover the systematic study including the clinical studies and various surveys that lay a foundation for the requirement of robotic assistive devices.

The designed exoskeleton presents three of the most basic movements of the human arm that facilitate activities of daily living (ADL). The design parameters are taken similar to the parameters of the upper-limb of a normal human being. Computed torque control (CTC) is applied to the system in order to actuate the system to the desired joint positions. The exoskeleton exhibits shoulder abduction/adduction, extension/flexion and elbow extension/flexion motions. The results of this work show that the CTC control successfully reduces the error in the exoskeleton joint positions.

ACKNOWLEDGMENT

I would first like to thank my advisor, Dr. Mukul Kumar Gupta, for the past four years at the University of Petroleum and Energy Studies. His guidance in control systems, dynamics, and persistence in science have always encouraged me during my post-graduate and doctoral studies. In my first year, Dr. Mukul spent enormous efforts guiding me in research and never lost his patience even when I struggled. I am thankful to my advisor for patiently listening to all of my puerile ideas and showing immense faith in me throughout. My co-supervisor, Dr. Amit Kumar Mondal motivated and guided me in writing good research papers. He would seek every chance to improve my writing skills that helped to build my confidence to submit my research in good journals and become a qualified researcher. Without his constant support, I would never be able to accomplish my Ph.D. study. All the knowledge and merit that my advisors passed on me has made me today and will continue benefiting my future life.

In addition to my Supervisor, I would like to express my profuse appreciation and thankfulness to Dr. S. J. Chopra (Chancellor), Dr. Sunil Rai (Vice-Chancellor), Dr. Kamal Bansal (Dean), and Dr. Jitendra Kumar Pandey (Assoc. Dean - Research) for their support in helping me pursue a graduate career at the University of Petroleum & Energy Studies (UPES). I would also like to thank Dr. Ajay Kumar Srivastava, Dr. Deepak Bharadwaj, Dr. Vivek Kaundal (L&T Technology Services), Dr. S. M Tauseef, Dr. Shyam Pandey, Dr. Girish Chandran, Dr. Pankaj Sharma, Dr. S. Garimella, Dr. Suresh Kumar, and Dr. P. S. Ranjit, for their valuable suggestions and guidance at every stage of this work.

I would also like to acknowledge the funding support received from the Research & Development Department, UPES, under the SEED grant scheme, which was instrumental in my graduate research and getting this dissertation completed in time. I would also like to thank the lab technicians at the Workshop lab, Mechatronics and CAM lab, and CAD lab for helping me carry out the simulations and prototype fabrication at different stages of my research.

I am deeply thankful to all my colleagues at the University of Petroleum and Energy Studies: Ms. Megha Katiyar, Mr. Debajyoti Bose, Mr. K. Balaji, Dr. S.R.V.S Prasanna, Mr. P. Sairam, Ms. Meera C. S, Ms. B. Aslesha, Ms. Varnita Verma, Ms. Srawanthi Medhi, Mr. Satyajith Chowdhary, Mr. Glen B. H, and Mr. Chakradhar for their invaluable comments and suggestions during group meetings. A sincere note of thanks to faculty members of the Mechanical Engineering Department, UPES including, Mr. Narayan Khatri, Dr. S. K. Kurre, Mr. Swapnil Bhurat, Dr. Natraj Mishra, Dr. Abhay Kumar, Dr. P. Suresh Kumar, Dr. Jitendra Yadav, Dr. Roushan Kumar, Dr. Deepak Bharadwaj, Mr. Prashant Shukla, Mr. Suraj Meshram, Ms. Lunu Saikia, Ms. Geethanjali Raghav, Mr. Ram Kunwer, Mr. Dishant Beniwal, Mr. Ashish K Saran, Dr. Doonga Ramesh Kumar, Mr. Ramesh M, Dr. Amneesh Singhla, Mr. Avani Kumar, and Mr. V. Senthil Kumar for their continuous encouragement and support.

Finally, I would like to thank my parents and family members for their constant support and love at every stage of my life. Completing this degree would never be possible without their love and encouragement.

TABLE OF CONTENTS

LIST OF FIGURES

LIST OF TABLES

LIST OF SYMBOLS

P_x, P_y, P_z	Robot position coordinates
${}^{i}r_i$	Position Vector
${}^{0}T_i$	Transformation Matrix
L K	Lagrangian Kinetic Energy
P	Potential Energy
m	Mass, Kg
g	Acceleration due to gravity, $m\text{-}s^{-1}$
I	Inertia Tensor
q	Ɵ (Joint Displacement)
$\dot{q}$	Joint Velocity
$\ddot{q}$	Joint Acceleration
M_{ij}	Mass matrix
h_{ijk}	Coriolis Matrix
G_i	Gravity Matrix
τ_i	Torque at link i, N-m
t	Time
K_p	Position gain
K_d	Velocity gain
α	Angle about the common normal
Ɵ	Theta
ω	Frequency
D-H	Denavit-Hartenberg
CTC	Computed Torque Control
DOF	Degree of Freedom
GH	Glenohumeral
ADL	Activities of Daily Living
Tr	Trace
sEMG	Surface Electromyography

CHAPTER 1 INTRODUCTION

A wearable exoskeleton device consists of links and joints that closely resembles the structure of the human body. An individual needs an assistive device for rehabilitation of weak/stroke-affected limbs, movement disorder, or for enhancing muscular strength. In the case of movement disorder, the capabilities of the individual remain limited that further diminishes the quality of life. To improve the functionality of the affected limb, orthoses, and physiotherapy are used to provide physical rehabilitation [1]. The exoskeleton technology consists of Upper limb and Lower extremity exoskeletons. These can be divided into two categories – Prosthesis and Orthosis [2]. A prosthesis is used as the replacement for the missing body parts while in orthosis external components are used to assist the motion of the weak, disabled body parts. These devices have been introduced under neuro-rehabilitation because they mimic human limb and guide the patient’s limb, covering several degrees of freedom, following proper anatomy [3].

1.1 ROBOTIC REHABILITATION THERAPY

Robotic rehabilitation therapy has better results in improving motor functions in patients and the effects of single joint robotic training and multi-joint robotic training are the same [4] The reason behind the disability can be a stroke, loss of muscle function, accidental reasons, etc.

Figure 1.1 Loss of muscle function [5]

Although physiotherapy sessions could be helpful, there is a strong possibility of inaccurate movements of body parts as in physiotherapy, movements are performed manually [6]. Conventional rehabilitation sessions without assistive devices for patients with lower limb disabilities is much more strenuous, as it would require at least two physiotherapists to train the patient. Also, there are strong chances of inconsistency in the pattern of walking [7]. The disadvantages of manual physiotherapy can be eliminated with the help of externally assistive devices. This technology-based treatment provides interactivity, intensity, flexibility, and adaptiveness to the patient's performance and needs [8]–[10]. Even after the development of such devices, the efficiency of these robot-assisted therapy sessions, when compared to manual physiotherapy sessions, remains uncertain. Clinical trials such as [11]–[22], [23] that have been performed in order to validate the efficiency and efficacy of robotic treatment.

Robotic exoskeletons work on the autonomous algorithms which are solely dependent on physiological measurements of the human effort [24]. These measurements not only provide the real-time body input but acts as feedback about the performance of the assistive devices. With the new upcoming sensor technologies, direct physiological state data is not taken in form of velocities, force, or neuro-interface instead as skin conductance, heart rate, oxygen saturation, etc. which makes the user unaware of the accessories and the reaction of the user becomes conscious free.

Robotic assistive devices act as a body-in-loop framework and the assistive device continuously tries to adapt to the user conditions [25]. Skill transfer and human-in-loop are fresh issues in the field of robotic exoskeleton based rehabilitation. Qiang et al. [26] discussed synergy-based control by skill transfer. In the study, control of the lower-limb exoskeleton has been achieved by transferring motor skills. The experimentation mainly considered body synergy while developing exoskeleton control in order to maintain consistency in the gait pattern of the patients with hemiplegia having asymmetrical gait. Considering human-in-loop control, the research [27] proposed this strategy for gait rehabilitation using a unilateral exoskeleton robot. The unilateral lower-limb exoskeleton robot is attached to the affected limb and the gait pattern is coordinated with the healthy leg on the opposite side. An adaptive controller is also incorporated to surpass unknown non-linear disturbances. Though, more extensive studies are still required to investigate the effect of these strategies on motor function.

There has been considerable progress in the field of assistive devices like NEUROExos, ARMin, MEDARM [28], etc. These devices include both for upper-limb and lower extremity exoskeleton devices and have been divided into two classes, namely, Active exoskeletons and passive exoskeletons [29]. Neurally impaired subjects require intensive training with feasible outcomes, which is a prime motive of the exoskeleton devices [30]. Many such devices are reviewed later in this paper, highlighting their advantages and disadvantages. These devices with multiple degrees of freedom have incorporated various techniques for controlling the device such as Neuro, Fuzzy [31], [32] technique, etc. For joint actuation, various actuators such as hydraulic, pneumatic actuators, electric motors, shape memory alloys, series elastic actuators, etc. have been used. In many cases, the feedback for the actuators is received from EMG/EEG sensors.

There is a high demand for portable rehabilitation systems as the present devices are expensive, complex, and have portability issues. These devices are feasible to use in clinics under the supervision of experts [33]. The portable rehabilitative devices provide ease of access to the patients that leads to an increase in the frequency of training [34]. According to the survey by Elaine Biddiss [35] in Canada, most users of Prosthetics rated cost and weight as the predominant issue, while the lightweight prosthetic solution was rated the first priority. The survey is related to the prosthetics, while the author reckons that similar feedback can be considered in the case of an orthosis.

1.2 MOTIVATION

The brain is an extremely complex organ in the human body. It controls almost all the body functions. In the case of stroke, the blood flow in the region that controls a particular body function seizes. As a result, the functionality of that body part is affected. In these cases, the patient has a very limited or no muscle function post-stroke or accident. The priming factors behind the burden of stroke have been identified by the study "Global burden of stroke and risk

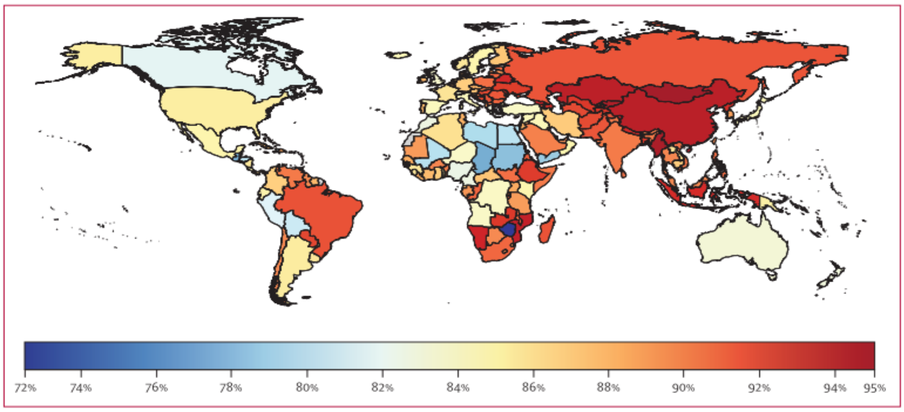

Figure 1.2 Stroke-related DALYs attributable to all modifiable risk factors combined for both sexes in 2013

factors in 188 countries, during 1990-2013" [36]. The study revealed stroke-related disability-adjusted life-years (DALYs) associated with potentially modifiable environmental, occupational, behavioral, physiological, and metabolic risk factors in different age, sex groups worldwide as shown in Figure 1.1 for the first time, air pollution turned out to be one of the leading contributors to stroke burden worldwide. Among all the factors that result in disability, stroke is ranked at number 5 in the United States [37]. These disabilities are rehabilitated with the help of a physiotherapist performing the muscle movement regularly to improve the muscle function.

Robotic assistive devices when appropriately applied give better results than conventional approaches, including a standardized training environment, adaptable support, intensifying the training sessions and doses, and subsequently reducing the burden on therapists [38]. To support the same, conventional therapy for hemiparetic patients typically perform 30 movement repetitions with an affected upper limb for a 45-min session, while with robotic assistance they achieved over 1000 repetitions per session [39]. Active participation from the patient is expected during recovery sessions and the same can be promoted via adaptive assistance [40], [41], avoiding slacking [42], automated task difficulty adaption [43], [44], motivation through feedback results [45]. The objective of this thesis is the design and analysis of a 3-DOF exoskeleton device that replicates most basic movements such as shoulder abduction/adduction, extension/flexion, and elbow extension/flexion of the human upper-limb. The study covers the kinematic and dynamic analysis of the system and validation of computed torque control for this application.

1.3 PRINCIPAL CONTRIBUTION

The principal contribution of this research work is the design and development of a new exoskeleton device for human upper-limb rehabilitation. The developed device aims to provide rehabilitation to patients suffering from neurological disorders that affect the muscle function of the human body. The key contributions include:

- Obtaining kinematics and dynamics of the exoskeleton model
- Validation of Computed torque control scheme to reduce errors during trajectory tracking analysis of the exoskeleton device.
- Development of the proposed exoskeleton device, obtain human upper-limb muscle potential using sEMG sensors for motor actuation.

1.4 THESIS OVERVIEW

A short overview of the chapters following this introduction is presented below:

- **Chapter 2:** The chapter discusses human upper-limb autonomy reasons behind the burden of neurological disorders. The chapter also presents a detailed review of past and current developments in the field of robotic exoskeleton technology. This chapter also discusses various clinical evaluations that have been carried using robotic rehabilitation devices and their efficiency over conventional training methods.
- **Chapter 3:** This chapter presents the mathematical modeling of the proposed exoskeleton device. Relevant equations are developed using the theory of robotics kinematics and dynamics. Denavit-Hartenberg (D-H) guidelines are used to develop the kinematic model of the system. The dynamic model is derived using Euler-Lagrange equations of motion. An insight into the design parameters, torque, and singularity positions has been presented as well.
- **Chapter 4:** This chapter presents the validation of the computed torque control scheme in the trajectory tracking analysis of the proposed exoskeleton device. The simulations have been conducted using the actual design parameters of the developed exoskeleton device.
- **Chapter 5:** This chapter explains the design and development of the robotics exoskeleton device. It presents the CAD model, the prototyping, and the components used in the process.
- **Chapter 6:** The final chapter summarises the research work as a general conclusion and recommendations for future work.

CHAPTER 2 LITERATURE SURVEY

There has been a great evolution in the field of assistive devices since 1936. The research on exoskeleton devices varies from the upper, lower extremity to full-body exoskeleton devices. The exoskeletons were first designed to enhance the physical potentials of the human body soon to find their application in the rehabilitation field due to their characteristics like precision and repeatability and named as robotic rehabilitation devices (RRD). This chapter explains the upper-limb anatomy and the deficiencies associated with it along with a detailed review of the current developments in this field.

2.1 UPPER-LIMB ANATOMY AND DEFICIENCIES

In this section, upper-limb anatomy has been briefly explained which is required to design a robotic exoskeleton device having optimum human-robot interaction (HRI).

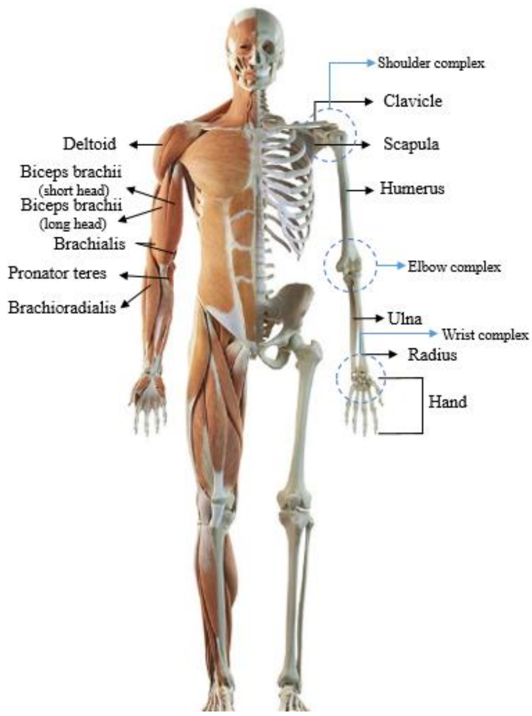

Figure 2.1 Human Upper-Limb Anatomy.

The shoulder complex consists of Clavicle Joint (Collarbone) and Scapula (Shoulder Blade). The Shoulder complex and elbow complex are connected with the Humerus, while the Elbow complex and wrist joint are connected with two bones Radius and Ulna that form the forearm as shown in Figure 2.1. Finally, the hand consists of Carpal bone, Metacarpal bones, and the Phalanges.

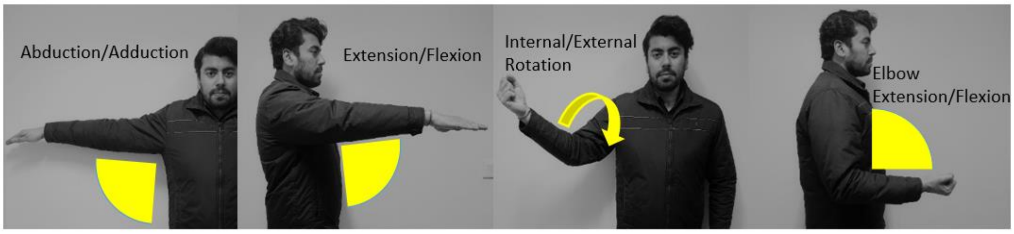

(a) (b) (c) (d)

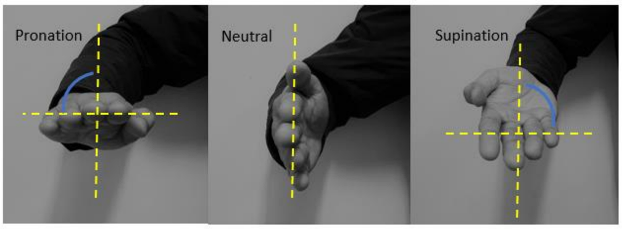

(e) (f) (g)

Figure 2.2 Common Upper limb Motions. (a) Shoulder Abduction/Adduction, (b) Shoulder Extension/Flexion, (c) Internal/External Rotation. (d) Elbow Extension/Flexion, (e) Forehand Pronation, (f) Neutral, (g) Forehand Supination

One of the most important features of the Shoulder complex is its instantaneous center of rotation (CoR) that changes with different positions of the upper-limb [2]. This increases the complexity of designing the exoskeleton that is required to replicate the motions of the shoulder complex.

Figure 2.2 shows the most important movements of the shoulder complex are shoulder abduction/adduction, Extension/Flexion while the elbow joint motions are Extension/Flexion, Internal/External rotation. The forearm region has two motions namely Pronation and supination [2], [28]. The normal movable range of the human shoulder is 75º in adduction and 180º in abduction, 60º in extension, and 180º in flexion. Similarly, the elbow range is between -5º to 145º [46].

S.K Jain studied congenital limb deficiency in 200 patients from 1984 to 1990 at Artificial Limb Centre Pune, India [47]. The study was done to identify the cause of limb deficiency and the following associative factors were found: Drugs, Previous abortions, previous premature births, previous cesarean births, Injury to the abdomen during pregnancy, Radiation during pregnancy, Heredity, etc.

The study also disclosed that the number of males suffering from limb deficiency was more than their female counterparts. Another study [48] by T. R. Scotland and H.R. Galway was done on children suffering from congenital and acquired upper limb deficiency from 1965 to 1975. The study was done to find reasons, usefulness, and feedback of the prosthetic devices worn by the patients during the study period. Patients with congenital deficiency and trauma were included in the study. The level of deficiency is explained in Table 2.1:

Table 2.1 Level of deficiencies [48].

Deficiency Level	**Right**	**Left**	**Bilateral**
Shoulder disarticulation	2	4	3

Below elbow	24	40	-
Above elbow	1	3	1
Below wrist	11	16	-
Above wrist	5	6	-

One of the most prominent reasons for the requirement of a rehabilitation device is the occurrence of stroke among the people, making it the third most common cause of deaths and disability [33], [49], [50]. In India, as per Census 2011, about 2.21% (2.68 Cr) of 121 Cr population is disabled [51] as shown in Figure 2.3. Out of 2.68 Cr disabled population, 56% (1.5 Cr) are males and 44% (1.18) Cr is female. Among the disabled persons, 20% of the people have a movement-related disability [51].

Stroke or cerebrovascular causes most of the disease burden in developing countries[52]. Reports suggest 3 percent of the world's disability caused due to strokes itself in 1990. The typical age of people suffering from strokes is 55-65 years [49] and the lifetime cost for health services per patient is estimated between US$59,800 and US$230,000 [53]. This trauma happening at younger age accumulates the social burden.

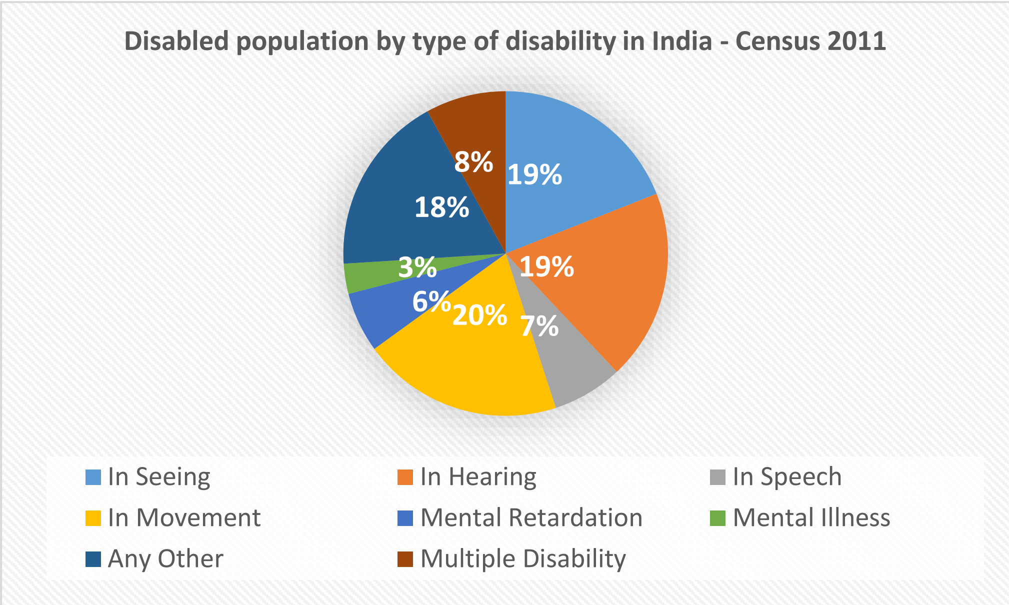

Figure 2.3 Disabled population by type of disability in India - Census 2011 [51].

The major causes of strokes in India are cerebral venous thrombosis, rheumatic heart disease, and tubercular meningitis [49] multiple sclerosis, cerebral palsy [54], and Parkinson’s disease [1], [55]. Table 2.2 shows the WHO report on the most common incidences that increase the burden of diseases in the respective regions, clearly showing stroke among the top 20 incidences.

Table 2.2 WHO report on the region-wise distribution of the top incidences [52]

	Africa	**Eastern Mediterranean**	**The Americas**	**Western Pacific**	**South-East Asia**	**Europe**	**World**
Stroke, first-ever Injuriesd	0.7	0.4	0.9	3.3	1.8	2.0	9.0
Diarrhoeal disease	912.9	424.9	543.1	1 255.9	1 276.5	207.1	4 620.4
Malaria	203.9	8.6	2.9	2.7	23.3	0.0	241.3
HIV infection	1.9	0.1	0.2	0.1	0.2	0.2	2.8
Tetanus	0.1	0.1	0.0	0.0	0.1	0.0	0.3
Pertussis	5.2	1.6	1.2	2.1	7.5	0.7	18.4
Dengue	0.1	0.5	1.4	2.3	4.6	0.0	9.0

Tuberculosis	1.4	0.6	0.4	2.1	2.8	0.6	7.8
Meningitis	0.3	0.1	0.1	0.1	0.2	0.0	0.7
Measles	5.3	1.0	0.0	3.3	17.4	0.2	27.1
Congestive heart failure	0.5	0.4	0.8	1.3	1.4	1.3	5.7
Lower respiratory infections	131.3	52.7	45.4	46.2	134.6	19.0	429.2
Malignant neoplasms – all sites	0.7	0.5	2.3	3.2	1.7	3.1	11.4
Injuries due to: **road traffic accidents**	4.7	2.8	2.2	4.1	8.6	1.8	24.3

falls	2.8	3.6	3.3	8.0	14.4	5.3	37.3
fires	1.7	1.5	0.3	0.7	5.9	0.8	10.9
violence	4.5	2.0	5.9	1.0	2.2	1.6	17.2
Complications of pregnancy:							
maternal hemorrhage	3.0	1.6	1.2	1.4	4.0	0.7	12.0
maternal sepsis	1.2	0.7	0.6	0.6	1.7	0.3	5.2
hypertensive disorders	2.1	1.2	0.8	1.1	2.8	0.5	8.4
obstructed labor	1.1	0.5	0.1	0.4	1.9	0.0	4.0
unsafe abortion	4.8	2.9	4.0	0.8	7.4	0.5	20.4

2.2 CLINICAL REVIEWS AND EVALUATION OF VARIOUS ROBOTIC EXOSKELETONS

Spinal cord injury (SCI) and stroke are the primary reasons for the requirement of Upper Limb Rehabilitation systems among patients. Even though the field of robotic rehabilitation systems is just a few years old, a comprehensive amount of research is being conducted all around the world due to robotic rehabilitation systems proving to be much more effective than traditional physiotherapy. Most of the robotic rehabilitation systems allow control of the articular joint by guiding the patient’s limbs according to the anatomy of the body. The results in spanning multiple numbers of DOFs and the corresponding workspaces. One such Robotic rehabilitation system is the Arm Light Exoskeleton (ALEx) as shown in Figure 2.4. After analyzing 16 upper limb muscles and the movement execution in 6 patients, it was concluded that it reduced the muscular activity of the shoulder’s abductors and increased the activity of the elbow flexors. However, the movements enabled by the exoskeleton were reduced in comparison to the natural movements of the body [11].

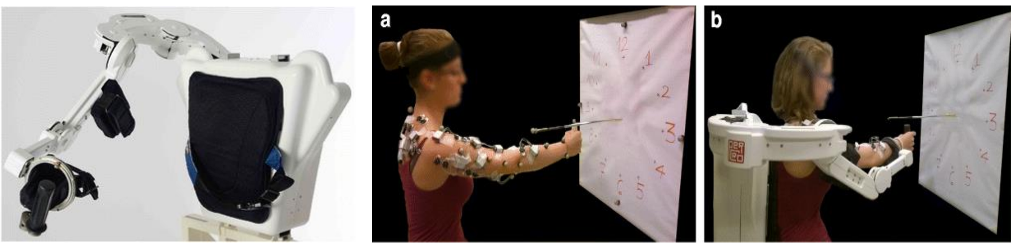

Figure 2.4 Arm Light Exoskeleton (ALEx), experimental setup in a and b [11].

Kyle at Rice University, used MAHI Exo II, DOF 5, for robotic rehabilitation via resistance therapy for patients with SCI. Over the course of treatment, the data pertaining to the patient’s movement quality was also analyzed using back driving evaluation mode. The outcome of the treatment initiated more extensive research into better control and treatment strategies and the Assist-as-Needed rehabilitation study [12]. Signal Processing has also played a major role in the robotics rehabilitation system as demonstrated by F. Xiao et al. in China. Xiao et al evaluated the assist ability of a cable-driven 7 DOF exoskeleton by collecting the surface electromyography signals of major muscle groups. These muscles were associated with upper limb movement. Xiao et al eventually concluded that post-stroke patients can be sent through constructive rehabilitation through exoskeleton [15].

The above discussed robotic Rehabilitation Systems definitely have brought advancement in the field of rehabilitation however they still possess a few critical issues such as portability, ease of use, and the high cost of manufacturing. To overcome the aforementioned issues Chinese researchers J. Huang et al developed a low-cost, portable, and in-home rehabilitation system which is an upper limb exoskeleton robot named RUPERT with 5 DOF. RUPERT is actuated by the means of pneumatic muscles which makes it lighter than many exoskeleton robots. It assists the patient, both in the clinic and at home, with performing daily life activities in a virtual environment. The proposed system was received positively by the patients and has good future prospects [16]. Another upper limb rehabilitation system that used virtual environments for therapy was developed by W. Qingcong et al. using a novel patient-active admittance control strategy which was validated during the course of development of the system. It was developed for patients with arm motor issues and performed daily life functions in a virtual environment. Further, to validate the patient-active control strategy a virtual airplane game was conducted [17]. A light exoskeleton was also developed by A. Frisoli et al in Italy. The exoskeleton assisted the patients with passive and active reaching exercises based on an impedance control strategy. The exoskeleton successfully tailored to the patient’s individual needs allowing them to regain motor functions [18].

One of the most significant examples of efficiency in motor recovery in Robotic-assisted training (RT) when compared to conventional training (CT) is the study conducted by Zhang et al [23]. The meta-analysis results are based on the whole group studies concluded that the motor recovery Fugl-Meyer Assessment (FMA score) in the RT group was significantly greater than the CT

	RT			CT				Std. Mean Difference	
Study or Subgroup	Mean	SD	Total	Mean	SD	Total	Weight	IV, Random, 95% CI	Year
Volpe 2000	12	3	30	10	4	26	9.5%	0.56 [0.03, 1.10]	2000
Lum 2002	3.3	0.7	13	1.6	0.3	14	5.4%	3.10 [1.93, 4.28]	2002
Masiero 2006	13.1	5.6	10	7.1	8.5	10	6.8%	0.80 [−0.12, 1.72]	2006
Rosati 2007	17.2	6.5	12	8.9	8.3	12	7.2%	1.08 [0.21, 1.94]	2007
Masiero 2007	12.8	5.5	17	7.5	9.5	18	8.4%	0.66 [−0.02, 1.35]	2007
Rabadi 2008	8.03	1.76	10	9.05	1.91	10	7.0%	−0.53 [−1.43, 0.36]	2008
Volpe 2008	15.73	2	11	15.1	1.7	10	7.2%	0.32 [−0.54, 1.19]	2008
Houseman 2009	3.3	2.4	15	2.2	2.6	16	8.2%	0.43 [−0.29, 1.14]	2009
Liao 2011	51.2	8.82	10	40.9	13.14	10	6.8%	0.88 [−0.05, 1.81]	2011
Reinkensmeyer 2012	27.4	11.4	13	23.8	8	13	7.8%	0.35 [−0.42, 1.13]	2012
Sale 2014(a)	35.46	12.24	26	23.96	17.51	27	9.3%	0.75 [0.19, 1.31]	2014
Sale 2014(b)	73.27	27.02	11	98.13	16.9	9	6.6%	−1.03 [−1.98, −0.08]	2014
Klamroth-Margansk 2014	3.25	1.68	38	2.47	1.67	35	10.0%	0.46 [−0.00, 0.93]	2014
Total (95% CI)			**216**			**210**	**100.0%**	**0.56 [0.19, 0.93]**	

Heterogeneity: $Tau^2 = 0.30$; $Chi^2 = 38.03$, $df = 12$ ($P = 0.0002$); $I^2 = 68\%$
Test for overall effect: $Z = 2.99$ ($P = 0.003$)

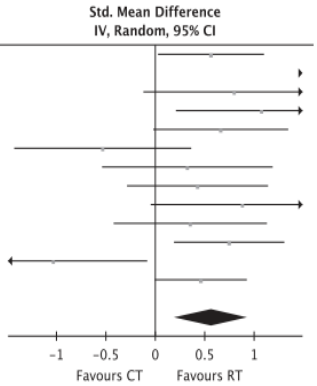

group.

Figure 2.5 Comparison of the Fugl-Meyer score after intervention between robotic-assisted therapy (RT) and conventional therapy (CT). CI, confidence interval [23].

In the second meta-analysis, two subgroups of RT were created. In the first subgroup, CT alone was compared with the combination of RT and CT (additional RT). In the second subgroup, CT alone was compared with RT alone (substitutional RT) as shown in Figure 2.6.

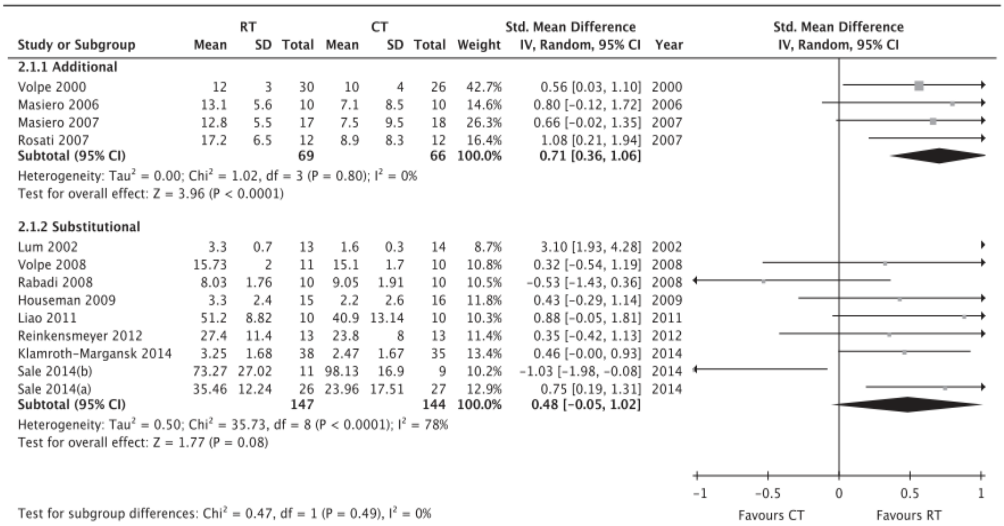

Figure 2.6 Comparison of the Fugl-Meyer score after intervention in two subgroups (additional subgroup; substitutional subgroup) [23].

Table 2.3 shows the results of various trials that were conducted. The outcome measures used in the trials were the Fugl-Meyer Assessment Scale (FMA), Motor Power Score (MP), Motor Status Score (MSS), Range of Motion, and Wolf Motor Function Test for motor controls. Ashworth Scale and Modified Ashworth Scale (MAS) for spasticity. Functional Independence Measure (FIM), Arm Motor Ability Test, Barthel Index, and Rancho Los Amigos Functional Test for functioning.

Table 2.3 Clinical reviews and evaluations of Upper Limb robotic rehabilitation devices.

Authors	**Type of Study**	**Aim**	**Results**	**Year**
Mehrholz et al [20]	Randomized controlled trials (RCT)	To evaluate effectiveness	Improvements in ADL, muscular	2015

			strength, and hand functions	
Peter et al [19]	RCT	To evaluate effectiveness	In 30 trials, significant improvement in FMA while FIM was significant in half of the cases.	2011
Sheng et al [21]	RCT	To evaluate effectiveness	All participants gained certain improvement in terms of physical function or strength and range of motion after training.	2016
Pirondini et al [11]	Three-dimensional point-to-point reaching movements	Use of ALEx for post-stroke upper limb robotic-assisted rehabilitation	Analysis of healthy subjects supported the use of exoskeleton for robot-assisted rehabilitation	2016
Xiao et al [15]	Fixed target movements	To evaluate effectiveness	Cable-driven exoskeleton demonstrated that it can provide effective movement	2018

			assistance to post-stroke patients.	
Lo et al [7]	RCT	To evaluate effectiveness	The study suggests mixed results on the effectiveness of Robotic rehabilitation over conventional rehabilitation.	2017
Zhang et al [23]	RCT	Evaluate the effectiveness of Conventional and Robotic training in improving the motor recovery of paretic upper limb	Motor recovery (FMA score) in the Robot-assisted therapy group was significantly greater than the conventional therapy group.	2017
Bertani et al [13]	RCT	Effectiveness of robotic exoskeleton in comparison to other types of intervention.	Especially in chronic stroke patients, robot-assisted rehabilitation is more effective in improving upper-limb recovery. No significant benefit of RT over CT in	2017

			the sub-acute phase after stroke.	
Singh et al [14]	RCT, non-RCT	Evaluate clinical outcomes and feasibility of RT of Upper limb in SCI patients.	Increased range of motion, grip, pinch, and muscle strength	2018

2.3 SIGNAL ACQUISITION FOR EXOSKELETON DEVICES

It is necessary to monitor human intentions/muscle activities to automatically control these robotic exoskeleton devices. They are either controlled manually with predefined commands or with the help of various sensors placed on the human body. There has been a continuous evolution in the field of Signal acquisition from the human body. The most commonly used sensors for gathering human intentions are EMG (Electromyography) and EEG (Electromyography) sensors [56]–[63]. The surface electromyography (sEMG) sensor electrode configuration is shown in Figure 2.7. Apart from EMG and EEG, surface muscle pressure monitoring systems have also been developed [64], [65]. These sensors assist in establishing human-robot interaction (HRI).

[66], [67] are some of the works towards the improvement of HRI in robotic exoskeleton devices.

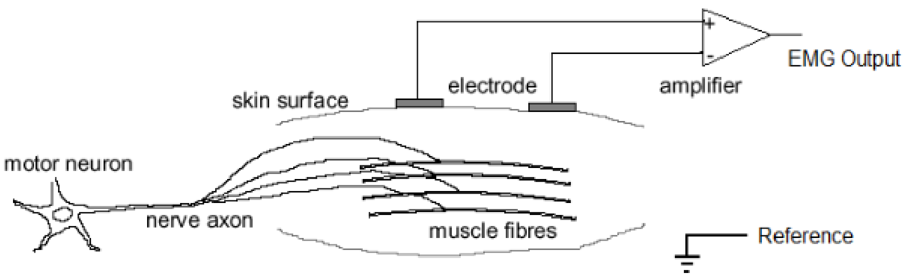

Figure 2.7 sEMG sensor electrode configuration [68].

EEG sensor is a great leap forward in the development of robotic exoskeleton technology. EEG sensors are a popular tool to investigate human intentions to actuate correct assistive exoskeleton motions. While EMG sensors are often termed as the muscle-machine interface, the EEG sensor technology is well regarded as the brain-machine interface (BMI). At a particular point in time, the EEG contains entire brain activity visible at the location of the electrode and is considered the most practical and realistic non-invasive brain-machine interface technique. Other techniques like functional magnetic resonance imaging (fMRI), positron emission tomography (PET), and magnetoencephalography (MEG) are plagued with mobility issues and high cost [69].

EMG coupled with IMU (Inertial Measurement Unit) [70] sensor provides feedback with greater accuracy. While EMG sensors provide muscle potential, IMU sensors track the motion efficiently [57]. IMU sensor is made up of a gyroscope and accelerometer [71] that are used to detect deflection, distance, angular velocity, and rotation angle [72] of an object. To enhance motor stability, a fusion of various above-mentioned sensors has been done in the research [73]. Though this work pertains to the lower-limb exoskeleton device, such efforts are also beneficial for the upper-limb exoskeleton interfaces. The results of the experiment demonstrated that fusion of the sensor data from both EEG and EMG sensors resulted in enhanced human stability.

2.4 CONTROL ALGORITHMS FOR EXOSKELETONS

The control system is an important part of every electro-mechanical system. Being a highly non-linear system, wearable robotic exoskeleton devices are often plagued with external disturbances and performance issues. To eliminate such issues, a unique control strategy is required for every such system. The main consideration of the exoskeleton control design is how to achieve the best control performances. However, other important issues like safety and stability have to be considered. Some of the most significant control algorithms adopted for wearable robotic exoskeleton devices categorized according to the model system, the physical parameters, the hierarchy, and the usage are adaptive control, adaptive-neural control, impedance control, adaptive-impedance control, neural network control, sliding mode control, fuzzy, neuro-fuzzy, robust control, robust-sliding mode control, admittance control, etc.

An adaptive control strategy is a physical parameter based control system [74]. This control strategy is used to control the force of human-robot interaction. An adaptive controller is generally used to adapt to the high external changes like the user's physical condition. One such application [75] uses an adaptive controller employing neural-network technology. The main objective of the application is to compensate for the input saturation effect of the actuator by using a learning algorithm in the presence of unknown system dynamics. Sana et al. [76] implemented the robust sliding-mode control algorithm on three degrees of freedom robot to control the flexion/ extension movements of the wrist, the elbow, and the shoulder. Efficient tracking of desired trajectories in position and velocity were obtained by using the sliding mode law. Kang et al.

[77] proposed a safety improved adaptive controller for a 5 DOF upper-limb exoskeleton. The results prove that the controller accumulated unknown uncertainties.

Yi et al. [78] proposed an active disturbance rejection control (ADRC) based strategy for tracking the gait trajectory of a lower-limb exoskeleton robot. A performance comparison was conducted with the conventional proportional integral derivative PID controller. Experimental results show that the ADRC strategy is superior to PID control in tracking the target gait. Besides these control strategies, to make the patient suffering from neurological disorders perform a certain task by controlling a device, brain-machine interface (BMI) techniques have been developed.

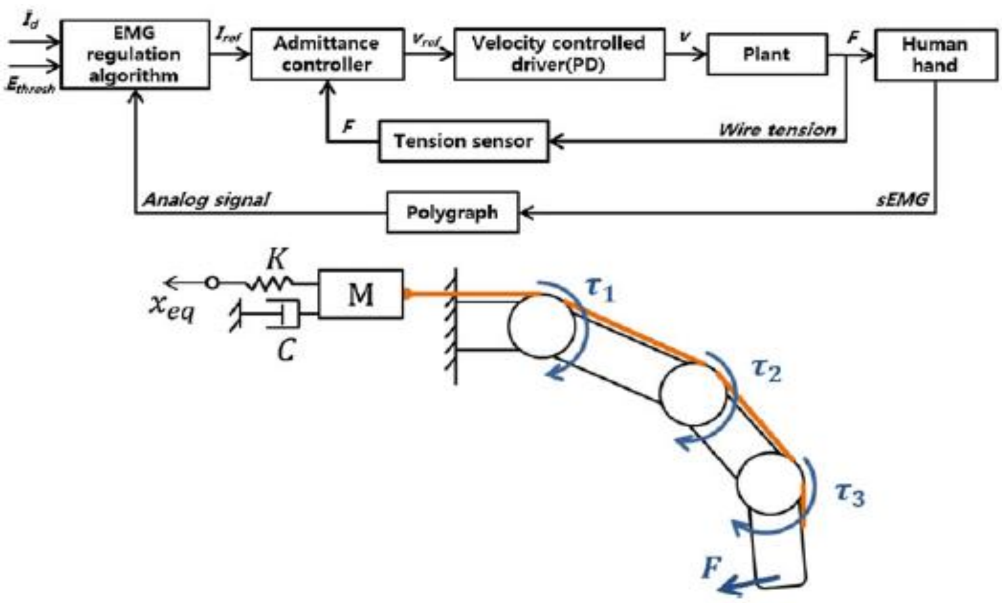

Figure 2.8 Control algorithm and schematic of impedance control exercise [79]

Zhijun et al. [80] proposed adaptive-neural control using BMI. The BMI-based closed-loop adaptive control is designed to improve the performance and directly control the robot through the human mind. Research [79] at SNU, Korea proposed various control algorithms for the hand exoskeleton device SNU Exo-Glove. Three exercise control algorithms: isotonic, isokinetic, and impedance control were proposed. For each of the three exercise control algorithm, an EMG regulation algorithm is proposed. Figure 2.8 shows the impedance control schematic.

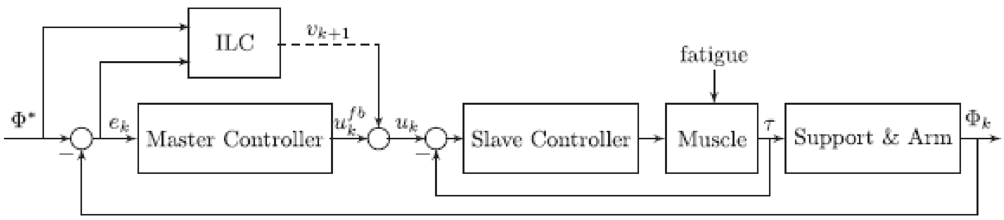

Figure 2.9 The iterative learning control scheme [81]

Wenkang et al. [81] proposed an iterative learning control (ILC) as shown in Figure 2.9. ILC was used for robot-assisted stroke rehabilitation to reduce the effects of muscle fatigue during the rehabilitation process.

2.5 EXOSKELETON ACTUATORS

Various types of actuators used in exoskeleton devices are based on the control methodologies, application, linkage configurations, and ease of actuation and handling. The most common types of actuators are:

- Electric Motors
- Pneumatic Actuators
- Hydraulic Actuators
- Series Elastic Actuators
- Pneumatic Artificial Muscle Actuators

Of the above-listed actuators, Electric Motors are the commonest choice [1], [82] due to their ease of control, actuation, maintenance, compactness, and portability. However, they are held back because of the high impedance values. The pneumatic actuators composed of the pneumatic cylinder offers high power to weight ratio if the weight of the compressor unit required for cylinder actuation is not considered. The hydraulic actuators are the most powerful among the above mentioned, but it is relatively heavier and suffers from fluid leakage problems, which is not suitable for rehabilitation application. Another innovation in the field of actuators is pneumatic muscle actuators [83]. These actuators have a very good power/weight ratio like pneumatic actuators and exhibit the properties of the human muscle system [84]. They are light and transfer force in a single direction with the help of internal rubber structure and braided mesh shell [1]. Electric motors are the most widely used actuators in upper and lower limb exoskeletons due to their reliability, favorable torque to weight ratio, high speed, good overloading capacity, and precision. There are two types of electric actuators: AC motors and DC motors, mostly brushless. Because permanent-magnet motors provide high torque despite the motor shaft being stationary, they are preferred by most in the industry. In the case of mobile exoskeleton devices, a lightweight motor is ideal to use. Brushed DC motors provide high torque, high efficiency, and performance [85].

Weight is a critical factor while choosing actuators for an exoskeleton and due to the low weight of pneumatic actuators; they are favorable when weight is a constraint in exoskeleton design. They are highly compliant in nature but due to their non-linear performance, they are difficult to control and slow in operation. Furthermore, since they operate using air, they also need a portable air supply, which adds weight to the system, but it still manages to keep the overall weight of the system less than the traditional systems. Hydraulic actuators use fluid under high pressure to convert hydraulic power into mechanical work. They have variable stiffness ability i.e. the system arrangement is highly flexible, has a good specific power i.e. the power to weight ratio. However, it is noisy in nature and requires complex components to work properly. They provide high output forces even though they are compact in size, which reduces power consumption. Electric, Pneumatic, Hydraulic actuators have their pros and cons. Some are slow, nonlinear in performance while others are heavy and noisy. Combining the advantages of different actuation systems novel exoskeletons have been developed.

Series Elastic Actuators comprises of a BLDC motor in conjunction with a spring in series, which provides 'stiffness' between the load and the motor. Torsional springs are used instead of linear springs in the case of Rotary series elastic actuators. These are almost zero impedance actuating systems and provide very accurate torque control. They provide high force fidelity, variable stiffness, good force control bandwidth, and low friction. Pneumatic artificial muscle consists of a flexible inflatable membrane enclosed within a fibrous material with one end attached to the load and the other end to the gas /air valve. As air is pumped into the membrane, it expands radially while contracting in the axial direction and thus exerts a force on the load in the axial direction. PAMs mimic muscles exhibiting nonlinear behavior and hence are difficult to control [85]. However, they do provide high power to weight and power to volume ratio, which are 5 times the values offered by electric actuators. During high-level performance requirements, these actuators are not durable [86]. Another advancement in the field of artificial muscle actuators is fluidic artificial muscles (FAM) [87].

2.6 WEARABLE EXOSKELETON DEVICES

There has been a great evolution in the field of assistive devices since 1936. The research on exoskeleton devices varies from the upper limb to the lower limb exoskeleton devices. Lelai Zhou et. al [29] designed a passive upper-limb exoskeleton for the brachial plexus injury. The exoskeleton device has been designed in order to compensate for the arm weight and in-hand objects. The device is a wearable exoskeleton and has five degrees of freedom. Soumya Kanti Manna et.al developed a working prototype of an exoskeleton device named EXORN. The exoskeleton has ten degrees of freedom and is wearable by the human arm. The designed exoskeleton resembles the human joint ranges. The mechanical structure can also be attached to the human arm [28]. Kazuo et.al developed three degrees of freedom mobile exoskeleton that uses users EMG signals as the input signal for the robot controllers. [46]. Mohamed G. B. Atia et al proposed a 2DOF low-cost upper limb exoskeleton having two revolute joints and with dual modes i.e. portable and cart-mounted. For the calculations of the joint angles of the user's arm, inertial measurement units (IMU Razor) is used [88]. This system does not have the facility to alter the lengths on the joints as per the upper-limbs of different users. Yogeswaran et al. [57] developed an upper limb exoskeleton for rehabilitation based on EMG and IMU sensor feedback. The EMG sensor is used for forearm strength detection and the IMU sensor is used for forearm motion detection. In addition, a graphical user interface (GUI) has been designed using LabVIEW. The EMG sensors receive signals from target muscle through Ag-AgCl electrodes, which is used for motor actuation. Spinal cord injury (SCI) and stroke are the primary reasons for the need for Upper Limb Rehabilitation systems among patients.

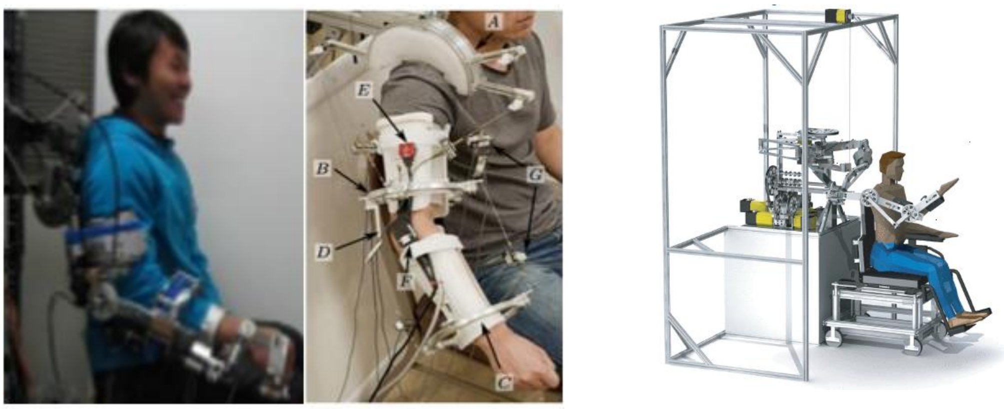

(a) (b) (c)

Figure 2.10 Exoskeleton Devices (a) SUEFUL-7 [2] (b) CAREX [2] (c) MEDARM

One of the most notable works in the field of robotic rehabilitation devices is Cyberdyne's Hybrid Assistive Limb (HAL). The working principle of HAL includes reading Bio-electric Signals (BES) that are sent by the brain to actuate the target muscles [89]. HAL is used for various non-military applications such as physical therapy, assistance to disabled persons, and accommodates workers to carry heavier loads, assistance for rescue activities on disaster sites. The lower-limb medical version of HAL The full-body exoskeleton by Cyberdyne is in the research and development phase. Dual-arm exoskeletons such as [90] are a leap forward towards the development of new human-cooperative strategies to detect human subject's movement efforts. The subject's movement intentions were extracted from muscular efforts. A six-axis force/torque sensor was used to estimate the muscular-effort. Various experiments were also conducted to prove the effectiveness of the proposed system.

ReWalk [91] developed by Argo Medical Technologies [92] is a device that provides valuable exercise and therapy [93]. ReWalk is a rehabilitation robot for spinal cord injury and contains motors at hip and knee joints. The actuation is obtained when the user bends his/her body forward, which is sensed by the system and the system follows the natural gait. CAREX [30] is a cable-driven arm rehabilitation robot. To replace the rigid heavy links, cuffs are fixed to the human limbs. Cables drive these cuffs while motors drive these cables. The absence of a rigid link makes the structure comparatively lighter than other limb rehabilitation devices. 6-REXOS [94] is a 6 DOF upper-limb exoskeleton primarily focused on improving physical human-robot interaction (pHRI) and kinematic redundancy. In [95] a wrist and forearm rehabilitation robot has been designed. The exoskeleton has three degrees of freedom namely supination/pronation, flexion/extension, and abduction/adduction. Three DC motors are used to actuate these motions. MEDARM [96] is five degrees of freedom rehabilitation system for the shoulder complex as shown in Figure 2.10. The purpose of the design is to stabilize the movements of the upper limb. Moreover, the exoskeleton is designed to avoid singularity and mimic the natural motions of the human shoulder joint. Electric motors are used along with the cable and belt transmission mechanism. The robot also provides a wide range of adjustments to suit different users. ARMin [97] is an upper limb exoskeleton for training and therapy to improve the activities of daily living. ARMin has six degrees of freedom and it is adaptable to different body types. It uses optical hand support to avoid uncomfortable hand postures. There are three different modes of training available in the ARMin GUI namely, Movement therapy, Game therapy, and ADL training. Table 2.4 shows the various upper limb exoskeleton devices developed for different applications.

Table 2.4 Upper Limb Exoskeleton System

Author	**Year**	**Actuator used**	**DOF**	**Limb**	**Field of Application**
Manna & Bhaumik [28]	2013	Brushless DC servo motor & DC Geared Motor	10	Upper limb	Rehabilitation therapy
Kiguchi and Hayashi [98]	2012	DC encoded motors	7	Upper limb	Power assist
Lo and Xie [99]	2014	Brushless DC servo motors	5	Upper Limb	Rehabilitation
Ying et al. [30]	2012	DC motors	5	Upper Limb	Rehabilitation
Atia *et al.* [88]	2017	Motors	2	Upper Limb	Assist
Beigzadeh *et al.* [100]	2015	DC Motors	1	Upper Limb	Assist

Mahdavian *et al.* [101]		DC Motors	3 2(for shoulder)	Upper Limb	Rehabilitation
Kiguchi *et al.* [46]	2007	DC Motors	3	Upper Limb	Rehabilitation and motion assist
Hong *et al.* [102]	2012	Motors	10	Upper Limb	Assistance
Lu *et al.* [33]	2011	DC encoded motors	2	Upper Limb	Stroke and rehabilitation
Gopura and Kiguchi [103]	2007	DC motors	3	Upper Limb	Forearm motion assist
Noda *et al.* [104]	2014	Pneumatic-Electric Hybrid Actuator	1	Upper Limb	Assist
Lo and Xie [105]	2012	pneumatic muscle actuators	8 actuated DOF and	upper-limb	Stroke

			2 passive DOF		
Lu *et al.* [106]	2013	Cable Pully	4	upper-limb	Paralysis
Nef *et al.* [97]	2007	brushed DC motors	6	upper-limb	Movement Therapy and rehabilitation
Hasegawa *et al.* [107]		DC motors	4	upper-limb	Meal assistance
Gupta *et al.* [108]	2006	Electric motors	5	upper-limb	Rehabilitation and training
Mao and Agrawal [30]	2012	Motors and cable	5	upper-limb	neural rehabilitation
Kiguchi *et al* [109]	2003	DC motors	2	upper-limb	Assistance and shoulder support
Gopura and Kiguchi [110]	2009	DC motors	7	upper-limb	Shoulder Assist

Frisoli *et al.* [111]	2009	frameless DC motor	5	upper-limb	Assisted rehabilitation in virtual reality
Rocon *et al.* [112]	2007	dc motor	4	upper-limb	Rehabilitation Tremor Assessment and Suppression
Martinez *et al.*[95]	2013	dc motor	3	upper-limb	Forearm and wrist Rehabilitation
Gunasekara *et al.* [94]	2015	DC motors	4	Upper limb	motion assistance
Johnson *et al.* [113]	2001	electric motors	5	Upper limb	Limb assistance
Sasaki *et al.* [114]	2005	Pneumatic	1	Upper limb	Motion assist at the wrist
Klein *et al.* [115]	2008	Pneumatic	4	Upper limb	rehabilitation, stroke

Sugar *et al.* [116]	2007	Pneumatic	4	Upper limb	Assistance
Mistry *et al.* [117]	2005	Hydraulic	7	Upper limb	Motor Behavioral Study
Schiele and Hirzinger [118]	2011	Motors	8 Active and 6 Passive	Upper Limb	Force-feedback telemanipulation
Gupta *et al.* [108]	2006	Electric motors	5	Upper Limb	Training and Rehabilitation
S. Ball *et al.* [96]	2007	Electric motors	5	Upper Limb	Rehabilitation
Schill *et al.* [119]	2011	Stepper Motors and Fluidic actuators	4	Upper Limb	Assistance
Wang *et al.* [120]	2019	Motors	3	Upper Limb	Rehabilitation

More such exoskeleton systems and their brief review can be found in [2], [69], [82], [92], [121]–[125].

2.7 CONCLUSIONS FROM LITERATURE SURVEY

- Movement related disability has been a prominent issue worldwide. In India, 20% of the disabled population has some kind of movement-related disability. The results of various clinical tests as shown in Table 3 strongly suggest that the use of Robot-assisted training (RT) can be integrated into clinical practice.

- Individuals can expect to pay a hefty amount ($75,000-$350,000 USD) for an exoskeleton. Even if the patient manages to purchase the device, the initial amount may not include the cost of being trained. These training charges may vary depending upon the experience and education level of the trainers or training clinicians. Moreover, the additional costs for maintenance or warranty can be expected. These monetary costs present a major challenge in the path of exoskeletons for personal use.

- The user-centered design technique is also one of the prominent needs of hardware development [7] as the current systems are not sufficiently safe to operate physically with people [63]. It is required that the robot is adaptable to different individuals [34] in order to avoid uncomfortable or unnatural posture and has multiple degrees of freedom so as to provide better rehabilitative results.

- The burden of stroke is set to increase over the next decades in low and middle-income countries, most of which are located in the Indian subcontinent and Africa. The scientific community must also work to reduce the overall cost of procurement of exoskeletons by individuals. This is a particularly dire limitation as 85% of all stroke deaths occur in low and middle-income countries. A significant reduction in initial cost can motivate more people to adopt these robotic devices.

CHAPTER 3 MATHEMATICAL MODELING OF THE EXOSKELETON

A set of mathematical expressions of the robot describe the joint torque values and joint position with respect to time. This chapter presents the mathematical modeling of the proposed exoskeleton device. Relevant equations are developed using the theory of robotics kinematics and dynamics. Denavit-Hartenberg (D-H) guidelines are used to develop the kinematic model of the system. The dynamic model is derived using Euler-Lagrange equations of motion. An insight into the design parameters, torque, and singularity positions has been presented as well.

3.1 KINEMATIC ANALYSIS

The kinematic analysis consists of the forward and inverse kinematics of the robotic system. The forward kinematics provides the coordinates of the point in space that the end effector of the system achieves while knowing the joint angles. With inverse kinematics, the desired point in the workspace is known and the joint angles are calculated.

3.1.1 FORWARD KINEMATIC ANALYSIS OF 3-DOF UPPER-LIMB EXOSKELETON

The forward kinematics is obtained after calculating the DH-parameters of the proposed robotic exoskeleton device. The proposed design has a similarity with the human upper-limb. The kinematic model of the design is shown in Figure 3.1. The D-H parameters of the model are shown in Table 5.

Table 3.1 DH parameters of 3-DOF upper-limb exoskeleton

#	ϴ	d	a	α
0-1	Θ_1	L_1	0	90°
1-2	Θ_2	0	L_2	0°
2-H	Θ_3	0	L_3	0°

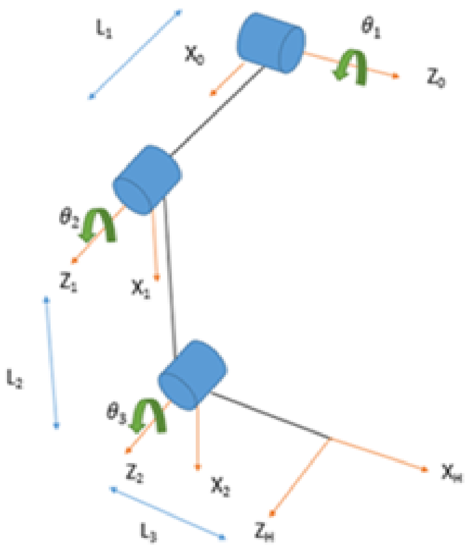

Figure 3.1 Kinematic configuration of Exoskeleton device

The Transformation matrix of each link is as follows:

$$A_1 = \begin{bmatrix} \cos\theta_1 & -\sin\theta_1 & 0 & 0 \\ \sin\theta_1 & \cos\theta_1 & 0 & 0 \\ 0 & 0 & 1 & 0 \\ 0 & 0 & 0 & 1 \end{bmatrix} \times$$

$$\begin{bmatrix} 1 & 0 & 0 & 0 \\ 0 & 1 & 0 & 0 \\ 0 & 0 & 1 & l_1 \\ 0 & 0 & 0 & 1 \end{bmatrix} \times \begin{bmatrix} 1 & 0 & 0 & 0 \\ 0 & 1 & 0 & 0 \\ 0 & 0 & 1 & 0 \\ 0 & 0 & 0 & 1 \end{bmatrix} \times \begin{bmatrix} 1 & 0 & 0 & 0 \\ 0 & \cos 90 & -\sin 90 & 0 \\ 0 & \sin 90 & \cos 90 & 0 \\ 0 & 0 & 0 & 1 \end{bmatrix}$$

$$= \begin{bmatrix} -\sin\theta_1 & 0 & \cos\theta_1 & -l_1 \sin\theta_1 \\ \cos\theta_1 & 0 & \sin\theta_1 & l_1 \cos\theta_1 \\ 0 & 1 & 0 & 0 \\ 0 & 0 & 0 & 1 \end{bmatrix} \tag{3.1}$$

Similarly,

$$A_2 = \begin{bmatrix} \cos\theta_2 & -\sin\theta_2 & 0 & l_2 \cos\theta_2 \\ \sin\theta_2 & \cos\theta_2 & 0 & l_2 \sin\theta_2 \\ 0 & 0 & 1 & 0 \\ 0 & 0 & 0 & 1 \end{bmatrix} \tag{3.2}$$

$$A_3 = \begin{bmatrix} -\sin\theta_3 & -\cos\theta_3 & 0 & -l_3\sin\theta_3 \\ \cos\theta_3 & -\sin\theta_3 & 0 & l_3\cos\theta_3 \\ 0 & 0 & 1 & 0 \\ 0 & 0 & 0 & 1 \end{bmatrix} \quad (3.3)$$

$$A_{hand} = A_1 \times A_2 \times A_3 \quad (3.4)$$

Where A_{hand} shows the position and orientation of the end effector of a robotic exoskeleton.

3.1.2 EXOSKELETON WORKSPACE

In order to calculate the workspace from the forward kinematics of the robotic system, all the reachable points of the end effector are plotted. Figure 3.2 shows all the reachable points by the end effector of the robotic exoskeleton.

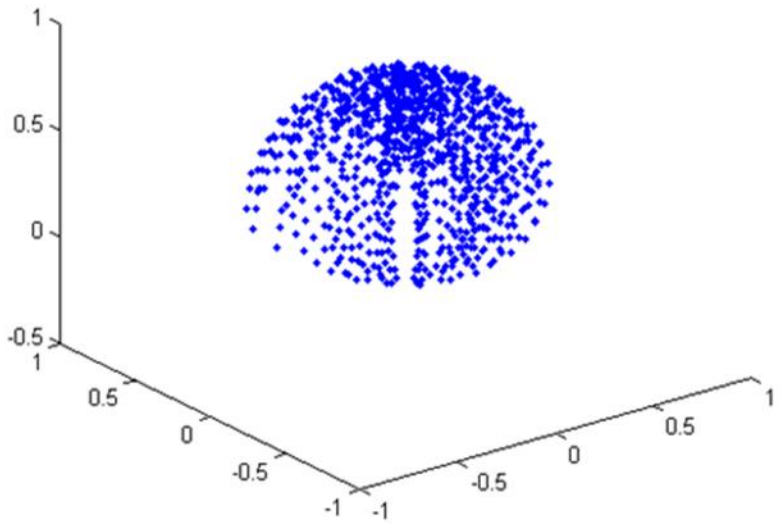

Figure 3.2 3-DOF Exoskeleton Workspace

Robotic workspace typically shows the orientation and position of the end effector on different locations within its reach [126], which entirely depends upon the forward kinematics and joint angle (*θ*) range of each joint. To generate the 3D plot, joint positions of the end effector (*Px, Py, Pz*) are required.

3.1.3 JACOBIAN

The transformation from joint velocities to the end effector velocity is described by a matrix, called Jacobian. The jacobian matrix, which is dependent on manipulator configuration is a linear mapping from velocities in joint space to velocities in Cartesian space. The Jacobin is one of the most important tools for the characterization of differential motions of the manipulator the mapping between differential changes is linear and can be expressed as

$$Ve(t) = J(q)\dot{q} \tag{3.5}$$

Where, $J(q) = 3X1$ manipulator jacobian,

$\dot{q} = nX1$ vector of n joints

This can be written in column vectors of the jacobian,

$$Ve(t) = [J_1(q)J_2(q)J_3(q)] \tag{3.6}$$

$$Ve(t) = \begin{bmatrix} v \\ w \end{bmatrix} = \begin{bmatrix} \dot{d} \\ \dot{\theta} \end{bmatrix} = J(q)\dot{q} \tag{3.7}$$

The rotary Jacobian can be written as follows

$$J_i(q) = \begin{bmatrix} P_{i-1} X\, {}^{i-1}_{n}P \\ P_{i-1} \end{bmatrix} \tag{3.8}$$

The origin of frame {n} at the end effector is $O_n = [0 \quad 0 \quad 0 \quad 1]^T$. This applies to the origin of any frame i.e. for any value of n. Each column of the jacobian matrix can be calculated separately as

$$J_1(q) = \begin{bmatrix} P_0 X\, {}^0P_3 \\ P_0 \end{bmatrix},\ J_2(q) = \begin{bmatrix} P_1 X\, {}^1P_3 \\ P_1 \end{bmatrix},\ J_3(q) = \begin{bmatrix} P_2 X\, {}^2P_3 \\ P_2 \end{bmatrix} \tag{3.9}$$

The individual Jacobian matrix can be combined to form a total Jacobian matrix as shown below

$$J = [J_1 \quad J_2 \quad J_3] \tag{3.10}$$

The calculation of jacobian is shown in Appendix B.

3.1.4 STATIC FORCE ANALYSIS

Assuming that the self-weight of the exoskeleton 'F' acting on the joints is given by

$$F = [f_x \quad f_y \quad f_z \quad m_x \quad m_y \quad m_z]^T \tag{3.11}$$

Where f_x, f_y, f_z are the forces along the *x*-, *y*-, and *z*-axes of the hand frame, and m_x, m_y, m_z are the moments about the *x*-, *y*-, and *z*-axes.

Thus,
$$\tau_{static} = J(q)^T \mathbf{F} \tag{3.12}$$

The computation of static load analysis has been explained in Appendix C

Static torque of the three joints of the exoskeleton at $\theta_1 = \begin{bmatrix} 0 & 75^\circ & 150^\circ \end{bmatrix}$; $\theta_2 = \begin{bmatrix} 0 & 70^\circ & 140^\circ \end{bmatrix}$; $\theta_3 = \begin{bmatrix} 0 & 65^\circ & 130^\circ \end{bmatrix}$ is calculated as

$$\text{Static Torque } (N\text{-}m) = \begin{bmatrix} 0 & 0 & 0 \\ 18.0600 & -5.1327 & -5.5768 \\ 10.7800 & -7.6226 & 0.0000 \end{bmatrix} \tag{3.13}$$

The values of the static torque are obtained for the self-weight of the exoskeleton. The significance of the values of theta has been explained in section 3.2.2.

3.2 DYNAMIC ANALYSIS

3.2.1 DYNAMIC MODELLING OF THE 3-DOF EXOSKELETON

The exoskeleton joint torques are calculated using Lagrangian, *L=K-P*. Where P is the potential energy and K is the kinetic energy of the system.

$$L = \frac{1}{2}\sum_{i=1}^{n}\sum_{j=1}^{i}\sum_{k=1}^{i} Tr\left[({}^{0}T_{j-1} Q_j \,{}^{j-1}T_i) I_i ({}^{0}T_{k-1} Q_k \,{}^{k-1}T_i)^T \right] \dot{q}_j \dot{q}_k + \sum_{i=1}^{n} m_i g \,{}^{0}T_i \,{}^{i}\bar{r}_i \tag{3.14}$$

The Lagrangian formulation begins with the determination of the kinematic model. Already we have the kinematic model for the exoskeleton robot. Her all the joints are revolute joint. Value of Q_j are obtained by the partial differentiation of the homogeneous transformation matrix.

$$Q_1 = \begin{bmatrix} 0 & -1 & 0 & 0 \\ 1 & 0 & 0 & 0 \\ 0 & 0 & 0 & 0 \\ 0 & 0 & 0 & 0 \end{bmatrix} \tag{3.15}$$

$$Q_2 = \begin{bmatrix} 0 & -1 & 0 & 0 \\ 1 & 0 & 0 & 0 \\ 0 & 0 & 0 & 0 \\ 0 & 0 & 0 & 0 \end{bmatrix} \tag{3.16}$$

$$Q_3 = \begin{bmatrix} 0 & -1 & 0 & 0 \\ 1 & 0 & 0 & 0 \\ 0 & 0 & 0 & 0 \\ 0 & 0 & 0 & 0 \end{bmatrix} \tag{3.17}$$

Since all the joints are revolute $Q_1=Q_2=Q_3$, the inertial tensors I_1, I_2, and I_3 for the links of length l_1, l_2, and l_3 can be obtained by

$$I_i = \begin{bmatrix} \frac{1}{2}(-I_{xx}+I_{yy}+I_{zz}) & I_{xy} & I_{xz} & m_i\bar{x}_i \\ I_{xy} & \frac{1}{2}(I_{xx}-I_{yy}+I_{zz}) & I_{yz} & m_i\bar{y}_i \\ I_{xz} & I_{yz} & \frac{1}{2}(I_{xx}+I_{yy}-I_{zz}) & m_i\bar{z}_i \\ m_i\bar{x}_i & m_i\bar{y}_i & m_i\bar{z}_i & m_i \end{bmatrix} \tag{3.18}$$

Where for link 1:

$$\bar{x}_i = 30.47$$
$$\bar{y}_i = 40.70$$
$$\bar{z}_i = 20.00$$

$$I_1 = \begin{bmatrix} -366323.02 & -29747.06 & 99469.88 & 4972.704 \\ -29747.06 & 586717.77 & 132848.21 & 6642.24 \\ 99469.88 & 132848.21 & 88788.75 & 3264 \\ 4972.704 & 6642.24 & 3264 & 163.20 \end{bmatrix} \quad (3.19)$$

The units of the components of I_1, I_2, and I_3 are in grams and millimeters.

Link 2:

$$\bar{x}_i = 4.93$$
$$\bar{y}_i = 102.29$$
$$\bar{z}_i = 144.22$$

$$I_2 = \begin{bmatrix} 2243540.35 & 120641.62 & 185133.02 & 1153.86 \\ 120641.62 & 2482831.98 & 3452804.16 & 23940.97 \\ 185133.02 & 3452804.16 & 4870375.63 & 33754.691 \\ 1153.86 & 23940.97 & 33754.69 & 234.05 \end{bmatrix} \quad (3.20)$$

Link 3:

$$\bar{x}_i = 204.20$$
$$\bar{y}_i = 25.81$$
$$\bar{z}_i = 217.50$$

$$I_3 = \begin{bmatrix} 10616723.815 & 1341465.91 & 11508862.43 & 51199.066 \\ 1341465.91 & 225326.405 & 1594473.85 & 6471.3413 \\ 11508862.43 & 1594473.85 & 16068705.815 & 54533.775 \\ 51199.066 & 6471.3413 & 54533.775 & 250.73 \end{bmatrix} \tag{3.21}$$

According to the Euler-Lagrange dynamic formulation, τ is generally termed as torque at joint i, which drives link i of the manipulator. It is given by

$$\tau_i = \frac{d}{dt}\left(\frac{\delta L}{\delta \dot{q}_i}\right) - \frac{\delta L}{\delta q_i} \tag{3.22}$$

Torque τ_i is applied to link i after carrying out the differentiation.

$$\tau_i = \sum_{j=1}^{n} M_{ij}(q)\ddot{q}_j + \sum_{j=1}^{n}\sum_{k=1}^{n} h_{ijk}\dot{q}_j\dot{q}_k + G_i \tag{3.23}$$

for $i = 1,2,\ldots,n$

The first step required the computation of matrices d_{ij}, which are required to compute all other coefficients. The next step is applied to compute the elements of the inertia matrix M_{ij} using the equation shown below:

Where, $$M_{ij} = \sum_{p=\max(i,j)}^{n} Tr\left[d_{pj} I_p d_{pi}^T\right] \tag{3.24}$$

For a 3-link robotic exoskeleton the computation of values of d_{ij} in included in Appendix C

$$M = \begin{bmatrix} m_{11} & m_{12} & m_{13} \\ m_{21} & m_{22} & m_{23} \\ m_{31} & m_{32} & m_{33} \end{bmatrix} \tag{3.25}$$

Where *M* is the mass matrix of the system. The computation of the mass matrix is also included in Appendix C.

In the upcoming steps, the Coriolis and Centrifugal force coefficients, h_{ijk} for i, j, k=1,2,3 are obtained from the equation as explained below

$$h_{ijk} = \sum_{p=\max(i,j,k)}^{n} Tr\left[\frac{\partial(d_{pk})}{\partial q_p} I_p d_{pi}^T \right] \tag{3.26}$$

The Coriolis and Centrifugal coefficient matrix *H* for the 3-link exoskeleton robot is calculated as

$$\begin{aligned} H_1 = {} & h_{111}\dot{\theta}_1\dot{\theta}_1 + h_{112}\dot{\theta}_1\dot{\theta}_2 + h_{113}\dot{\theta}_1\dot{\theta}_3 + h_{121}\dot{\theta}_2\dot{\theta}_1 + h_{122}\dot{\theta}_2\dot{\theta}_2 \\ & + h_{123}\dot{\theta}_2\dot{\theta}_3 + h_{131}\dot{\theta}_3\dot{\theta}_1 + h_{132}\dot{\theta}_3\dot{\theta}_2\ h_{133}\dot{\theta}_3\dot{\theta}_3 \end{aligned} \tag{3.27}$$

$$H_2 = h_{211}\dot{\theta}_1\dot{\theta}_1 + h_{212}\dot{\theta}_1\dot{\theta}_2 + h_{213}\dot{\theta}_1\dot{\theta}_3 + h_{221}\dot{\theta}_2\dot{\theta}_1 + h_{222}\dot{\theta}_2\dot{\theta}_2$$
$$+h_{223}\dot{\theta}_2\dot{\theta}_3 + h_{231}\dot{\theta}_3\dot{\theta}_1 + h_{232}\dot{\theta}_3\dot{\theta}_2 + h_{233}\dot{\theta}_3\dot{\theta}_3 \tag{3.28}$$

$$H_3 = h_{311}\dot{\theta}_1\dot{\theta}_1 + h_{312}\dot{\theta}_1\dot{\theta}_2 + h_{313}\dot{\theta}_1\dot{\theta}_3 + h_{321}\dot{\theta}_2\dot{\theta}_1 +$$
$$h_{322}\dot{\theta}_2\dot{\theta}_2 + h_{323}\dot{\theta}_2\dot{\theta}_3 + h_{331}\dot{\theta}_3\dot{\theta}_1 + h_{332}\dot{\theta}_3\dot{\theta}_2 + h_{333}\dot{\theta}_3\dot{\theta}_3 \tag{3.29}$$

$$H = \begin{bmatrix} H_1 & H_2 & H_3 \end{bmatrix} \tag{3.30}$$

Detailed computation of the Coriolis and Centrifugal coefficient matrix is explained in Appendix C.

Computation of the gravity loading at the three joints which results in gravity matrix is shown below

$$G_i = -\sum_{p=i}^{n} m_p g d_{pi} \, {}^{p}\overline{r_p} \tag{3.31}$$

$$G_1 = -(m_1 g d_{11} r_1 + m_2 g d_{21} r_2 + m_3 g d_{31} r_3) \tag{3.32}$$

$$G_2 = -(m_2 g d_{22} r_2 + m_3 g d_{32} r_3) \tag{3.33}$$

$$G_3 = -(m_3 g d_{33} r_3) \tag{3.34}$$

$$G = \begin{bmatrix} G_1 & G_2 & G_3 \end{bmatrix} \tag{3.35}$$

The complete dynamic model of the exoskeleton robot is obtained by substituting the above results. The robotic equation of motion in the matrix form is

$$\begin{bmatrix} \tau_1 \\ \tau_2 \\ \tau_3 \end{bmatrix} = \begin{bmatrix} m_{11} & m_{12} & m_{13} \\ m_{21} & m_{22} & m_{23} \\ m_{31} & m_{32} & m_{33} \end{bmatrix} \times \begin{bmatrix} \ddot{\theta}_1 \\ \ddot{\theta}_2 \\ \ddot{\theta}_3 \end{bmatrix} + \begin{bmatrix} H_1 \\ H_2 \\ H_3 \end{bmatrix} + \begin{bmatrix} G_1 \\ G_2 \\ G_3 \end{bmatrix} \tag{3.36}$$

Dynamic Torque *(N-m)* for the desired trajectory of each joint is calculated as

$$\begin{bmatrix} 0 & -1.3468 & 1.2065 & 6.5534 & -2.2534 & 0 \\ -0.0003 & -1.5953 & -0.9489 & 0.5156 & 0.2969 & 0.0001 \\ -0.0001 & -1.4437 & -1.8215 & -0.8855 & 0.2045 & -0.0000 \end{bmatrix} \tag{3.37}$$

The 3-DOF upper-limb exoskeleton consisting of all revolute joints and link lengths $l_1 = 180\ mm$, $l_2 = 260\ mm$, $l_3 = 385\ mm$ as per the measurement of an individual with height 189 cm. Link l_2 and l_3 have variable lengths in the form of a sliding mechanism that can shorten or lengthen the links associated with the upper arm and forearm. The links are made up of aluminum alloy 6061. The joint torque is calculated after applying the payload in the form of arm weight on each link. For a healthy individual with a weight of 70kg, the entire mass of the upper arm is 3.47kg which includes the weight of the Forearm – 1.12 kg; Upper arm – 1.89 kg, and Hand – 0.46 kg. kg [127].

3.2.2 TRAJECTORY PLANNING

The trajectory is the sequence of motions of the joint with respect to time [128]. The trajectory of the robot depends both on the dynamics and kinematics of the robot. Link 1 is fixed on the rear side of the shoulder joint to facilitate abduction/adduction motion. The range of motion of the human upper-limb for the shoulder abduction/adduction, extension/flexion, and elbow extension/flexion is given in Table 3.2.

Table 3.2 Movement range of required upper-limb motions [129][58]

Upper-limb movement	**Movement range**	**Exoskeleton range**
Shoulder abduction/adduction	180°/0°	150°
Shoulder flexion/extension	150°-180°/-40° to -50°	140°
Elbow flexion/extension	135°-140°/0°	130°

For the safety of the patient/wearer, only positive motions (shoulder abduction, shoulder flexion, elbow flexion/extension) is considered. The range of movement varies from one individual to another. The exoskeleton movement range of different links is set below the maximum range of human upper-limb as per the biomechanics of the human arm. To achieve a smooth and continuous motion, a fifth-order trajectory has been designed.

As mentioned in the table above, the trajectory has been designed using the maximum degree of movements in the exoskeleton's individual joints.

For Joint 1:

$$\begin{aligned}
\theta_1 &= a_0 + a_1 t + a_2 t^2 + a_3 t^3 + a_4 t^4 + a_5 t^5 \\
\dot{\theta}_1 &= a_1 + 2a_2 t + 3a_3 t^2 + 4a_4 t^3 + 5a_5 t^4 \\
\ddot{\theta}_1 &= 2a_2 + 6a_3 t + 12a_4 t^2 + 20a_5 t^4
\end{aligned} \tag{3.38}$$

Applying the boundary conditions

$$\begin{aligned}
t_i &= 0, \theta_i = 0^\circ; \\
t_f &= 5, \theta_f = 150^\circ; \\
t_i &= 0, \dot{\theta}_i = 0^\circ; \\
t_f &= 5, \dot{\theta}_f = 0^\circ; \\
t_i &= 0, \ddot{\theta}_i = 0^\circ; \\
t_f &= 5, \ddot{\theta}_f = 0^\circ
\end{aligned}$$

Computing the coefficient, the joint trajectory is obtained as follows

$$\theta_1 = 12t^3 - 3.6t^4 + 0.2880t^5 \tag{3.39}$$

For Joint 2:

$$\begin{aligned}
\theta_2 &= b_0 + b_1 t + b_2 t^2 + b_3 t^3 + b_4 t^4 + b_5 t^5 \\
\dot{\theta}_2 &= b_1 + 2b_2 t + 3b_3 t^2 + 4b_4 t^3 + 5b_5 t^4 \\
\ddot{\theta}_2 &= 2b_2 + 6b_3 t + 12b_4 t^2 + 20b_5 t^4
\end{aligned} \tag{3.40}$$

Applying the boundary conditions

$$\begin{aligned}
t_i &= 0, \theta_i = 0^\circ; \\
t_f &= 5, \theta_f = 140^\circ; \\
t_i &= 0, \dot{\theta}_i = 0^\circ; \\
t_f &= 5, \dot{\theta}_f = 0^\circ; \\
t_i &= 0, \ddot{\theta}_i = 0^\circ; \\
t_f &= 5, \ddot{\theta}_f = 0^\circ
\end{aligned}$$

Computing the coefficient, the joint trajectory is obtained as follows

$$\theta_2 = 11.2t^3 - 3.36t^4 + 0.2688t^5 \tag{3.41}$$

For Joint 3:

$$\begin{aligned}
\theta_3 &= c_0 + c_1 t + c_2 t^2 + c_3 t^3 + c_4 t^4 + c_5 t^5 \\
\dot{\theta}_3 &= c_1 + 2c_2 t + 3c_3 t^2 + 4c_4 t^3 + 5c_5 t^4 \\
\ddot{\theta}_3 &= 2c_2 + 6c_3 t + 12c_4 t^2 + 20c_5 t^4
\end{aligned} \tag{3.42}$$

Applying the boundary conditions

$$t_i = 0, \theta_i = 0^\circ;$$
$$t_f = 5, \theta_f = 130^\circ;$$
$$t_i = 0, \dot{\theta}_i = 0^\circ;$$
$$t_f = 5, \dot{\theta}_f = 0^\circ;$$
$$t_i = 0, \ddot{\theta}_i = 0^\circ;$$
$$t_f = 5, \ddot{\theta}_f = 0^\circ$$

Computing the coefficient, the joint trajectory is obtained as follows

$$\theta_3 = 10.4t^3 - 3.12t^4 + 0.2496t^5 \tag{3.43}$$

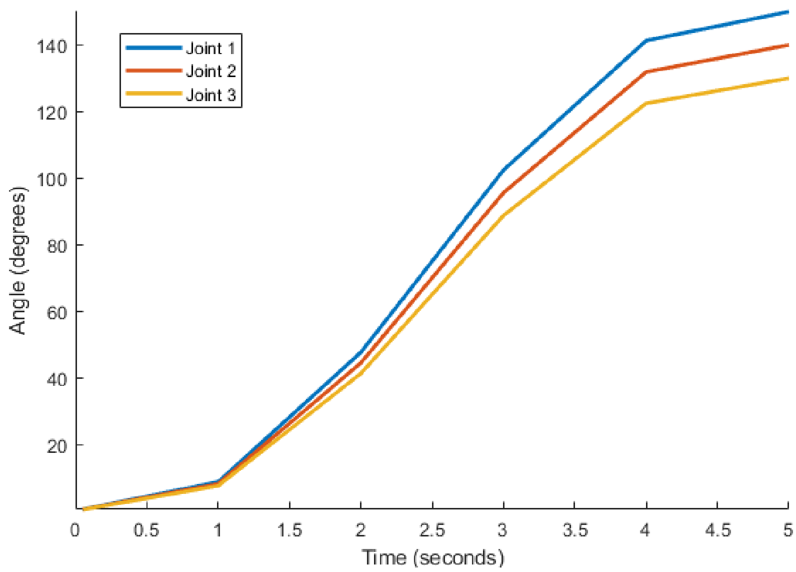

Figure 3.3 Joint angular response with respect to time.

3.3 SUMMARY

The primary contribution of this chapter towards the thesis work is the kinematic and dynamic analysis for the mathematical modeling of the proposed model. The relation between the joint angles, dynamics, and trajectory tracking analysis presents a detailed insight into the configuration of the exoskeleton mechanisms.

CHAPTER 4 CONTROL ARCHITECTURE

It is well known that robotic systems are highly nonlinear [130], complicated, and dynamically coupled [131]. Without the implementation of a suitable control technique, the non-linearity of robotic systems results in uncertainty. The control requires the knowledge of the mathematical model and some sort of intelligence. Whereas, the required mathematical modeling is obtained from basic physical laws governing robot dynamics and associated devices. A robot performs the specified tasks in its environment, which can be divided into two classes: contact type task and non-contact type tasks. The non-contact type tasks involved the manipulation of the end –effector in space to do desired work. While in contact type tasks the end effector interacts with the environment. The Computed Torque Control (CTC) has been employed in the system. The globally asymptotically stability of CTC makes it a very effective motion control system [132]. The controller in CTC modifies the system to effectively decouple and linearize by employing nonlinear feedback of joint velocities and its actual positions [133]. The schematic representation of the control system is shown in Figure 4.1.

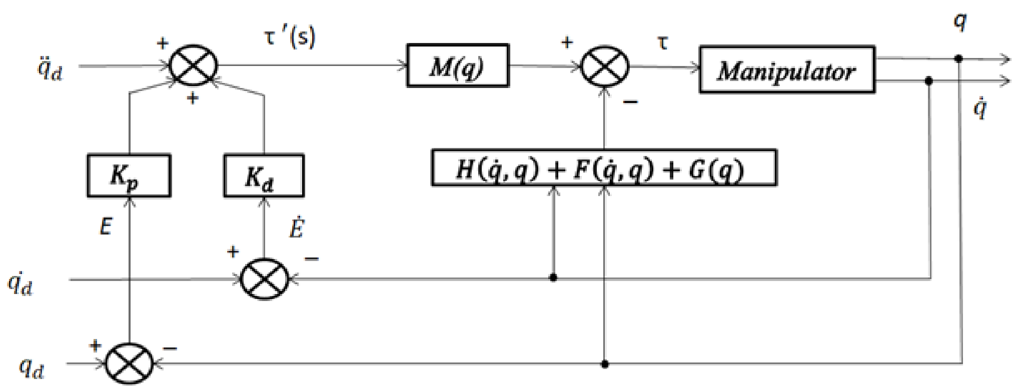

Figure 4.1 Computed torque control law for the nonlinear controller

The joint torques τ based on rigid body dynamics.

$$\tau = M(q)\ddot{q} + H(q,\dot{q}) + G(q) \tag{4.1}$$

The dynamic control of manipulator motions and /or interaction forces requires knowledge of forces or torque that must be exerted on the manipulator's joints to move the links and the end effector from the present location to the desired location, with or without the constraints of a particular planned end-effector trajectory, and or planned end-effector force/torque.

In both the situations of the desired end-effector location and the desired end-effector force, the control of the individual joint's location is important. Hence it is an obvious requirement that each joint is controlled by a position servo. If the body of the robot is to move very slowly or to move one joint at a time, then the control is simple because coupled dynamics forces are negligible.

The contributions of overall non-rigid body effects and frictions, $F(q,\dot{q})$ has been neglected in the system. The errors in the controller are defined as

$$\begin{aligned} E(t) &= q_d(t) - q(t) \\ \dot{E}(t) &= \dot{q}_d(t) - \dot{q}(t) \end{aligned} \tag{4.2}$$

Where q and q_d are actual and desired positions of the robot. K_p and K_d are positions and velocity gains.

Though the links are assumed to be rigid bodies, the flexibility of the links very much constrains the selection of control gains [133]. All mechanical elements produce resonance at frequencies other than natural frequency due to unmodelled structural flexibility. The controller must be designed in such a way to avoid the excitation of these unmodelled resonances.

$$\omega_{res} = \omega_0 \sqrt{\frac{I_0}{I_{\max}}} \tag{4.3}$$

Where ω_{res} is the resonance frequency, ω_0 is the actual structural frequency at I_0 which is effective inertia. The controller must prevent the excitation of the design above natural frequency ω_n to ensure structural stability. The natural frequency is given by

$$\omega_n \leq 0.5\omega_{res} \tag{4.4}$$

Where,

$$\omega_n = \sqrt{K_p} \tag{4.5}$$

From the above equations, we have

$$\omega_n \leq 0.5\omega_0 \sqrt{\frac{I_0}{I_{\max}}} \tag{4.6}$$

Therefore,

$$K_p \leq (0.5\omega_0)^2 \frac{I_0}{I_{\max}} \tag{4.7}$$

The Computed Torque Control (CTC) employs uses nonlinear feedback to linearize the error dynamics. This in turn provides better trajectory tracking performance. The Simulink model of the joint trajectory is shown in Figure 4.2.

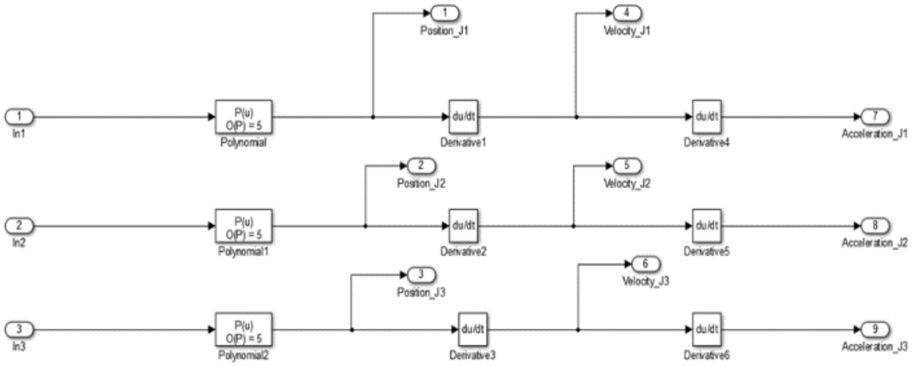

Figure 4.2 Joint trajectory Simulink model

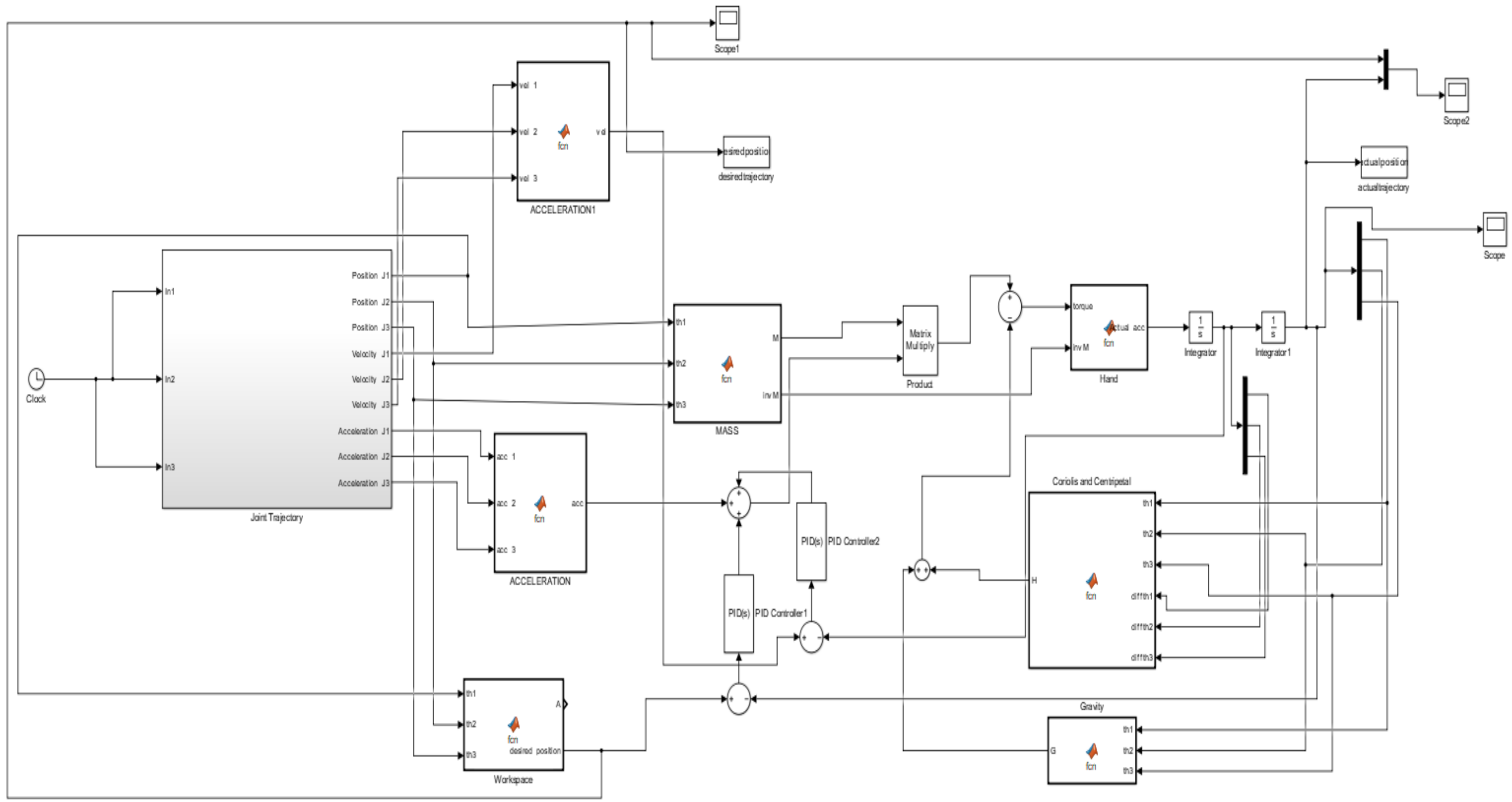

Figure 4.3 CTC control architecture

4.1 CTC SIMULATION

Simulations for the CTC control algorithm were carried using the actual design parameters of the exoskeleton robot. Figure 4.4 shows the desired and the actual joint positions of the 3-DOF exoskeleton after the application of the control system. Figure 4.5 shows the comparison of required and actual joint trajectories before the application of the CTC control scheme. The simulation clearly shows the final joint positions missing the required values by a great margin. The comparison of both as shown in Figure 4.6 and with minimal error in the output after the application of CTC control, Figure 4.7 clearly validates the performance of the CTC control system for the proposed design.

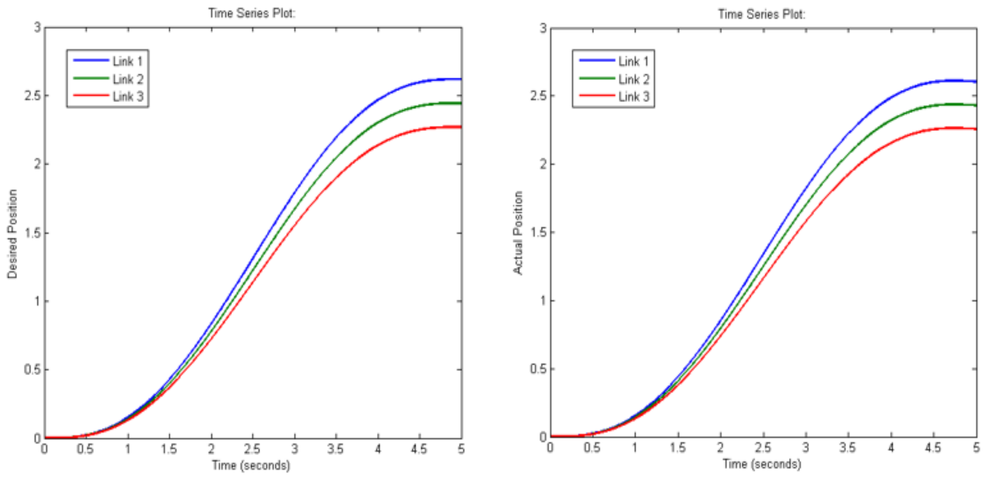

(a) Desired joint positions (b) Actual joint positions

Figure 4.4 Desired joint positions and actual joint positions

Figure 4.3 shows the designed controller that employs the basic principles of the computed torque control (CTC). Figure 4.5 shows the error comparison.

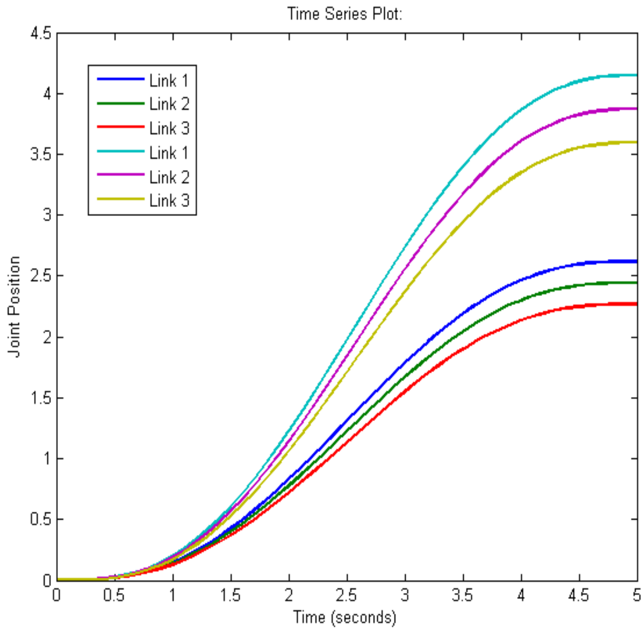

Figure 4.5 Comparison of actual and required joint trajectories of 3-DOF exoskeleton before application of CTC scheme

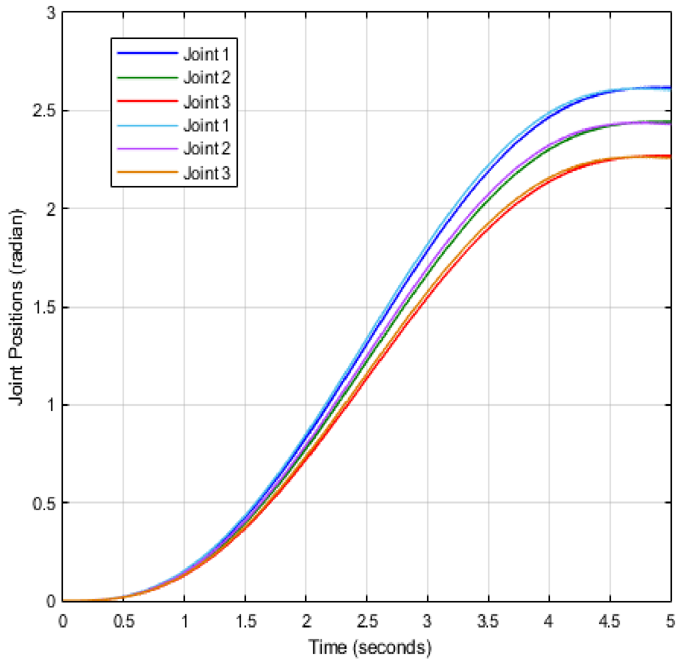

Figure 4.6 Comparison of actual and desired positions after application of CTC

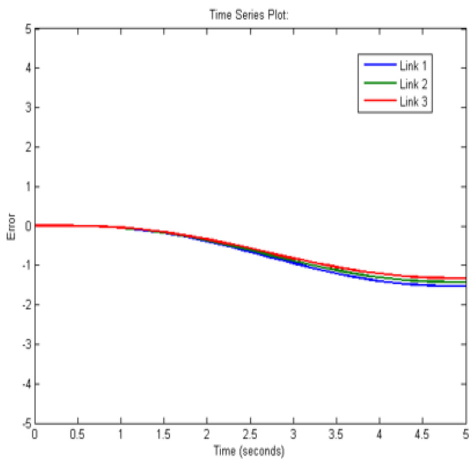

(a) Without the application of CTC

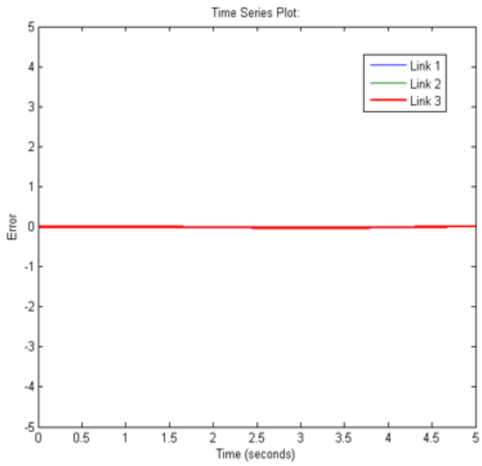

(b) With CTC control

Figure 4.7. Joint position error without application of CTC and with CTC control

4.2 SUMMARY

This chapter contributes to the development of the CTC control system for the robotic exoskeleton. Without the application of a control system, the non-linear behavior of the dynamic system failed to accomplish the required trajectory. The results clearly validate that the application of CTC control reduces the errors in the output joint positions, making direct use of the complete dynamic model of the system to cancel the effect of gravity, Coriolis and centrifugal force, etc.

CHAPTER 5 DEVELOPMENT OF EXOSKELETON PROTOTYPE

The developed exoskeleton device performs three of the most basic movements of the human upper-limb. These movements are shoulder abduction/adduction, extension/flexion and elbow extension/flexion motions. The material used for the fabrication of exoskeleton linkages is Aluminium 6061-T6. The aluminum 6061-T6 is one of the most commonly used aluminum alloys for structural applications. The Al 6061 also features higher strength than Al 6063. The T6 refers to the temper or degree of hardness, achieved by precipitation hardening. At the same time, Al 6061 offers good machinability.

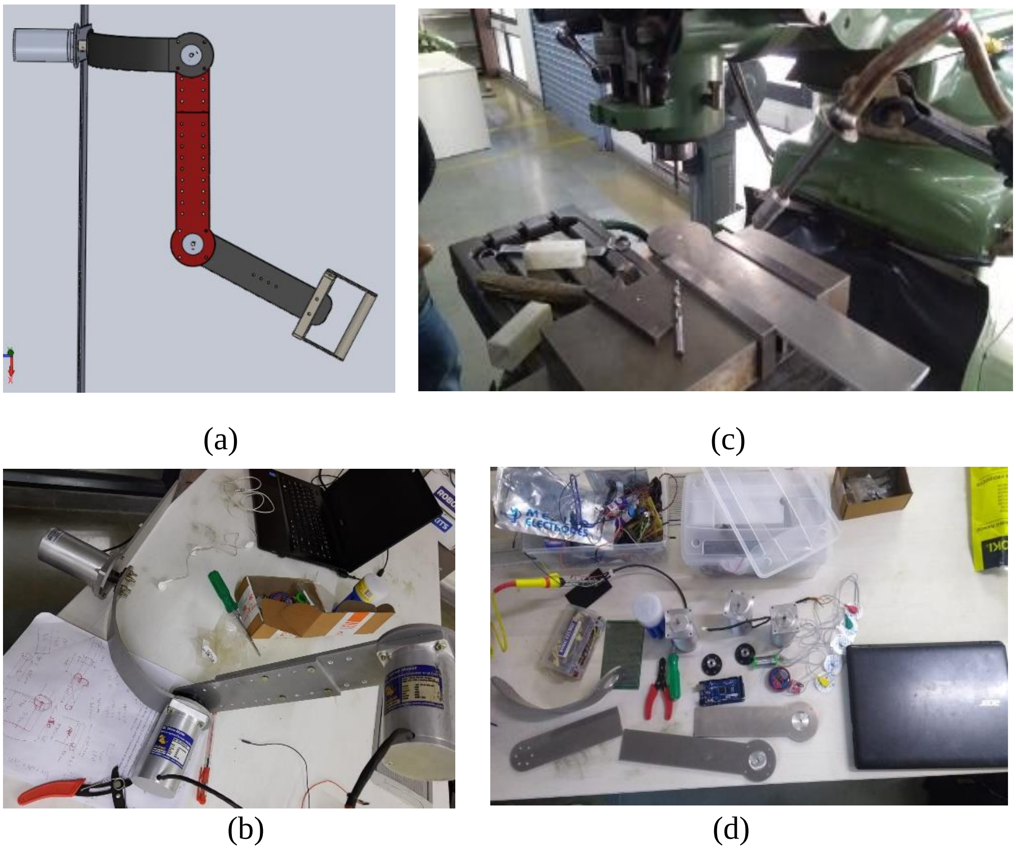

Figure 5.1 (a), (b) SolidWorks models of the proposed exoskeleton, (c) Machining of linkages on vertical milling center, (d) Exoskeleton linkages after machining

Table 5.1 Instruments and machinery used

Sl. No.	Instrument/Equipment /Machine	Application	Image
1	Aluminum 6061-T6	Exoskeleton linkages	
2	Bosch Metal Cutter	Al 6061-T6 sheet cutting	
3	Wire EDM	Profile cutting	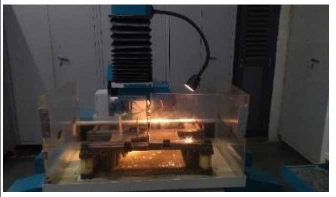
5	Radial drilling machine	Drilling	
6	Arduino Mega	Primary robot controller	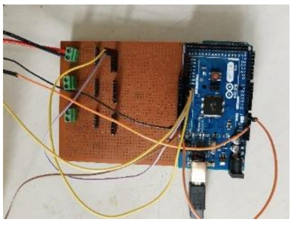

7	DC Servo Encoder Motor	Exoskeleton Actuator	
8	EMG Sensors	Electromyography signal processor	
9	Ag/Agcl Electrodes	Muscle potential signal	
10	Arc welding system	Structural welding	

11	Obstacle avoidance IR sensor	Safety sensor	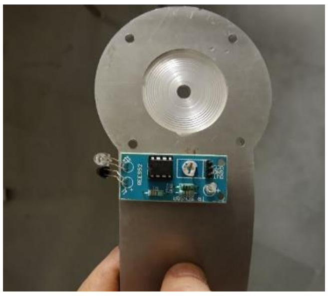
12	IMU Razor 9DOF sensor	Angular observations	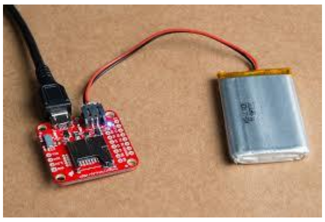
13	Robotic Coupling	Power transmission	

5.1 SPECIFICATION OF COMPONENTS

Various materials and components have been used in order to fabricate the prototype of the exoskeleton model as explained below.

5.1.1 ALUMINIUM 6061-T6

Aluminum 6061 is the most widely used alloy in the 6000 series. 6061 aluminum plates are precipitation-hardened containing silicon and magnesium and its major alloying elements. It caters medium to high strength with good toughness and corrosion-resistant characteristics [134][135]. Figure 5.2 shows the comparison of various tempers of Al 6061 alloy. Clearly, the T6 offers more machinability than other tempers.

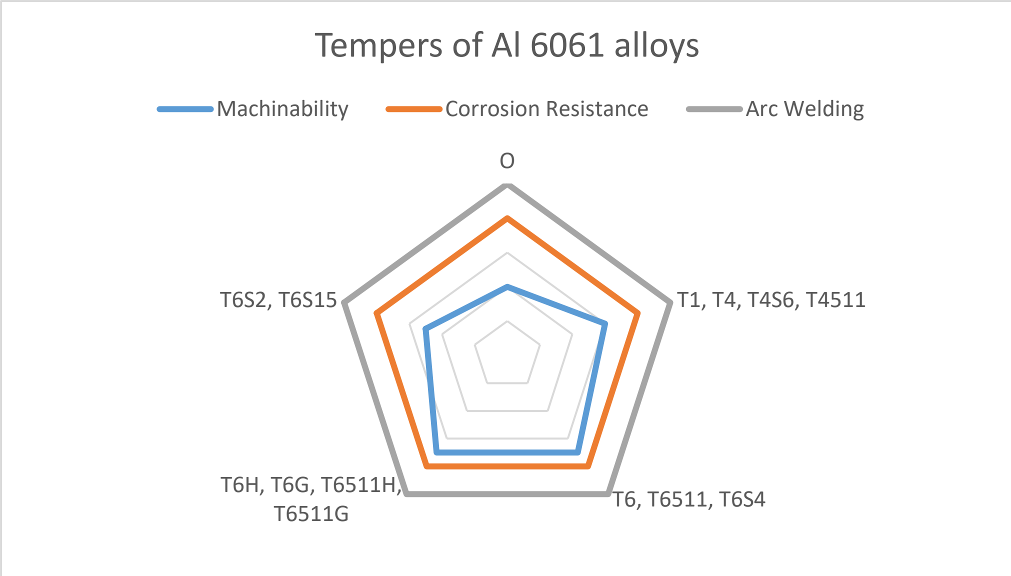

Figure 5.2 Comparative characteristics of related alloys/tempers

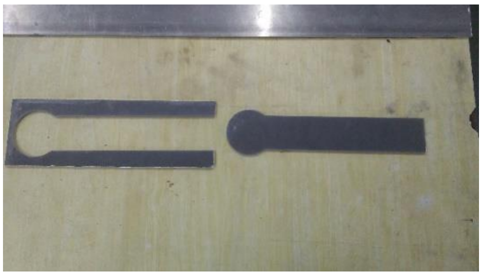
(a)


(b)


(c)

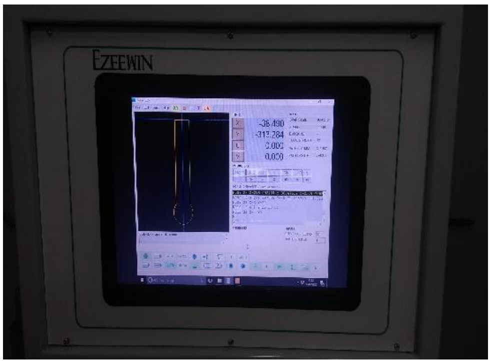

(d)

Figure 5.3 High order of machinability of Al 6061-T6 alloy, Robotic link post- (a) Wire-EDM cutting, (b) Milling, (c) Drilling, (d) Wire EDM control panel

5.1.2 EZEECUT NXG CNC WIRE CUT EDM MACHINE

EZEECUT NXG CNC wire cut EDM machine comprises of

- Machine tool
- Pulse generator
- Coolant unit

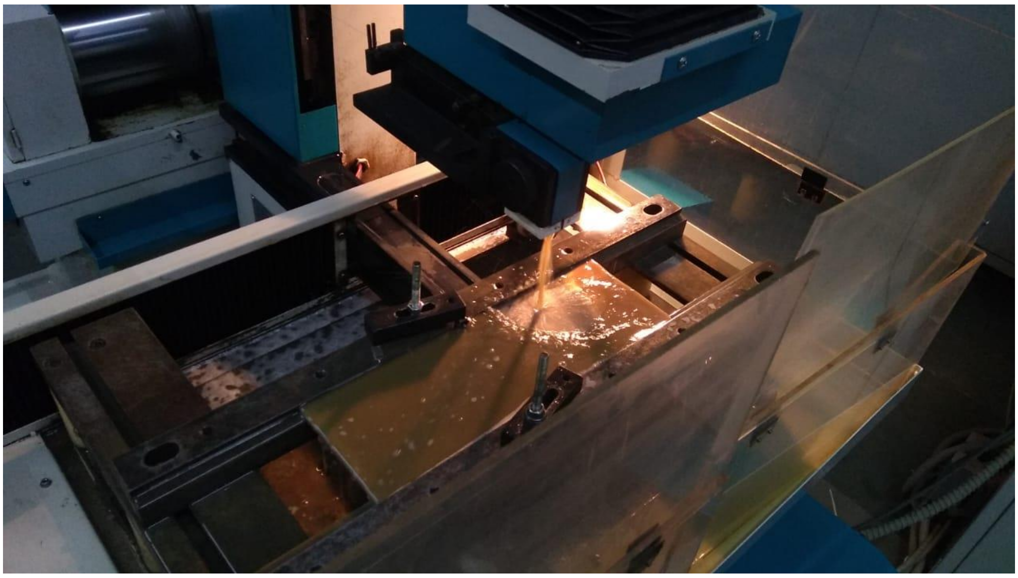

Figure 5.4 EZEECUT NXG CNC wire cut EDM machine cutting an Al6061-T6 sheet with 5mm thickness.

The machine tool mainly comprises of the work table normally referred to as X_Y table, Z-axis quill with motor, wire tension unit with rollers, wire feed drum assembly with others. The work table moves on the X and Y axis in steps of 1-micron employing stepper motors. The auxiliary table parallel to the X-Y table also moves using stepper motors.

The wire feed drum assembly provides help to the wire to reciprocate for the EDM process. The machine is capable of producing the taper cutting of ± 3 deg over 100mm with the help of the movement of the auxiliary table.

5.1.3 ARDUINO MEGA 2560 MICROCONTROLLER

The 3-DOF upper-limb robotic exoskeleton uses Arduino Mega 2560 R3 microcontroller board. The microcontroller has 54 digital I/O pins, 16 analog pins that are used for analog inputs only. It also has 4 UART pins for serial communication. In the 3-DOF exoskeleton project, the Rhino DC servo Encoder motors are used. The motors are actuated using the UART communication protocol. The Tx and Rx pins of the microcontroller are used to drive motors and receive feedback. The analog pins A0, A1, A2 are used to capture rectified analog input from EMG sensors.

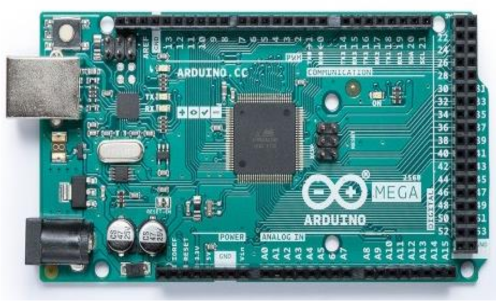

(a)

(b)

Figure 5.5 (a) Arduino 2560 R3 microcontroller board, (b) Microcontroller connections.

5.1.4 RHINO DC SERVO MOTOR

RMCS-220X High-Torque Encoder DC Servo Motor and Driver UART, I2C, PPM, and Analog input interface (Max. 15Vdc and 7A)

Key features:

- The motor has a 0.2º encoder resolution
- The motor has 10RPM max speed and 200kg-cm torque.
- Motor speed control interface via UART, I2C, PPM, and analog input.

- Speed and position control
- Max-speed, damping, P-Gain, I-Gain, and speed feedback settings are adjustable.

Table 5.2 Mechanical specifications of Rhino RMCS-220X

Specifications	Details
Dimensions	120mm*60mm*65mm
Weight	350gms

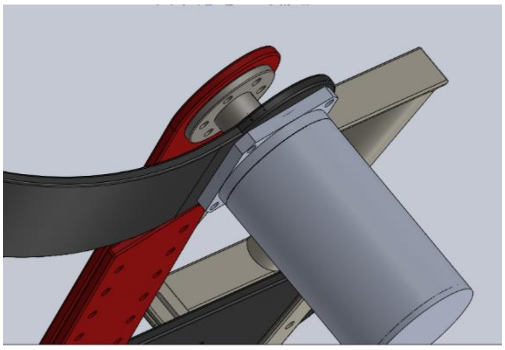

(a)

(b)

Figure 5.6 (a) CAD model and (b) Actual Rhino DC servo motor

Table 5.3 Encoder specifications of Rhino RMCS-220X

Specification	Details
Counts per rotation	1800

Degrees per count on the output shaft	0.2 deg per count

5.1.5 EMG SENSOR (ADVANCER TECHNOLOGIES MUSCLE SENSOR V3)

It is necessary to monitor human intentions/muscle activities to automatically control these robotic exoskeleton devices. They are either controlled manually with predefined commands or with the help of various sensors placed on the human body. There has been a continuous evolution in the field of Signal acquisition from the human body. The most commonly used sensors for gathering human intentions are EMG (Electromyography) and EEG (Electromyography) sensors [56]–[63]. The surface electromyography (sEMG) sensor electrode configuration is shown in Figure 5.6. Apart from EMG and EEG, surface muscle pressure monitoring systems have also been developed [64], [65]. These sensors assist in establishing human-robot interaction (HRI). [66], [67] are some of the works towards the improvement of HRI in robotic exoskeleton devices.

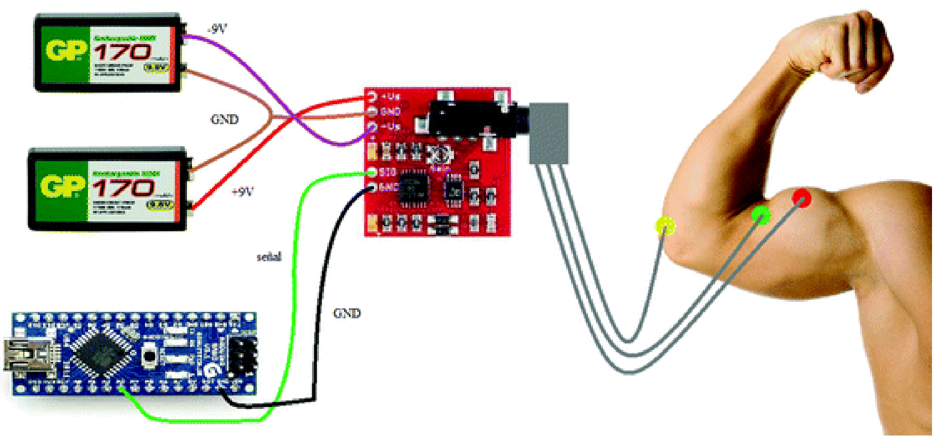

Figure 5.7 EMG sensor electrode connection with target muscle.

EMG coupled with IMU (Inertial Measurement Unit) [70] sensor provides feedback with greater accuracy. While EMG sensors provide muscle potential, IMU sensors track the motion efficiently [57]. IMU sensor is made up of a gyroscope and accelerometer [71] that are used to detect deflection, distance, angular velocity, and rotation angle [72] of an object.

Measuring muscle activation via electric potential, referred to as electromyography (EMG), has traditionally been used for medical research and diagnosis of neuromuscular disorders. However, with the advent of ever shrinking yet more powerful microcontrollers and integrated circuits, EMG circuits and sensors have found their way into prosthetics, robotics, and other control systems. Figure 5.8 shows the sEMG sensor pin layout.

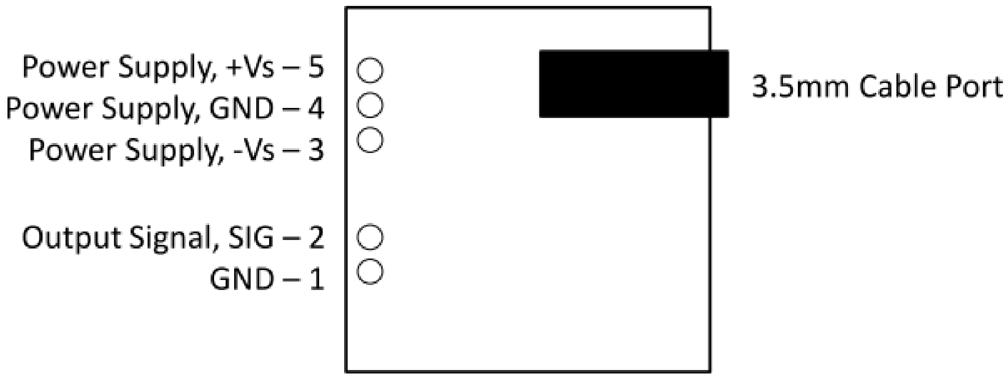

Figure 5.8 Three-lead sEMG Sensor pin layout

5.1.6 IR OBSTACLE AVOIDANCE SENSOR

Infrared sensors are used as obstacle sensors in the robotic exoskeleton application. These sensors emit and/or detect infrared radiation in order to sense the surroundings.

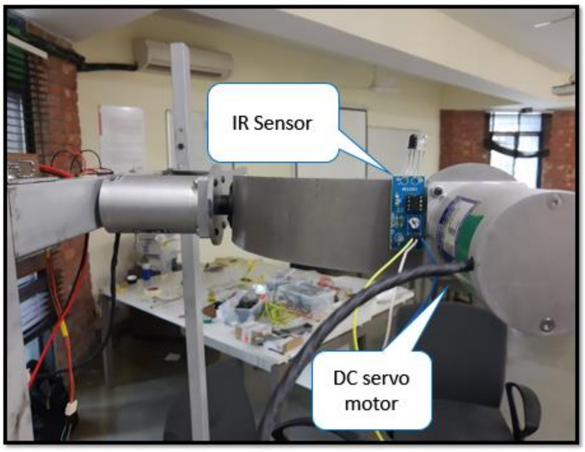

Figure 5.9 IR sensor placement on exoskeleton arm

When this sensor is used for obstacle detection, the sensor transmits an infrared signal. This signal bounces off the surface of the object and it is received by the infrared receiver.

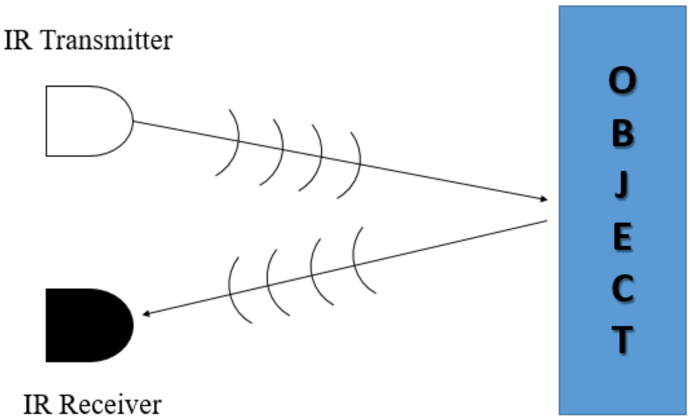

Figure 5.10 Working principle of IR sensors

When the IR transmitter emits radiation, it reaches the object and some of the radiation reflects back to the IR receiver. Based on the intensity of the reception by the IR receiver, the output of the sensor is defined.

5.1.7 IMU RAZOR (9DOF)

(a) (b)

Figure 5.11 (a) IMU Razor, (b) IMU sensor readings in microcontroller serial monitor

The 9DoF Razor's MPU-9250 features three, three-axis sensors a gyroscope, an accelerometer, and a magnetometer which gives it the ability to sense linear acceleration, angular rotation velocity, and magnetic field vectors. The IMU sensor has been used to get accurate angular velocity and position of the robotic link in real-time.

5.1.8 NEMA 23 COUPLING

EasyMech Nema 23 shaft couplings with 6.35mm internal diameter have been used for power transmission from the DC servo motor shaft with a 6mm diameter to the respective robotic linkage. The coupling is made up of mild steel with 6 holes near the circumference of the coupling with a 5.2mm diameter. The coupling provides a good hold of the motor shaft and ensures the safe operation of the robot. The coupling can be attached to the output shaft of the motor via an allen key using M4x6 socket screws.

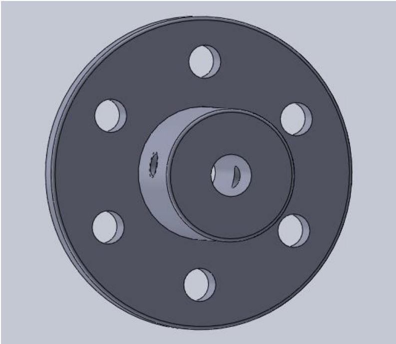

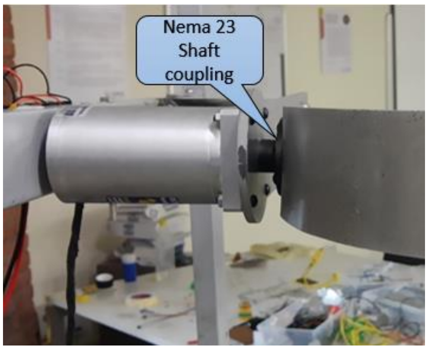

(a) (b)

Figure 5.12 (a) SolidWorks part design of Nema 23 coupling, (b) Nema 23 coupling on the exoskeleton.

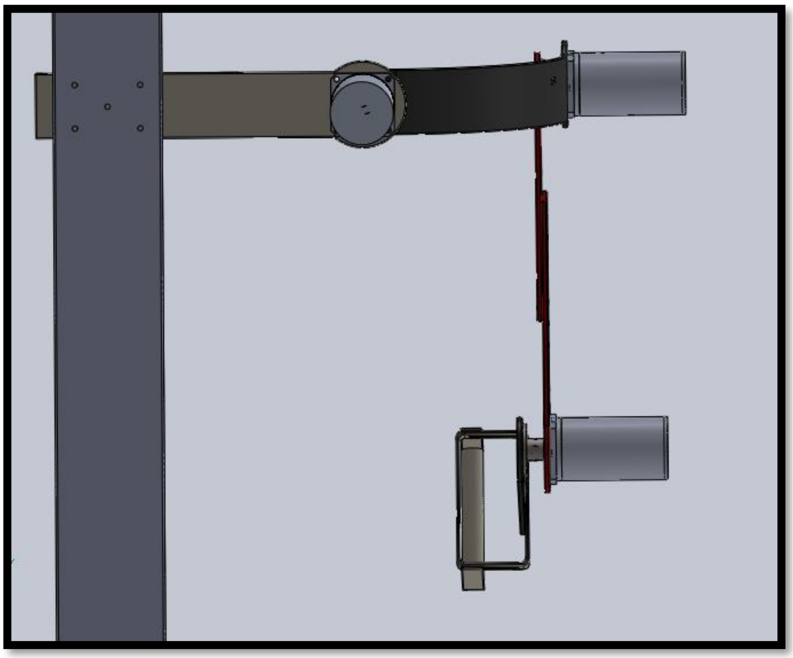

(a)

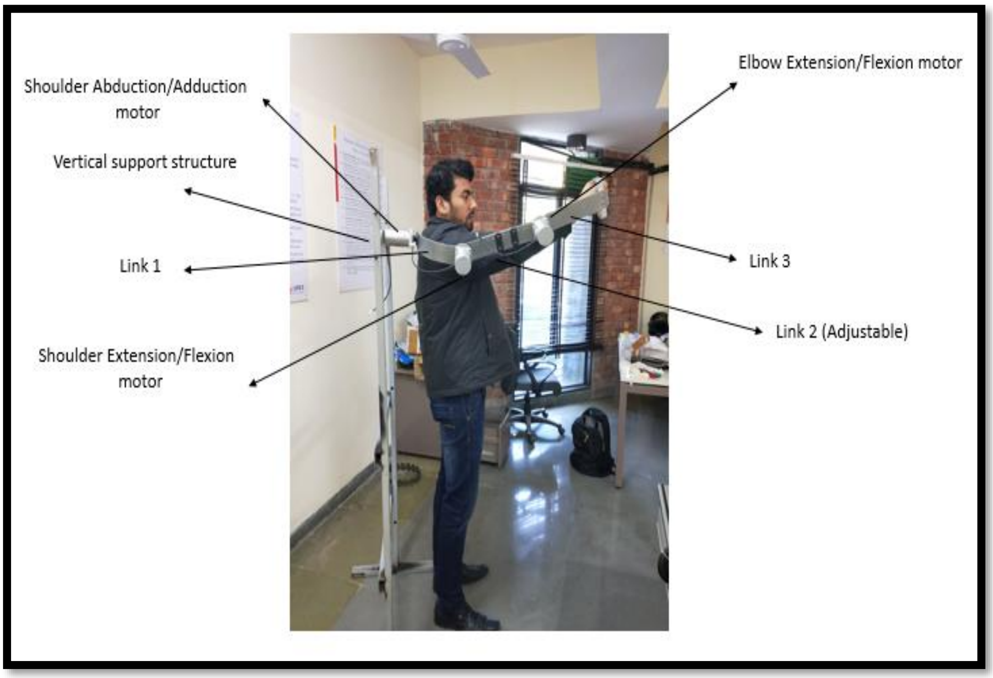

(b)

Figure 5.13 3-DOF Exoskeleton system (a) CAD model (b) Prototype

5.2 STATIC LOAD ANALYSIS

The static load analysis of the proposed system has been carried out to validate the system load-carrying capability at the proposed payload of the human arm. Results of Joint displacement, von misses stress, and static strain simulation for every exoskeleton linkage is shown.

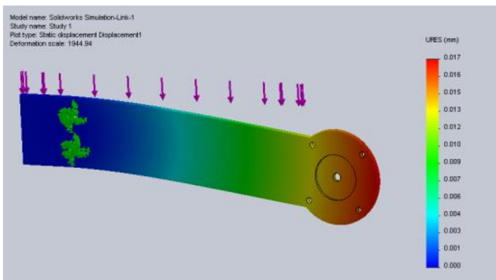

(a)

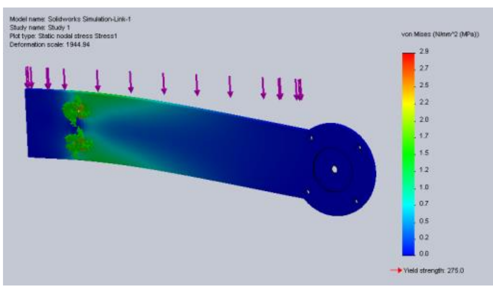

(b)

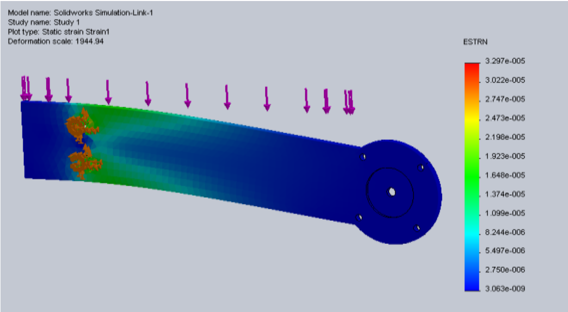

(c)

Figure 5.14. (a) Joint displacement, (b) von misses stress, and (c) static strain simulation for Link 1

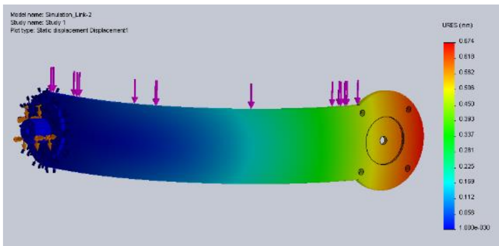

(a)

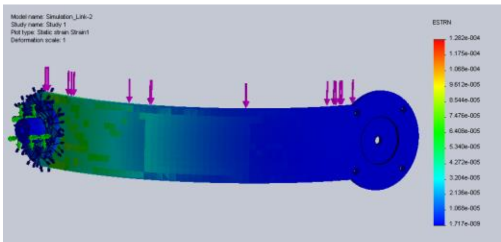

(b)

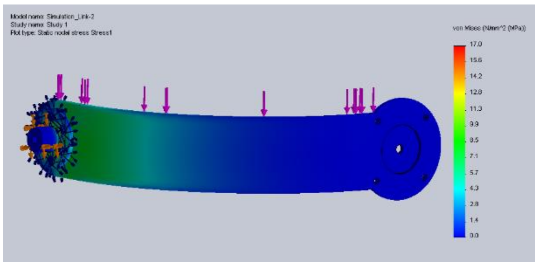

(c)

Figure 5.15. (a) Joint displacement, (b) von misses stress and, (c) static strain simulation for Link 2

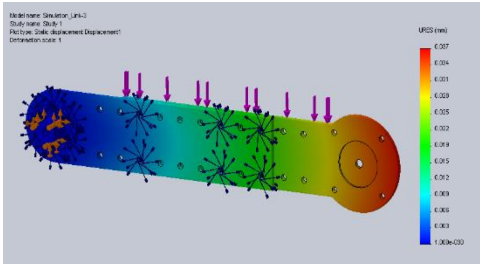

(a)

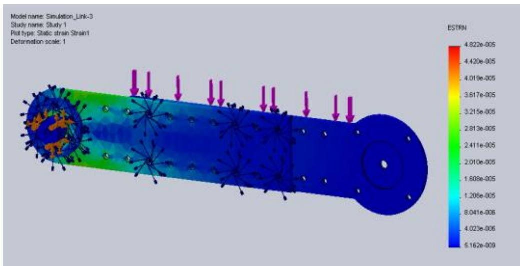

(b)

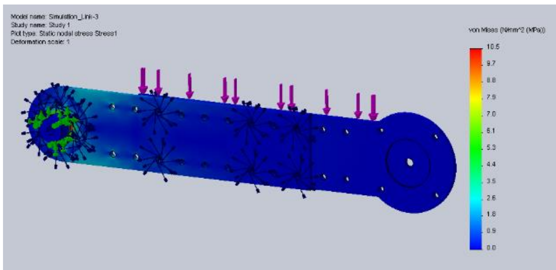

(c)

Figure 5.16. (a) Joint displacement, (b) von misses stress and, (c) static strain simulation for Link 3

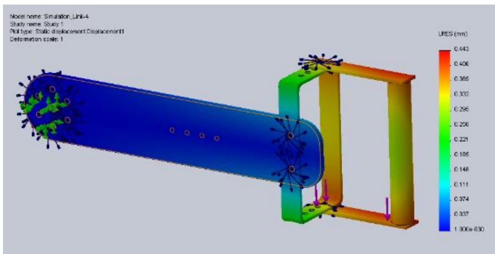

(a)

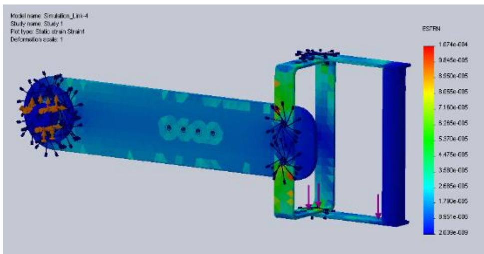

(b)

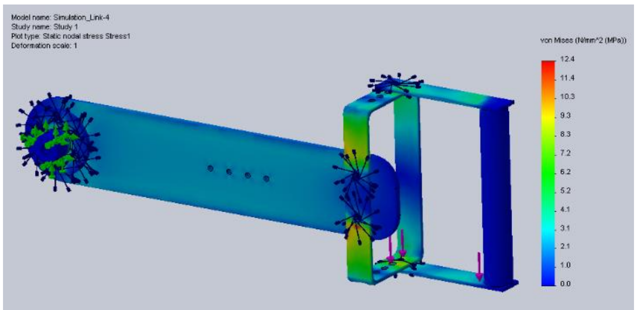

(c)

Figure 5.17. (a) Joint displacement, (b) von misses stress and, (c) static strain simulation for Link 4

5.3 SUMMARY

In the chapter development of the exoskeleton prototype is discussed. The developed exoskeleton is highly economical and light. The robotic structure makes use of Al6061-T6 which offers high stiffness and loading characteristics. The sEMG sensors provide muscle potential to the control that compares the potential with the predefined threshold thus actuates the servo motor of the associated part. The drawback of the sEMG sensors is that the threshold of the sEMG sensor varies highly between individuals and their placement. The future simulations on the system will be carried using EEG sensors. This chapter also contributes to the static load analysis of the design for the proposed payload which is the human arm's weight taken as distributed load. Though the device is proposed for rehabilitation, it can also be used as an assistive exoskeleton in the future.

CHAPTER 6 CONCLUSION AND FUTURE WORK

6.1 CONCLUSION

The chapter includes a brief discussion together with the conclusion of the thesis and the future directions of this study. The thesis addressed the issues related to the developments and clinical evaluations of robotic exoskeletons for human upper-limb rehabilitation. The major contributions of the thesis are:

- The exoskeleton system modeling that includes kinematic and dynamic analysis with CTC control simulations. The results of the simulation have been included in the thesis.
- The prototype of a 3DOF exoskeleton robot as per the proposed design.
- The designed 3-DOF upper-limb exoskeleton is a step towards making a low-cost exoskeleton device that can perform simple movements to help individuals in activities of daily living.

The thesis consists of six chapters: Introduction, Literature Survey, Mathematical Modelling of the Exoskeleton, Control Architecture, Development of Exoskeleton Prototype, and Conclusion and Future Work. The conclusion of the entire study at large is explained below.

The impediments in the path of Robotic rehabilitation devices (RRD) include cost constraints, safety issues, equipment size, and complexity. If the exoskeleton is meant to support multiple joints in the human body, it is obvious that the number of actuators, increasing the weight of the device. In order to overcome the fatigue related to physiotherapy lessons at the clinic, the exoskeleton device must provide better pHRI along with improved repetitions of activities of daily living (ADL).

Movement related disability has been a prominent issue worldwide. In India, 20% of the disabled population has some kind of movement-related disability. The results of various clinical tests as shown in Table 3 strongly suggest that the use of Robot-assisted training (RT) can be integrated into clinical practice. Whereas, in order to further solidify this claim, there is a strong need to design new tests apart from FMA, FIM, and point to point movements. Moreover, adaptive and neural-network control algorithms have found greater application in the field of robotic exoskeletons. The scientific community must also work to reduce the overall cost of procurement of exoskeletons by individuals. This is a particularly dire limitation as 85% of all stroke deaths occur in low and middle-income countries. A significant reduction in initial cost can motivate more people to adopt these robotic devices. It has also been observed that the outcomes of robotic rehabilitation therapy present better results in improving motor functions in patients and the effects of single joint robotic training and multi-joint robotic training are the same.

The burden of stroke is set to increase over the next decades in low and middle-income countries, most of which are located in the Indian subcontinent and Africa. Therefore, measures to prevent strokes must also run in parallel to efforts to decrease disability from stroke. Being a multidisciplinary project, the advancements in this area are pushing the boundaries of technological limitations. Robot-assisted therapy has matured enough and represents an embodiment of a paradigm shift in neuro-rehabilitation following a stroke.

6.2 FUTURE WORK

Future research on exoskeletons must focus on the use of exoskeletons for personal use. Moreover, future research should also focus on improving the overall health of individuals suffering from neurological disorders. Mobility and power consumption has had been a prominent issue in assistive and rehabilitation devices. Research in the area of passive exoskeleton devices could cater to the problem of power consumption in mobile devices. Apart from EMG based feedback, brain-machine interface through brain signals (EEG) are being used to control the movements. Electrooculogram (EOG) presents a wide scope for research. Being quite new technology it is used for generating feedback signals for the controller. EMG-based control is quite difficult as the proper acquisition of signals from the desired muscle is not possible due to muscle redundancy as there are other secondary muscles also involved in the same motion.

Dual-arm exoskeletons, hybrid exoskeletons, skill transfer, and human-in-loop are hot issues in exoskeleton technology and must be explored. The requirements for miniaturization and fast prototyping techniques in the field of medical robotics will surely benefit the advancement in assistive technologies. These devices have the potential to be successfully used at home. However, it is important that the user and scientific community set realistic expectations as the potential and capabilities of exoskeleton devices greatly vary between individuals and subject to current technological limitations. Further research is required in the field of rehabilitation robotics to replicate the natural movements of the patients and improve the safety, mobility, and reliability of these systems.

The developed exoskeleton device needs further improvements in the future with rigorous testing and clinical trials to evolve into a better device. The future work on the developed exoskeleton is ongoing and includes the addition of one more degree of freedom at the elbow joint for the internal and external rotation of the human arm, the introduction of planetary geared motors, switch type safety stoppers, stability analysis of the system.

REFERENCES

[1] P. Maciejasz, J. Eschweiler, K. Gerlach-Hahn, A. Jansen-Troy, and S. Leonhardt, “A survey on robotic devices for upper limb rehabilitation,” *J. Neuroeng. Rehabil.*, vol. 11, no. 1, pp. 1–29, 2014.

[2] R. A. R. C. Gopura, D. S. V Bandara, K. Kiguchi, and G. K. I. Man, “Developments in hardware systems of active upper-limb exoskeleton robots: A review,” *Rob. Auton. Syst.*, 2015.

[3] F. Molteni, G. Gasperini, G. Cannaviello, and E. Guanziroli, “Exoskeleton and End-Effector Robots for Upper and Lower Limbs Rehabilitation: Narrative Review,” *PM and R*, vol. 10, no. 9. pp. S174–S188, 2018.

[4] G. Grimaldi and M. Manto, “Functional impacts of exoskeleton-based rehabilitation in chronic stroke : multi-joint versus single-joint robotic training,” pp. 2–4, 2013.

[5] “Upper Limb Neurological Examination,” *Medistudents*, 2017. [Online]. Available: https://www.medistudents.com/en/learning/osce-skills/neurology/upper-limb-neurological-examination/.

[6] S. K. Manna and S. Bhaumik, “A Bioinspired 10 DOF Wearable Powered Arm Exoskeleton for Rehabilitation,” *J. Robot.*, vol. 2013, 2013.

[7] K. Lo, M. Stephenson, and C. Lockwood, “Mobility and Functional Ability in Adult Stroke Patients : a Systematic Review Protocol,” pp. 39–

48, 2017.

[8] C. Duret, A. Grosmaire, and H. I. Krebs, “Robot-Assisted Therapy in Upper Extremity Hemiparesis : Overview of an Evidence-Based Approach,” vol. 10, no. April, pp. 1–8, 2019.

[9] D. P. Losey, C. G. McDonald, E. Battaglia, and M. K. O’Malley, “A Review of Intent Detection, Arbitration, and Communication Aspects of Shared Control for Physical Human–Robot Interaction,” *Appl. Mech. Rev.*, vol. 70, no. 1, p. 10804, 2018.

[10] F. I. Birouaş, “Development and testing of a mixed feedback control system for robotic hand exoskeleton,” pp. 17–20, 2019.

[11] E. Pirondini *et al.*, “Evaluation of the effects of the Arm Light Exoskeleton on movement execution and muscle activities: A pilot study on healthy subjects,” *J. Neuroeng. Rehabil.*, vol. 13, no. 1, pp. 1–21, 2016.

[12] D. Kyle, “Clinical Evaluation of an Upper Limb Exoskeleton for Rehabilitation After Incomplete Spinal Cord Injury,” Rice University, 2015.

[13] R. Bertani, C. Melegari, M. C. De Cola, A. Bramanti, P. Bramanti, and R. S. Calabrò, “Effects of robot-assisted upper limb rehabilitation in stroke patients: a systematic review with meta-analysis,” *Neurol. Sci.*, vol. 38, no. 9, pp. 1561–1569, 2017.

[14] H. Singh *et al.*, “Robot-assisted upper extremity rehabilitation for

cervical spinal cord injuries: a systematic scoping review," *Disabil. Rehabil. Assist. Technol.*, vol. 13, no. 7, pp. 704–715, 2018.

[15] F. Xiao, Y. Gao, Y. Wang, Y. Zhu, and J. Zhao, "Design and evaluation of a 7-DOF cable-driven upper limb exoskeleton," *J. Mech. Sci. Technol.*, vol. 32, no. 2, pp. 855–864, 2018.

[16] J. Huang, X. Tu, and J. He, "Design and Evaluation of the RUPERT Wearable Upper Extremity Exoskeleton Robot for Clinical and In-Home Therapies," *IEEE Trans. Syst. Man, Cybern. Syst.*, vol. 46, no. 7, pp. 926–935, 2016.

[17] Q. Wu, X. Wang, B. Chen, and H. Wu, "Patient-active control of a powered exoskeleton targeting upper limb rehabilitation training," *Front. Neurol.*, vol. 9, no. OCT, 2018.

[18] A. Frisoli *et al.*, "Training and assessment of upper limb motor function with a robotic exoskeleton after stroke," *Proc. IEEE RAS EMBS Int. Conf. Biomed. Robot. Biomechatronics*, pp. 1782–1787, 2012.

[19] O. Péter, G. Fazekas, K. Zsiga, and Z. Dénes, "Robot-mediated upper limb physiotherapy: Review and recommendations for future clinical trials," *Int. J. Rehabil. Res.*, vol. 34, no. 3, pp. 196–202, 2011.

[20] M. J., P. T., K. J., and P. M., "Electromechanical and robot-assisted arm training for improving activities of daily living, arm function, and arm muscle strength after stroke," *Cochrane Database of Systematic Reviews*, no. 4. 2008.

[21] B. Sheng, Y. Zhang, W. Meng, C. Deng, and S. Xie, “Bilateral robots for upper-limb stroke rehabilitation: State of the art and future prospects,” *Med. Eng. Phys.*, vol. 38, no. 7, pp. 587–606, 2016.

[22] J. M. Veerbeek, A. C. Langbroek-Amersfoort, E. E. H. Van Wegen, C. G. M. Meskers, and G. Kwakkel, “Effects of Robot-Assisted Therapy for the Upper Limb after Stroke,” *Neurorehabil. Neural Repair*, vol. 31, no. 2, pp. 107–121, 2017.

[23] C. Zhang, C. W. P. Li-Tsang, and R. K. C. Au, “Robotic approaches for the rehabilitation of upper limb recovery after stroke: A systematic review and meta-analysis,” *Int. J. Rehabil. Res.*, vol. 40, no. 1, pp. 19–28, 2017.

[24] M. Xiloyannis, D. Chiaradia, A. Frisoli, and L. Masia, “Physiological and kinematic effects of a soft exosuit on arm movements,” pp. 1–15, 2019.

[25] E. Y. Y. Cheung, T. K. W. Ng, K. K. K. Yu, R. Lc, and G. L. Y. Cheing, “Robot-assisted training for people with spinal cord injury: A meta-analysis,” *Arch. Phys. Med. Rehabil.*, vol. 98, no. 11, pp. 2320–2331.e12, 2017.

[26] Q. Wei, Z. Li, K. Zhao, Y. Kang, and C. Y. Su, “Synergy-based Control of Assistive Lower-Limb Exoskeletons by Skill Transfer,” *IEEE/ASME Trans. Mechatronics*, vol. 4435, no. c, 2019.

[27] D. Wei *et al.*, “Human-in-the-Loop Control Strategy of Unilateral Exoskeleton Robots for Gait Rehabilitation,” *IEEE Trans. Cogn. Dev.*

Syst., vol. 8920, no. c, 2019.

[28] "A Bioinspired 10 DOF Wearable Powered Arm Exoskeleton for Rehabilitation," *J. Robot.*, vol. 2013, no. December, 2013.

[29] L. Zhou, Y. Li, and S. Bai, "A human-centered design optimization approach for robotic exoskeletons through biomechanical simulation," *Rob. Auton. Syst.*, vol. 91, pp. 337–347, 2017.

[30] Y. Mao and S. K. Agrawal, "Design of a cable-driven arm exoskeleton (CAREX) for neural rehabilitation," *IEEE Trans. Robot.*, vol. 28, no. 4, pp. 922–931, 2012.

[31] Z. Li, C. Su, G. Li, and H. Su, "Fuzzy Approximation-Based Adaptive Backstepping Control of an Exoskeleton for Human Upper Limbs," *IEEE Trans. Fuzzy Syst.*, vol. 23, no. 3, pp. 555–566, Jun. 2015.

[32] Z. Li, S. Xiao, S. S. Ge, and H. Su, "Constrained Multilegged Robot System Modeling and Fuzzy Control With Uncertain Kinematics and Dynamics Incorporating Foot Force Optimization," *IEEE Trans. Syst. Man, Cybern. Syst.*, vol. 46, no. 1, pp. 1–15, Jan. 2016.

[33] E. C. Lu *et al.*, "Development of a robotic device for upper limb stroke rehabilitation: A user-centered design approach," *Paladyn, J. Behav. Robot.*, vol. 2, no. 4, pp. 176–184, 2011.

[34] R. P. Matthew, E. J. Mica, W. Meinhold, J. A. Loeza, M. Tomizuka, and R. Bajcsy, "Introduction and initial exploration of an Active/Passive Exoskeleton framework for portable assistance," *IEEE Int. Conf. Intell.*

Robot. Syst., vol. 2015-Decem, pp. 5351–5356, 2015.

[35] E. Biddiss and T. Chau, “Dielectric elastomers as actuators for upper limb prosthetics: Challenges and opportunities,” *Med. Eng. Phys.*, vol. 30, no. 4, pp. 403–418, 2008.

[36] V. L. Feigin *et al.*, “Global burden of stroke and risk factors in 188 countries, during 1990–2013: a systematic analysis for the Global Burden of Disease Study 2013,” *Lancet Neurol.*, vol. 15, no. 9, pp. 913–924, 2016.

[37] “About Stroke,” 2019. [Online]. Available: https://www.stroke.org/en/about-stroke. [Accessed: 27-Nov-2019].

[38] R. Gassert and V. Dietz, “Rehabilitation robots for the treatment of sensorimotor deficits: A neurophysiological perspective,” *J. Neuroeng. Rehabil.*, vol. 15, no. 1, pp. 1–15, 2018.

[39] A. C. Lo *et al.*, “Robot-Assisted Therapy for Long-Term Upper-Limb Impairment after Stroke,” *N. Engl. J. Med.*, vol. 362, no. 19, pp. 1772–1783, 2010.

[40] R. Riener, L. Lünenburger, and G. Colombo, “Human-centered robotics applied to gait training and assessment.,” *J. Rehabil. Res. Dev.*, vol. 43, no. 5, pp. 679–693, 2006.

[41] V. Dietz and K. Fouad, “Restoration of sensorimotor functions after spinal cord injury,” *Brain*, vol. 137, no. 3, pp. 654–667, 2013.

[42] L. Marchal-Crespo, S. McHughen, S. C. Cramer, and D. J. Reinkensmeyer, “The effect of haptic guidance, aging, and initial skill level on motor learning of a steering task,” *Exp. Brain Res.*, vol. 201, no. 2, pp. 209–220, Mar. 2010.

[43] J.-C. Metzger *et al.*, “Assessment-driven selection and adaptation of exercise difficulty in robot-assisted therapy: a pilot study with a hand rehabilitation robot,” *J. Neuroeng. Rehabil.*, vol. 11, no. 1, p. 154, 2014.

[44] L. Zimmerli, C. Krewer, R. Gassert, F. Müller, R. Riener, and L. Lünenburger, “Validation of a mechanism to balance exercise difficulty in robot-assisted upper-extremity rehabilitation after stroke,” *J. Neuroeng. Rehabil.*, vol. 9, no. 1, p. 6, 2012.

[45] G. Saposnik, M. Levin, and null null, “Virtual reality in stroke rehabilitation: a meta-analysis and implications for clinicians,” *Stroke*, vol. 42, no. 5, pp. 1380–1386, 2011.

[46] K. Kiguchi, M. H. Rahman, M. Sasaki, and K. Teramoto, “Development of a 3DOF mobile exoskeleton robot for human upper-limb motion assist,” *Rob. Auton. Syst.*, vol. 56, no. 8, pp. 678–691, 2008.

[47] S. K. Jain, “A study of 200 cases of congenital limb deficiencies,” *Prosthet. Orthot. Int.*, vol. 18, no. 3, pp. 174–179, 1994.

[48] T. R. Scotland and H. R. Galway, “A long-term review of children with congenital and acquired upper limb deficiency,” *J. bone Jt. Surg.*, vol. 65-B, no. No. 3, pp. 346–349, 1993.

[49] P. M. Dalal, “Strokes in young in India,” *J. Int. Med. Sci. Acad.*, vol. 17, no. 2, pp. 79–83, 2004.

[50] C. Warlow, C. Sudlow, M. Dennis, J. Wardlaw, and P. Sandercock, “Stroke,” *Lancet*, vol. 362, no. 9391, pp. 1211–1224, 2003.

[51] National Sample Survey Office, “Disabled persons in India: A statistical profile,” pp. 0–107, 2016.

[52] World Health Organization, “The Global Burden of Disease: 2004 update,” *2004 Updat.*, p. 146, 2008.

[53] V. L. Feigin, C. M. M. Lawes, D. A. Bennett, and C. S. Anderson, “Stroke epidemiology: A review of population-based studies of incidence, prevalence, and case-fatality in the late 20th century,” *Lancet Neurol.*, vol. 2, no. 1, pp. 43–53, 2003.

[54] “Cerebral palsy,” 2016. [Online]. Available: https://www.mayoclinic.org/diseases-conditions/cerebral-palsy/symptoms-causes/syc-20353999.

[55] D. A. Elkouzi, “Understanding Parkinson’s.” [Online]. Available: http://www.parkinson.org/understanding-parkinsons/what-is-parkinsons.

[56] C. Bélaise, F. D. Maso, B. Michaud, K. Mombaur, and M. Begon, “An EMG-marker tracking optimisation method for estimating muscle forces,” *Multibody Syst Dyn*, 2017.

[57] Y. Ganesan, S. Gobee, and V. Durairajah, “Development of an Upper Limb Exoskeleton for Rehabilitation with Feedback from EMG and IMU Sensor,” *Procedia Comput. Sci.*, vol. 76, no. Iris, pp. 53–59, 2015.

[58] K. Kiguchi and Y. Hayashi, “An EMG-based control for an upper-limb power-assist exoskeleton robot,” *IEEE Trans. Syst. Man, Cybern. Part B Cybern.*, vol. 42, no. 4, pp. 1064–1071, 2012.

[59] R. A. R. C. Gopura, K. Kiguchi, and Y. Yi, “SUEFUL-7: A 7DOF upper-limb exoskeleton robot with muscle-model-oriented EMG-based control,” *2009 IEEE/RSJ Int. Conf. Intell. Robot. Syst. IROS 2009*, pp. 1126–1131, 2009.

[60] A. Dwivedi, Y. Kwon, A. J. Mcdaid, and M. Liarokapis, “A Learning Scheme for EMG Based Decoding of Dexterous , In-Hand Manipulation Motions,” no. August, 2019.

[61] A. Gupta, A. Mondal, and M. Gupta, “Kinematic, Dynamic Analysis and Control of 3 DOF Upper-limb Robotic Exoskeleton,” *J. Eur. des Systèmes Autom.*, vol. 52, no. 3, pp. 297–304, Aug. 2019.

[62] V. Verma, V. Chowdary, M. K. Gupta, and A. K. Mondal, “IoT and Robotics in Healthcare,” in *Medical Big Data and Internet of Medical Things*, CRC Press, 2018, pp. 245–269.

[63] M. Kalyoncu, “Design and Actuator Selection of a Lower Extremity Exoskeleton,” vol. 19, no. 2, pp. 623–632, 2014.

[64] M. D. S. D. Chandrasiri, R. K. P. S. Ranaweera, and R. A. R. C. Gopura,

"Development of a Surface Muscle Pressure Monitoring System for Wearable Robotic Devices," *2019 Moratuwa Eng. Res. Conf.*, pp. 544–549, 2019.

[65] J. M. P. Gunasekara, R. A. R. C. Gopura, T. S. S. Jayawardane, and S. W. H. M. T. D. Lalitharathne, "Control methodologies for upper limb exoskeleton robots," in *2012 IEEESICE International Symposium on System Integration (SII)*, 2012, pp. 19–24.

[66] X. Wu and Z. Li, "Cooperative Manipulation of Wearable Dual-Arm Exoskeletons Using Force Communication Between Partners," *IEEE Trans. Ind. Electron.*, vol. 0046, no. c, pp. 1–1, 2019.

[67] X. Wu, Z. Li, Z. Kan, and H. Gao, "Reference Trajectory Reshaping Optimization and Control of Robotic Exoskeletons for Human-Robot Co-Manipulation," *IEEE Trans. Cybern.*, pp. 1–12, 2019.

[68] M. Z. Jamal, "Signal Acquisition Using Surface EMG and Circuit Design Considerations for Robotic Prosthesis," in *Computational Intelligence in Electromyography Analysis*, G. R. Naik, Ed. Rijeka: IntechOpen, 2012.

[69] M. S. Al-Quraishi, I. Elamvazuthi, S. A. Daud, S. Parasuraman, and A. Borboni, "Eeg-based control for upper and lower limb exoskeletons and prostheses: A systematic review," *Sensors (Switzerland)*, vol. 18, no. 10, pp. 1–27, 2018.

[70] J. Narayan, A. Kalani, and S. K. Dwivedy, "Reference Trajectory based Jacobian Transpose Control of a Novel Lower Limb Exoskeleton System for Children," pp. 102–107, 2019.

[71] C. Yue, X. Lin, X. Zhang, J. Qiu, and H. Cheng, “Design and performance evaluation of a wearable sensing system for lower-limb exoskeleton,” *Appl. Bionics Biomech.*, vol. 2018, 2018.

[72] Y. Long, Z. J. Du, W. Wang, and W. Dong, “Development of a wearable exoskeleton rehabilitation system based on hybrid control mode,” *Int. J. Adv. Robot. Syst.*, vol. 13, no. 5, pp. 1–10, 2016.

[73] Z. Li *et al.*, “Hybrid Brain/Muscle Signals Powered Wearable Walking Exoskeleton Enhancing Motor Ability in Climbing Stairs Activity,” *IEEE Trans. Med. Robot. Bionics*, vol. 1, no. 4, pp. 218–227, 2019.

[74] K. Anam and A. A. Al-Jumaily, “Active exoskeleton control systems: State of the art,” *Procedia Eng.*, vol. 41, no. Iris, pp. 988–994, 2012.

[75] W. He, Z. Li, Y. Dong, and T. Zhao, “Design and Adaptive Control for an Upper Limb Robotic Exoskeleton in Presence of Input Saturation,” *IEEE Trans. Neural Networks Learn. Syst.*, vol. 30, no. 1, pp. 97–108, 2019.

[76] S. Bembli, N. K. Haddad, and S. Belghith, “Robustness Analysis of an Upper Limb Exoskeleton Controlled by Sliding Mode Algorithm,” *Mech. Mach. Sci.*, vol. 58, pp. 99–112, 2019.

[77] H. B. Kang and J. H. Wang, “Adaptive control of 5 DOF upper-limb exoskeleton robot with improved safety,” *ISA Trans.*, vol. 52, no. 6, pp. 844–852, 2013.

[78] Y. Long, Z. Du, L. Cong, W. Wang, Z. Zhang, and W. Dong, “Active

disturbance rejection control based human gait tracking for lower extremity rehabilitation exoskeleton," *ISA Trans.*, vol. 67, pp. 389–397, 2017.

[79] U. Jeong, H. K. In, and K. J. Cho, "Implementation of various control algorithms for hand rehabilitation exercise using wearable robotic hand," *Intell. Serv. Robot.*, vol. 6, no. 4, pp. 181–189, 2013.

[80] Z. Li, J. Li, S. Zhao, Y. Yuan, Y. Kang, and C. L. P. Chen, "Adaptive Neural Control of a Kinematically Redundant Exoskeleton Robot Using Brain-Machine Interfaces," *IEEE Trans. Neural Networks Learn. Syst.*, vol. 30, no. 12, pp. 3558–3571, 2019.

[81] W. Xu, B. Chu, and E. Rogers, "Iterative learning control for robotic-assisted upper limb stroke rehabilitation in the presence of muscle fatigue," *Control Eng. Pract.*, vol. 31, pp. 63–72, 2014.

[82] A. M. Stewart, C. G. Pretty, M. Adams, and X. Chen, "Review of Upper Limb Hybrid Exoskeletons," *IFAC-PapersOnLine*, vol. 50, no. 1, pp. 15169–15178, 2017.

[83] S. Balasubramanian, J. Ward, T. Sugar, and J. He, "Characterization of the Dynamic Properties of Pneumatic Muscle Actuators," *IEEE 10th Int. Conf. Rehabil. Robot.*, vol. 00, no. c, pp. 764–770, 2007.

[84] D. G. Caldwell, A. Razak, and M. Goodwin, "Braided Pneumatic Muscle Actuators," *IFAC Proc. Vol.*, vol. 26, no. 1, pp. 522–527, 1993.

[85] B. van Ninhuijs, L. A. van der Heide, J. W. Jansen, B. L. J. Gysen, D. J.

van der Pijl, and E. A. Lomonova, “Overview of Actuated Arm Support Systems and Their Applications,” *Actuators*, vol. 2, no. 4, pp. 86–110, 2013.

[86] H. Herr, “Exoskeletons and orthoses: classification, design challenges and future directions,” *J. Neuroeng. Rehabil.*, vol. 6, no. 1, p. 21, Jun. 2009.

[87] A. S. Camp, E. M. Chapman, and P. J. Cienfuegos, “Modeling and analysis of hydraulic piston actuation of McKibben fluidic artificial muscles for hand rehabilitation,” 2019.

[88] M. G. B. Atia, O. Salah, B. Medhat, and K. Ibrahim, “Design and analysis of low cost upper limb exoskeleton,” in *2017 12th International Conference on Computer Engineering and Systems (ICCES)*, 2017, pp. 80–84.

[89] “Cyberdyne HAL.” [Online]. Available: https://www.cyberdyne.jp.

[90] Z. Li, B. Huang, A. Ajoudani, C. Yang, C. Y. Su, and A. Bicchi, “Asymmetric Bimanual Control of Dual-Arm Exoskeletons for Human-Cooperative Manipulations,” *IEEE Trans. Robot.*, vol. 34, no. 1, pp. 264–271, 2018.

[91] J. Murtagh, “ReWalk: Robotic Exoskeletons for Spinal Cord Injury,” *CADTH issues Emerg. Heal. Technol.*, no. 141, 2015.

[92] R. Bogue, “Exoskeletons and robotic prosthetics: a review of recent developments,” *Ind. Robot An Int. J.*, vol. 36, no. 5, pp. 421–427, 2009.

[93] "ReWalk Personal 6.0," 2018. [Online]. Available: http://rewalk.com/.

[94] M. Gunasekara, R. Gopura, and S. Jayawardena, "6-REXOS: Upper limb exoskeleton robot with improved pHRI," *Int. J. Adv. Robot. Syst.*, vol. 12, 2015.

[95] J. A. Martinez, P. Ng, S. Lu, M. S. Campagna, and O. Celik, "Design of Wrist Gimbal: A forearm and wrist exoskeleton for stroke rehabilitation," *IEEE Int. Conf. Rehabil. Robot.*, 2013.

[96] S. J. Ball, I. E. Brown, and S. H. Scott, "MEDARM: A rehabilitation robot with 5DOF at the shoulder complex," *IEEE/ASME Int. Conf. Adv. Intell. Mechatronics, AIM*, 2007.

[97] T. Nef, M. Mihelj, G. Colombo, and R. Riener, "ARMin-robot for rehabilitation of the upper extremities," no. May, pp. 3152–3157, 2006.

[98] K. Kiguchi and Y. Hayashi, "An EMG-based control for an upper-limb power-assist exoskeleton robot," *IEEE Trans. Syst. Man, Cybern. Part B Cybern.*, vol. 42, no. 4, pp. 1064–1071, 2012.

[99] H. S. Lo and S. S. Q. Xie, "An upper limb exoskeleton with an optimized 4R spherical wrist mechanism for the shoulder joint," *IEEE/ASME Int. Conf. Adv. Intell. Mechatronics, AIM*, pp. 269–274, 2014.

[100] B. Beigzadeh, M. Ilami, and S. Najafian, "Design and development of one degree of freedom upper limb exoskeleton," *Int. Conf. Robot. Mechatronics, ICROM 2015*, pp. 223–228, 2015.

[101] M. Mahdavian, A. G. Toudeshki, and A. Yousefi-Koma, “Design and fabrication of a 3DoF upper limb exoskeleton,” *Int. Conf. Robot. Mechatronics, ICROM 2015*, pp. 342–346, 2015.

[102] M. B. Hong, S. J. Kim, and K. Kim, “Development of a 10-DOF robotic system for upper-limb power assistance,” *2012 9th Int. Conf. Ubiquitous Robot. Ambient Intell. URAI 2012*, no. Urai, pp. 61–62, 2012.

[103] R. A. R. C. Gopura and K. Kiguchi, “Development of an exoskeleton robot for human wrist and forearm motion assist,” *ICIIS 2007 - 2nd Int. Conf. Ind. Inf. Syst. 2007, Conf. Proc.*, no. August, pp. 535–540, 2007.

[104] T. Noda, T. Teramae, B. Ugurlu, and J. Morimoto, “Development of an upper limb exoskeleton powered via pneumatic electric hybrid actuators with bowden cable,” *IEEE Int. Conf. Intell. Robot. Syst.*, no. Iros, pp. 3573–3578, 2014.

[105] H. S. Lo and S. Q. Xie, “Exoskeleton robots for upper-limb rehabilitation: State of the art and future prospects,” *Med. Eng. Phys.*, vol. 34, no. 3, pp. 261–268, 2012.

[106] J. Lu, W. Chen, and M. Tomizuka, *Kinematic design and analysis of a 6-DOF upper limb exoskeleton model for a brain-machine interface study*, vol. 46, no. 5. IFAC, 2013.

[107] Y. Hasegawa, T. Kikai, K. Eguchi, and S. Shimada, “Exoskeletal meal assistance system (EMAS III) for progressive muscle dystrophy patient,” *IEEE/ASME Int. Conf. Adv. Intell. Mechatronics, AIM*, no. Emas Ii, pp. 279–284, 2014.

[108] A. Gupta and M. K. O'Malley, "Design of a haptic arm exoskeleton for training and rehabilitation," *IEEE/ASME Trans. Mechatronics*, vol. 11, no. 3, pp. 280–289, 2006.

[109] K. Kiguchi, K. Iwami, M. Yasuda, K. Watanabe, and T. Fukuda, "An Exoskeletal Robot for Human Shoulder Joint," vol. 8, no. 1, pp. 125–135, 2003.

[110] R. A. R. C. Gopura, K. Kiguchi, and Y. Yi, "SUEFUL-7: A 7DOF upper-limb exoskeleton robot with muscle-model-oriented EMG-based control," *2009 IEEE/RSJ Int. Conf. Intell. Robot. Syst. IROS 2009*, pp. 1126–1131, 2009.

[111] A. Frisoli, F. Salsedo, M. Bergamasco, B. Rossi, and M. C. Carboncini, "A force-feedback exoskeleton for upper-limb rehabilitation in virtual reality," *Appl. Bionics Biomech.*, vol. 6, no. 2, pp. 115–126, 2009.

[112] E. Rocon, J. M. Belda-Lois, A. F. Ruiz, M. Manto, J. C. Moreno, and J. L. Pons, "Design and validation of a rehabilitation robotic exoskeleton for tremor assessment and suppression," *IEEE Trans. Neural Syst. Rehabil. Eng.*, vol. 15, no. 1, pp. 367–378, 2007.

[113] G. R. Johnson, D. A. Carus, G. Parrini, S. S. Marchese, and R. Valeggi, "The design of a five degree of freedom powered orthosis for the upper limb," vol. 215, pp. 275–284, 1989.

[114] D. Sasaki, T. Noritsugu, and M. Takaiwa, "Development of active support splint driven by pneumatic soft actuator (ASSIST)," *Proc. - IEEE Int. Conf. Robot. Autom.*, vol. 2005, no. April, pp. 520–525, 2005.

[115] J. Klein *et al.*, "Biomimetic orthosis for the neurorehabilitation of the elbow and shoulder (BONES)," *Proc. 2nd Bienn. IEEE/RAS-EMBS Int. Conf. Biomed. Robot. Biomechatronics, BioRob 2008*, pp. 535–541, 2008.

[116] T. G. Sugar *et al.*, "Design and control of RUPERT: A device for robotic upper extremity repetitive therapy," *IEEE Trans. Neural Syst. Rehabil. Eng.*, vol. 15, no. 1, pp. 336–346, 2007.

[117] M. Mistry, P. Mohajerian, and S. Schaal, "An exoskeleton robot for human arm movement study," *2005 IEEE/RSJ Int. Conf. Intell. Robot. Syst. IROS*, pp. 3114–3119, 2005.

[118] A. Schiele and G. Hirzinger, "A new generation of ergonomic exoskeletons - The high-performance X-Arm-2 for space robotics telepresence," *IEEE Int. Conf. Intell. Robot. Syst.*, pp. 2158–2165, 2011.

[119] O. Schill *et al.*, "OrthoJacket: An active FES-hybrid orthosis for the paralysed upper extremity," *Biomed. Tech.*, vol. 56, no. 1, pp. 35–44, 2011.

[120] W. Wang, L. Qin, X. Yuan, X. Ming, T. Sun, and Y. Liu, "Bionic control of exoskeleton robot based on motion intention for rehabilitation training," *Adv. Robot.*, vol. 33, no. 12, pp. 590–601, 2019.

[121] E. Biddiss and T. Chau, "Dielectric elastomers as actuators for upper limb prosthetics: Challenges and opportunities," *Med. Eng. Phys.*, vol. 30, no. 4, pp. 403–418, 2008.

[122] J. Maciejasz Pawełand Eschweiler, K. Gerlach-Hahn, A. Jansen-Troy, and S. Leonhardt, “A survey on robotic devices for upper limb rehabilitation,” *J. Neuroeng. Rehabil.*, vol. 11, no. 1, pp. 1–29, 2014.

[123] H. S. Lo and S. Q. Xie, “Exoskeleton robots for upper-limb rehabilitation: State of the art and future prospects,” *Med. Eng. Phys.*, vol. 34, no. 3, pp. 261–268, 2012.

[124] G. Aguiar Noury, H. Bradwell, S. Thill, and R. Jones, “User-defined challenges and desiderata for robotics and autonomous systems in health and social care settings,” *Adv. Robot.*, vol. 33, no. 7–8, pp. 309–324, 2019.

[125] M. Barsotti, D. Leonardis, C. Loconsole, M. Solazzi, and E. Sotgiu, “A full upper limb robotic exoskeleton for reaching and grasping rehabilitation triggered by MI-BCI,” *2015 IEEE Int. Conf. Rehabil. Robot.*, no. Mi, pp. 49–54, 2015.

[126] L. Zhang, S. Wang, and X. Miao, “Workspace Simulation and Analysis of a Dual-Arm Nursing Robot,” in *Intelligent Robotics and Applications*, 2019, pp. 26–34.

[127] D. Chakarov, I. Veneva, M. Tsveov, and T. Tiankov, “New Exoskeleton Arm Concept Design And Actuation For Haptic Interaction With Virtual Objects,” *J. Theor. Appl. Mech.*, vol. 44, no. 4, pp. 3–14, 2015.

[128] D. Bharadwaj and M. Prateek, “Kinematics and Dynamics of Lower Body of Autonomous Humanoid Biped Robot,” *Int. J. Innov. Technol. Explor. Eng.*, vol. 8, no. 4, pp. 141–146, 2019.

[129] X. Wang, Q. Song, X. Wang, and P. Liu, “Kinematics and Dynamics Analysis of a 3-DOF Upper-Limb Exoskeleton with an Internally Rotated Elbow Joint,” *Appl. Sci.*, vol. 8, no. 3, p. 464, 2018.

[130] A. Chemori, “Control of complex robotic systems: Challenges, design and experiments,” *2017 22nd Int. Conf. Methods Model. Autom. Robot. MMAR 2017*, pp. 622–631, 2017.

[131] Z. Song, J. Yi, D. Zhao, and X. Li, “A computed torque controller for uncertain robotic manipulator systems: Fuzzy approach,” *Fuzzy Sets Syst.*, vol. 154, no. 2, pp. 208–226, 2005.

[132] S. Han, H. Wang, and Y. Tian, “Adaptive computed torque control based on RBF network for a lower limb exoskeleton,” *Proc. - 2018 IEEE 15th Int. Work. Adv. Motion Control. AMC 2018*, pp. 35–40, 2018.

[133] R. K. Mittal and I. J. Nagrath, *Robotics and control*. New Delhi : Tata McGraw-Hill, 2003.

[134] ASM Aerospace Identification metals Inc, “Aluminum 6061,” *Http://Asm.Matweb.Com/*, 2019.

[135] “Understanding Extruded Aluminum Alloys -,” *Alcoa Eng. Prod.*, 2012.

APPENDIX A

Engineering drawings of the proposed model

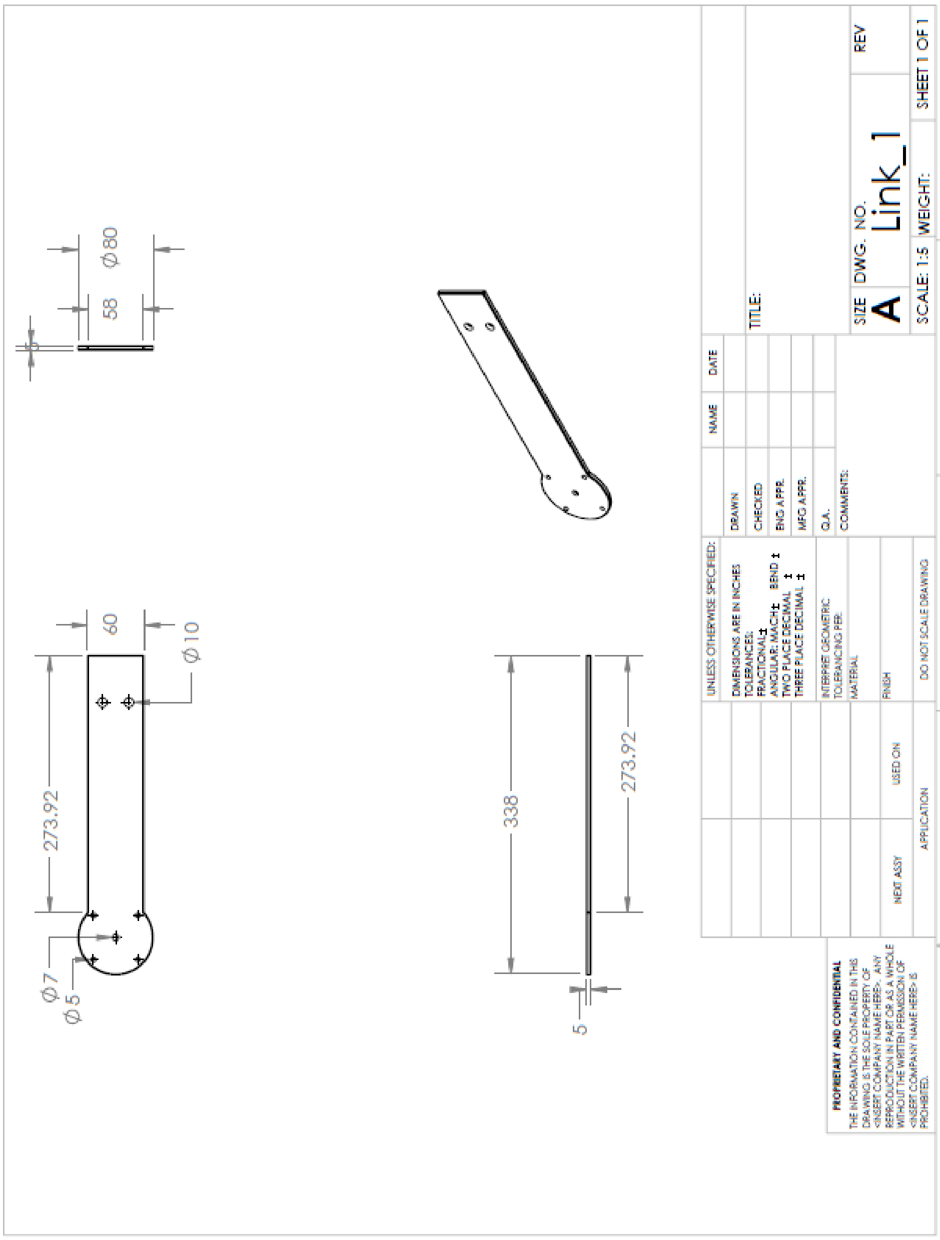

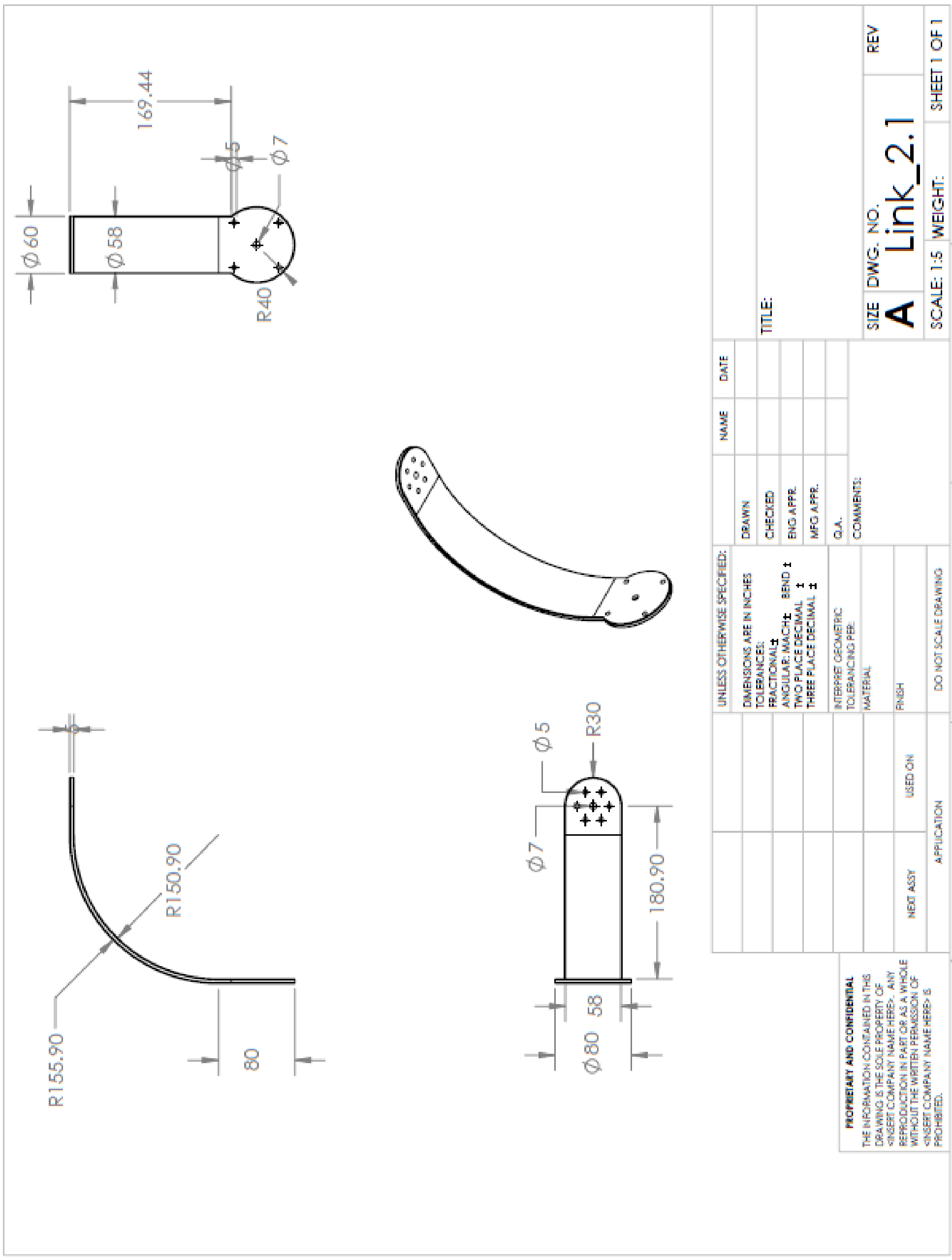
169.44
Ø60
Ø58
Ø5
Ø7
R40
R155.90
R150.90
80
Ø7
Ø5
R30
180.90
Ø80
58
UNLESS OTHERWISE SPECIFIED:
DIMENSIONS ARE IN INCHES
TOLERANCES:
FRACTIONAL±
ANGULAR: MACH± BEND ±
TWO PLACE DECIMAL ±
THREE PLACE DECIMAL ±
INTERPRET GEOMETRIC TOLERANCING PER:
MATERIAL
FINISH
DO NOT SCALE DRAWING
NAME
DATE
DRAWN
CHECKED
ENG APPR.
MFG APPR.
Q.A.
COMMENTS:
TITLE:
SIZE
A
DWG. NO.
Link_2.1
REV
SCALE: 1:5
WEIGHT:
SHEET 1 OF 1
NEXT ASSY
USED ON
APPLICATION
PROPRIETARY AND CONFIDENTIAL
THE INFORMATION CONTAINED IN THIS DRAWING IS THE SOLE PROPERTY OF <INSERT COMPANY NAME HERE>. ANY REPRODUCTION IN PART OR AS A WHOLE WITHOUT THE WRITTEN PERMISSION OF <INSERT COMPANY NAME HERE> IS PROHIBITED.
1
2
3
4
5

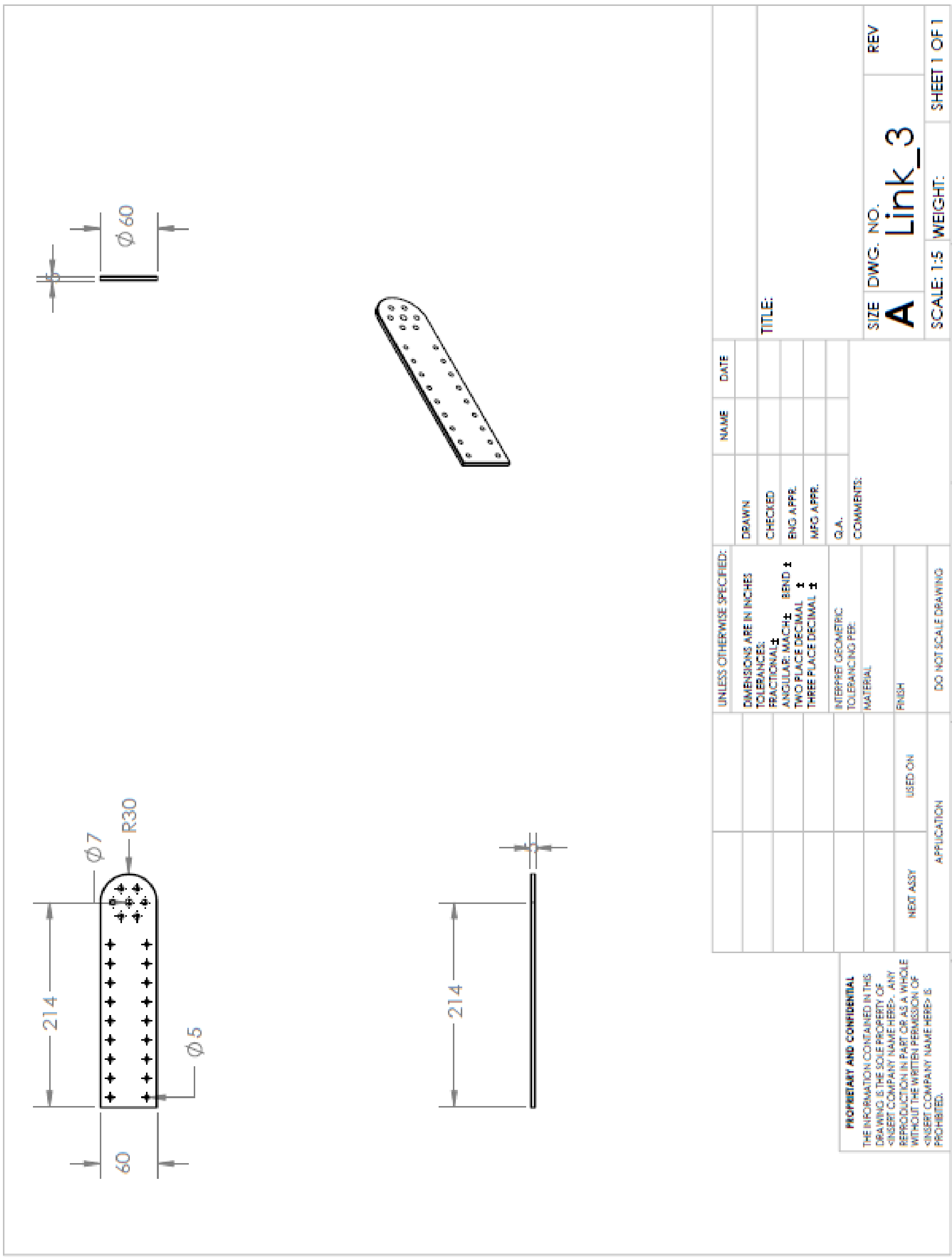
Ø60
214
Ø5
Ø7
R30
60
UNLESS OTHERWISE SPECIFIED:
DIMENSIONS ARE IN INCHES
TOLERANCES:
FRACTIONAL ±
ANGULAR: MACH ± BEND ±
TWO PLACE DECIMAL ±
THREE PLACE DECIMAL ±
INTERPRET GEOMETRIC
TOLERANCING PER:
MATERIAL
FINISH
DO NOT SCALE DRAWING
NEXT ASSY
USED ON
APPLICATION
NAME
DATE
DRAWN
CHECKED
ENG APPR.
MFG APPR.
Q.A.
COMMENTS:
TITLE:
SIZE
A
DWG. NO.
Link_3
REV
SCALE: 1:5
WEIGHT:
SHEET 1 OF 1
PROPRIETARY AND CONFIDENTIAL
THE INFORMATION CONTAINED IN THIS DRAWING IS THE SOLE PROPERTY OF <INSERT COMPANY NAME HERE>. ANY REPRODUCTION IN PART OR AS A WHOLE WITHOUT THE WRITTEN PERMISSION OF <INSERT COMPANY NAME HERE> IS PROHIBITED.

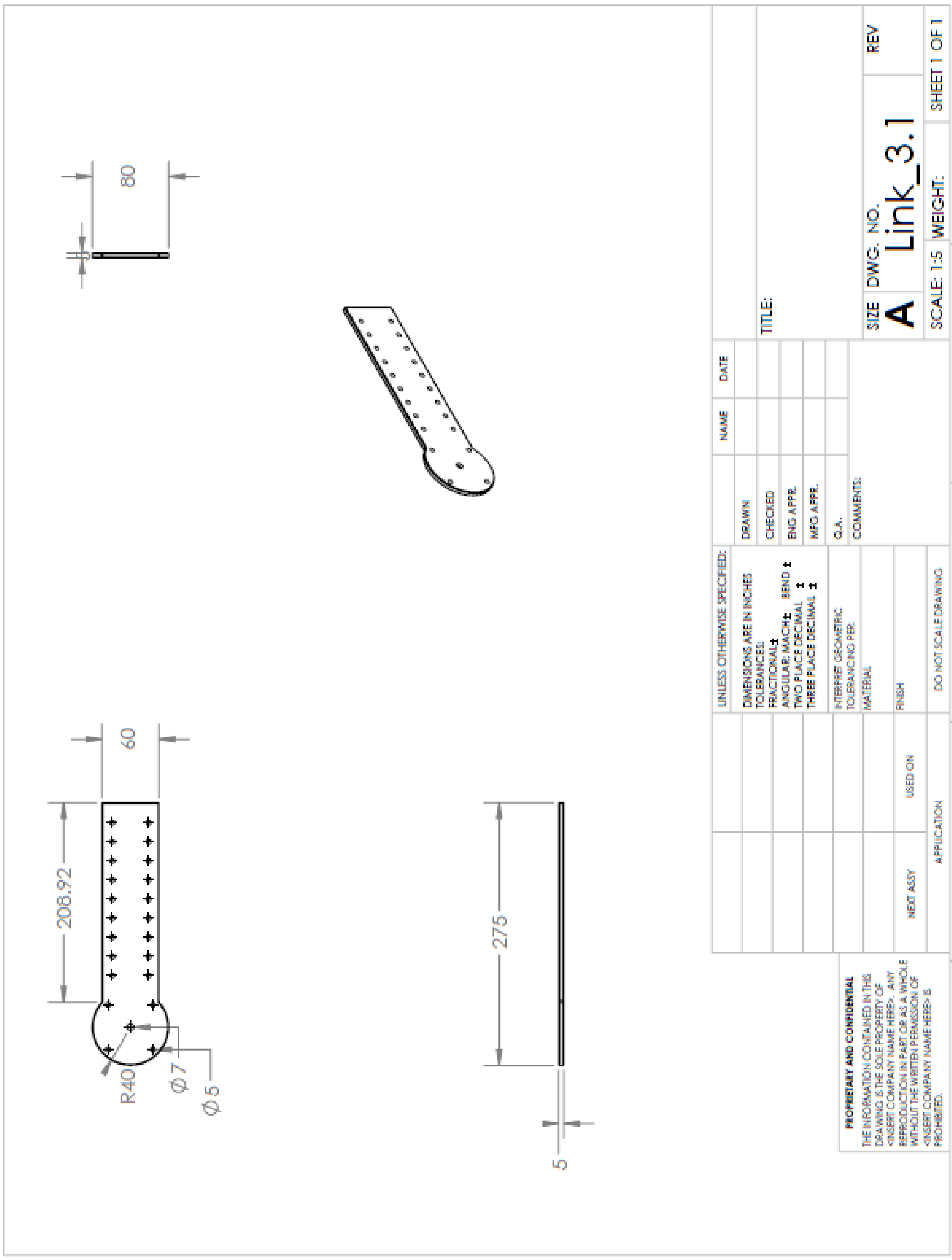

80
60
208.92
R40
Ø7
Ø5
275
5
UNLESS OTHERWISE SPECIFIED:
DIMENSIONS ARE IN INCHES
TOLERANCES:
FRACTIONAL±
ANGULAR: MACH± BEND ±
TWO PLACE DECIMAL ±
THREE PLACE DECIMAL ±
INTERPRET GEOMETRIC TOLERANCING PER:
MATERIAL
FINISH
DO NOT SCALE DRAWING
NEXT ASSY
USED ON
APPLICATION
DRAWN
CHECKED
ENG APPR.
MFG APPR.
Q.A.
COMMENTS:
NAME
DATE
TITLE:
SIZE
A
DWG. NO.
Link_3.1
REV
SCALE: 1:5
WEIGHT:
SHEET 1 OF 1
PROPRIETARY AND CONFIDENTIAL

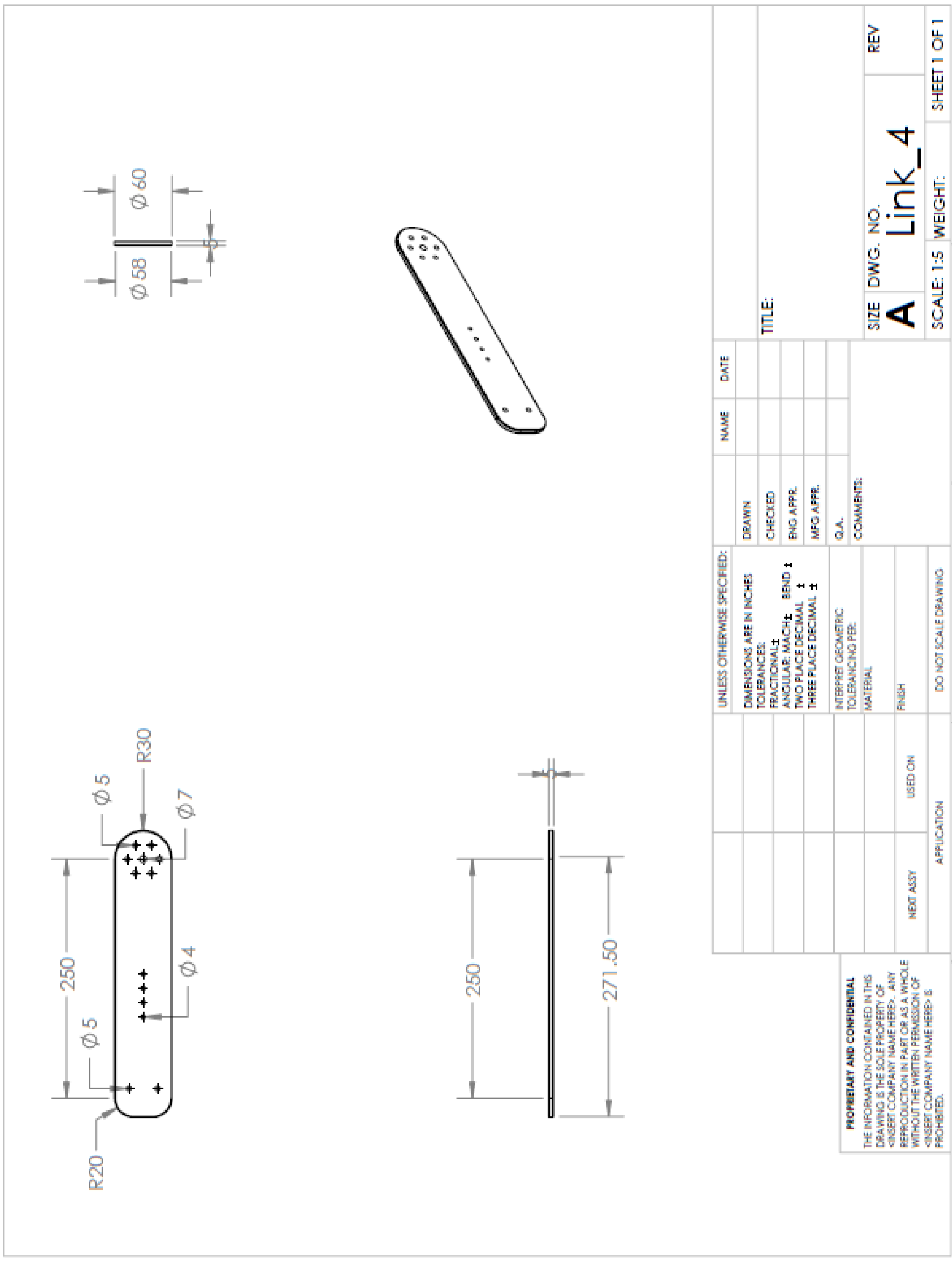
R20
Ø 5
250
Ø 4
Ø 7
Ø 5
R30
250
271.50
Ø 58
Ø 60
UNLESS OTHERWISE SPECIFIED:
DIMENSIONS ARE IN INCHES
TOLERANCES:
FRACTIONAL ±
ANGULAR: MACH ± BEND ±
TWO PLACE DECIMAL ±
THREE PLACE DECIMAL ±
INTERPRET GEOMETRIC TOLERANCING PER:
MATERIAL
FINISH
DO NOT SCALE DRAWING
NEXT ASSY
USED ON
APPLICATION
NAME
DATE
DRAWN
CHECKED
ENG APPR.
MFG APPR.
Q.A.
COMMENTS:
TITLE:
SIZE
A
DWG. NO.
Link_4
REV
SCALE: 1:5
WEIGHT:
SHEET 1 OF 1
PROPRIETARY AND CONFIDENTIAL
THE INFORMATION CONTAINED IN THIS DRAWING IS THE SOLE PROPERTY OF <INSERT COMPANY NAME HERE>. ANY REPRODUCTION IN PART OR AS A WHOLE WITHOUT THE WRITTEN PERMISSION OF <INSERT COMPANY NAME HERE> IS PROHIBITED.
5
4
3
2
1

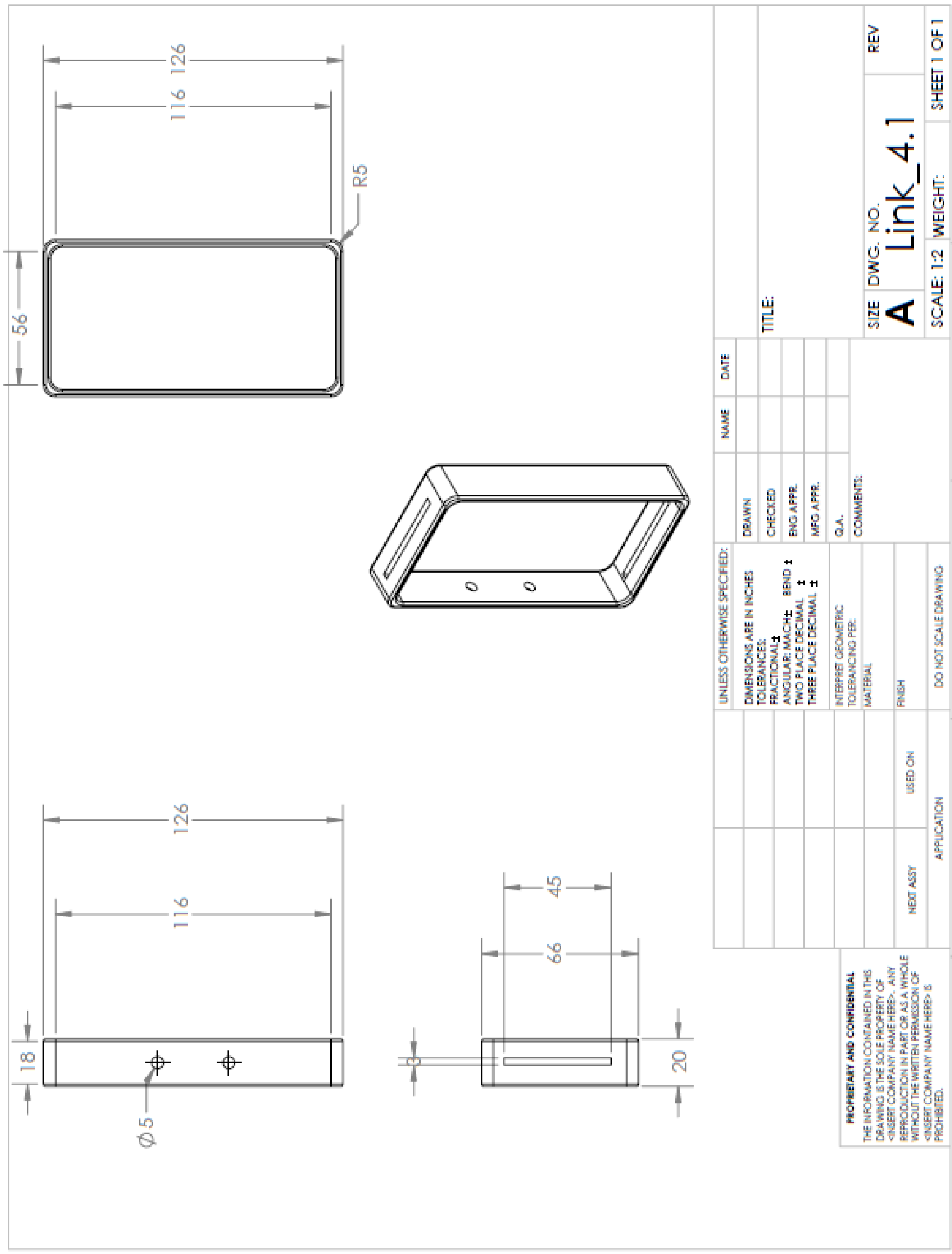
126
116
R5
56
18
Ø5
45
66
20
UNLESS OTHERWISE SPECIFIED:
DIMENSIONS ARE IN INCHES
TOLERANCES:
FRACTIONAL±
ANGULAR: MACH± BEND ±
TWO PLACE DECIMAL ±
THREE PLACE DECIMAL ±
INTERPRET GEOMETRIC TOLERANCING PER:
MATERIAL
FINISH
DO NOT SCALE DRAWING
NAME
DATE
DRAWN
CHECKED
ENG APPR.
MFG APPR.
Q.A.
COMMENTS:
TITLE:
SIZE
DWG. NO.
REV
A
Link_4.1
SCALE: 1:2
WEIGHT:
SHEET 1 OF 1
NEXT ASSY
USED ON
APPLICATION
PROPRIETARY AND CONFIDENTIAL
THE INFORMATION CONTAINED IN THIS DRAWING IS THE SOLE PROPERTY OF <INSERT COMPANY NAME HERE>. ANY REPRODUCTION IN PART OR AS A WHOLE WITHOUT THE WRITTEN PERMISSION OF <INSERT COMPANY NAME HERE> IS PROHIBITED.
1
2
3
4
5

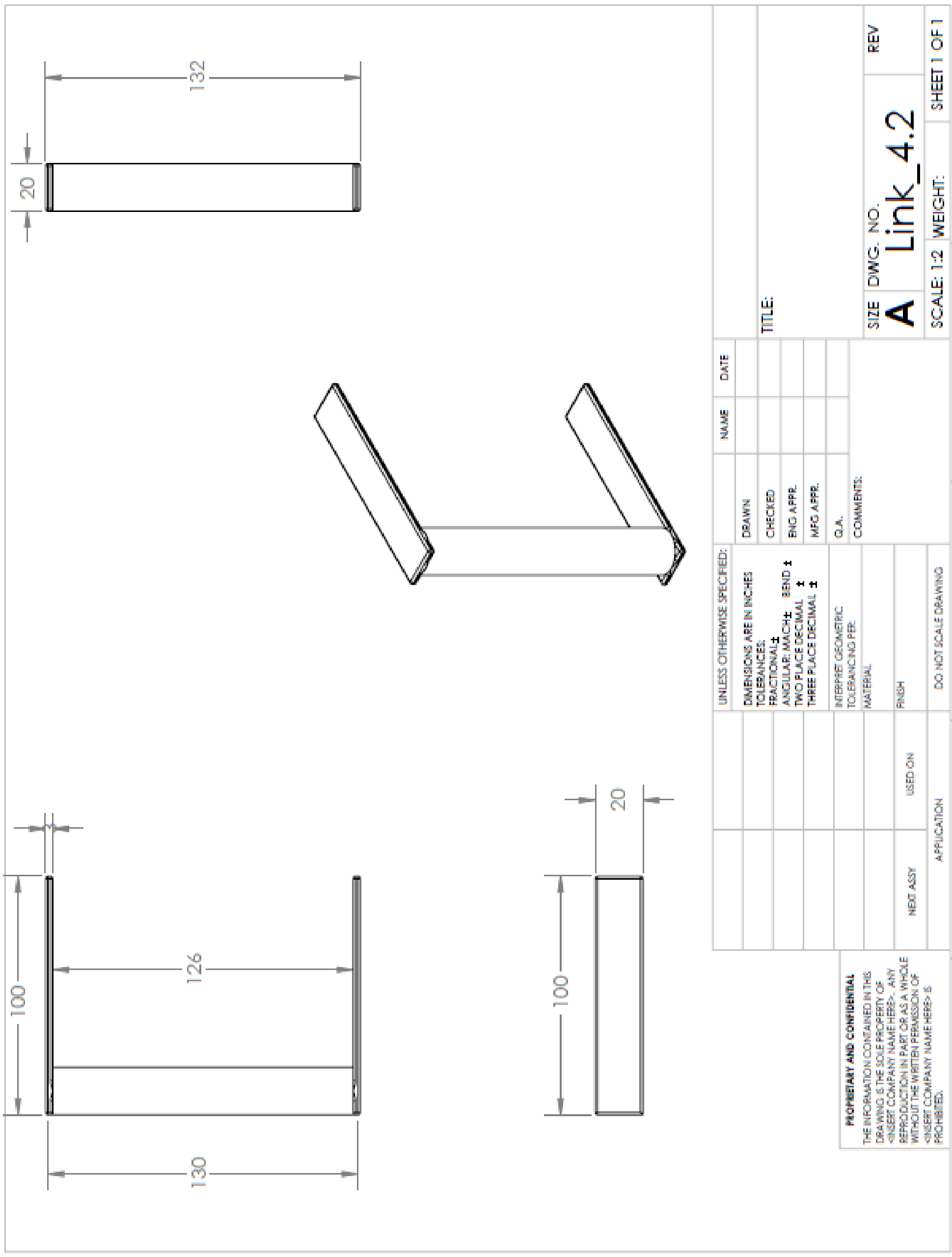
132
20
100
126
3
130
100
20
UNLESS OTHERWISE SPECIFIED:
DIMENSIONS ARE IN INCHES
TOLERANCES:
FRACTIONAL ±
ANGULAR: MACH ± BEND ±
TWO PLACE DECIMAL ±
THREE PLACE DECIMAL ±
INTERPRET GEOMETRIC TOLERANCING PER:
MATERIAL
FINISH
DO NOT SCALE DRAWING
NAME
DATE
DRAWN
CHECKED
ENG APPR.
MFG APPR.
Q.A.
COMMENTS:
TITLE:
SIZE
A
DWG. NO.
Link_4.2
REV
SCALE: 1:2
WEIGHT:
SHEET 1 OF 1
NEXT ASSY
USED ON
APPLICATION
PROPRIETARY AND CONFIDENTIAL
THE INFORMATION CONTAINED IN THIS DRAWING IS THE SOLE PROPERTY OF <INSERT COMPANY NAME HERE>. ANY REPRODUCTION IN PART OR AS A WHOLE WITHOUT THE WRITTEN PERMISSION OF <INSERT COMPANY NAME HERE> IS PROHIBITED.
1
2
3
4
5

APPENDIX B

Calculation of Jacobian

A =

$$\begin{bmatrix} \cos\theta_1\cos\theta_2\cos\theta_3 - \cos\theta_1\sin\theta_2\sin\theta_3 & -\cos\theta_1\cos\theta_2\sin\theta_3 - \cos\theta_1\cos\theta_3\sin\theta_2 & \sin\theta_1 & 13\cos\theta_1\cos\theta_2/50 - 77\cos\theta_1\sin\theta_2\sin\theta_3/200 + 77\cos\theta_1\cos\theta_2\cos\theta_3/200 \\ \cos\theta_2\cos\theta_3\sin\theta_1 - \sin\theta_1\sin\theta_2\sin\theta_3 & -\cos\theta_2\sin\theta_1\sin\theta_3 - \cos\theta_3\sin\theta_1\sin\theta_2 & -\cos\theta_1 & 13\cos\theta_2\sin\theta_1/50 - 77\sin\theta_1\sin\theta_2\sin\theta_3/200 + 77\cos\theta_2\cos\theta_3\sin\theta_1/200 \\ \cos\theta_2\sin\theta_3 + \cos\theta_3\sin\theta_2 & \cos\theta_2\cos\theta_3 - \sin\theta_2\sin\theta_3 & 0 & 13\sin\theta_2/50 + 77\cos\theta_2\sin\theta_3/200 + 77\cos\theta_3\sin\theta_2/200 + 9/50 \\ 0 & 0 & 0 & 1 \end{bmatrix}$$

P3 =

$$\begin{bmatrix} 13\cos\theta_1\cos\theta_2/50 - 77\cos\theta_1\sin\theta_2\sin\theta_3/200 + 77\cos\theta_1\cos\theta_2\cos\theta_3/200 \\ 13\cos\theta_2\sin\theta_1/50 - 77\sin\theta_1\sin\theta_2\sin\theta_3/200 + 77\cos\theta_2\cos\theta_3\sin\theta_1/20 \\ 13\sin\theta_2/50 + 77\cos\theta_2\sin\theta_3/200 + 77\cos\theta_3\sin\theta_2/200 + 9/50 \\ 0 \end{bmatrix}$$

P3Jacob =

$$\begin{bmatrix} 77\sin\theta_1\sin\theta_2\sin\theta_3/200 - 13\cos\theta_2\sin\theta_1/50 - 77\cos\theta_2\cos\theta_3\sin\theta_1/200 \\ 13\cos\theta_1\cos\theta_2/50 - 77\cos\theta_1\sin\theta_2\sin\theta_3/200 + 77\cos\theta_1\cos\theta_2\cos\theta_3/200 \\ 0 \\ 0 \end{bmatrix}$$

P3Jacobb =

$$\begin{bmatrix} 77\sin\theta_1\sin\theta_2\sin\theta_3/200 - 13\cos\theta_2\sin\theta_1/50 - 77\cos\theta_2\cos\theta_3\sin\theta_1/200 \\ 13\cos\theta_1\cos\theta_2/50 - 77\cos\theta_1\sin\theta_2\sin\theta_3/200 + 77\cos\theta_1\cos\theta_2\cos\theta_3/200 \\ 0 \end{bmatrix}$$

$$J_1(q) = \begin{bmatrix} P_0 X\, {}^0P_3 \\ P_0 \end{bmatrix}$$

J1 =

$$\begin{bmatrix} 77\sin\theta_1\sin\theta_2\sin\theta_3/200 - 13\cos\theta_2\sin\theta_1/50 - 77\cos\theta_2\cos\theta_3\sin\theta_1/200 \\ 13\cos\theta_1\cos\theta_2/50 - 77\cos\theta_1\sin\theta_2\sin\theta_3/200 + 77\cos\theta_1\cos\theta_2\cos\theta_3/200 \\ 0 \\ 0 \\ 0 \\ 1 \end{bmatrix}$$

Similarly,

$$J_2(q) = \begin{bmatrix} P_1 X\, {}^1P_3 \\ P_1 \end{bmatrix}$$

J2 =

$$\begin{bmatrix} -13\cos\theta_1\sin\theta_2/50 - 77\cos\theta_1\cos\theta_2\sin\theta_3/200 - 77\cos\theta_1\cos\theta_3\sin\theta_2/200 \\ -(13\sin\theta_1\sin\theta_2/50 - (77\cos\theta_2\sin\theta_1\sin\theta_3/200 - (77\cos\theta_3\sin\theta_1\sin\theta_2/200 \\ 13\cos\theta_2/50 + 77\cos\theta_2\cos\theta_3/200 - 77\sin\theta_2\sin\theta_3/200 \\ \sin\theta_1 \\ -\cos\theta_1 \\ 0 \end{bmatrix}$$

$$J_3(q) = \begin{bmatrix} P_2 X\, {}^2P_3 \\ P_2 \end{bmatrix}$$

J3 =

$$\begin{bmatrix} -77\cos\theta_1\cos\theta_2\sin\theta_3/200 - 77\cos\theta_1\cos\theta_3\sin\theta_2/200 \\ -(77\cos\theta_2\sin\theta_1\sin\theta_3/200 - 77\cos\theta_3\sin\theta_1\sin\theta_2/200 \\ 77\cos\theta_2\cos\theta_3/200 - 77\sin\theta_2\sin\theta_3/200 \\ \sin\theta_1 \\ -\cos\theta_1 \\ 0 \end{bmatrix}$$

$$J = [J_1 \quad J_2 \quad J_3]$$

J =

$$\begin{bmatrix} 77\sin\theta_1\sin\theta_2\sin\theta_3/200 - 13\cos\theta_2\sin\theta_1/50 - 77\cos\theta_2\cos\theta_3\sin\theta_1/200 & -13\cos\theta_1\sin\theta_2/50 - 77\cos\theta_1\cos\theta_2\sin\theta_3/200 - 77\cos\theta_1\cos\theta_3\sin\theta_2/200 & -77\cos\theta_1\cos\theta_2\sin\theta_3/200 - 77\cos\theta_1\cos\theta_3\sin\theta_2/200 \\ 13\cos\theta_1\cos\theta_2/50 - 77\cos\theta_1\sin\theta_2\sin\theta_3/200 + 77\cos\theta_1\cos\theta_2\cos\theta_3/200 & -13\sin\theta_1\sin\theta_2/50 - 77\cos\theta_2\sin\theta_1\sin\theta_3/200 - 77\cos\theta_3\sin\theta_1\sin\theta_2/200 & -77\cos\theta_2\sin\theta_1\sin\theta_3/200 - 77\cos\theta_3\sin\theta_1\sin\theta_2/200 \\ 0 & 13\cos\theta_2/50 + 77\cos\theta_2\cos\theta_3/200 - 77\sin\theta_2\sin\theta_3/200 & 77\cos\theta_2\cos\theta_3/200 - 77\sin\theta_2\sin\theta_3/200 \\ 0 & \sin\theta_1 & \sin\theta_1 \\ 0 & -\cos\theta_1 & -\cos\theta_1 \\ 1 & 0 & 0 \end{bmatrix}$$

APPENDIX C

Computation of d_{ij}:

$$d_{11} = A_0 Q_1 A_1 \,,$$

$$d_{21} = A_0 Q_1 A_1 A_2$$

$$d_{31} = A_0 Q_1 A_1 A_2 A_3$$

$$d_{22} = A_1 Q_2 A_2$$

$$d_{32} = A_1 Q_2 A_2 A_3$$

$$d_{33} = A_1 A_2 Q_3 A_3$$

$$d_{ij} = \begin{cases} {}^{0}T_{j-1} Q_j \, {}^{j-1}T_i & \text{for } j \le i \\ 0 & \text{for } j > i \end{cases}$$

$$\frac{\partial d_{ij}}{\partial p_k} = \begin{cases} {}^{0}T_{j-1} Q_j \, {}^{j-1}T_{k-1} Q_k \, {}^{k-1}T_i & \text{for i} \ge \text{k} \ge \text{j} \\ {}^{0}T_{k-1} Q_k \, {}^{k-1}T_{j-1} Q_j \, {}^{j-1}T_i & \text{for i} \ge \text{j} \ge \text{k} \\ 0 & \text{for i} < \text{j or i} < \text{k} \end{cases}$$

Computation of mass matrix:

$$m_{11} = trace(d_{11}I_1d'_{11}) + trace(d_{21}I_2d'_{21}) + trace(d_{31}I_3d'_{31})$$

$$m_{12} = trace(d_{22}I_2d'_{21}) + trace(d_{32}I_3d'_{31})$$

$$m_{13} = trace(d_{33}I_3d'_{31})$$

$$m_{21} = m_{12}$$

$$m_{31} = m_{13}$$

$$m_{22} = trace(d_{22}I_2d'_{22}) + trace(d_{32}I_3d'_{32})$$

$$m_{23} = trace(d_{33}I_3d'_{32})$$

$$m_{32} = m_{23}$$

$$m_{33} = trace(d_{33}I_3d'_{33})$$

$$M_1 = [m_{11} \quad m_{12} \quad m_{13}]$$

$$M_2 = [m_{21} \quad m_{22} \quad m_{23}]$$

$$M_3 = [m_{31} \quad m_{32} \quad m_{33}]$$

$$M = \begin{bmatrix} m_{11} & m_{12} & m_{13} \\ m_{21} & m_{22} & m_{23} \\ m_{31} & m_{32} & m_{33} \end{bmatrix}$$

Computation of Coriolis and Centrifugal coefficient matrix:

$$h_{111} = trace(A_0 Q_1 Q_2 A_1 I_1 d'_{11}) + trace(A_0 Q_1 A_1 Q_2 A_2 I_2 d'_{21})$$
$$+ trace(A_0 Q_1 A_1 A_2 Q_3 A_3 I_3 d'_{31})$$

$$h_{112} = trace(A_1 Q_2 Q_2 A_2 I_2 d'_{21}) + trace(A_1 Q_2 A_2 Q_3 A_3 I_3 d'_{31})$$

$$h_{113} = trace(A_1 A_2 Q_3 Q_3 A_3 I_3 d'_{31})$$

$$h_{121} = h_{112}$$

$$h_{131} = h_{113}$$

$$h_{123} = trace(A_1 A_2 Q_3 Q_3 A_3 I_3 d'_{31})$$

$$h_{132} = h_{123}$$

$$h_{133} = trace(A_1 A_2 Q_3 Q_3 A_3 I_3 d'_{31})$$

$$H_1 = h_{111}\dot{\theta}_1\dot{\theta}_1 + h_{112}\dot{\theta}_1\dot{\theta}_2 + h_{113}\dot{\theta}_1\dot{\theta}_3 + h_{121}\dot{\theta}_2\dot{\theta}_1 + h_{122}\dot{\theta}_2\dot{\theta}_2$$
$$+ h_{123}\dot{\theta}_2\dot{\theta}_3 + h_{131}\dot{\theta}_3\dot{\theta}_1 + h_{132}\dot{\theta}_3\dot{\theta}_2\ h_{133}\dot{\theta}_3\dot{\theta}_3$$

$$h_{211} = trace(A_0 Q_1 A_1 Q_2 A_2 I_2 d'_{22}) + trace(A_0 Q_1 A_1 A_2 Q_3 A_3 I_3 d'_{32})$$

$$h_{212} = trace(A_1 Q_2 A_2 I_2 d'_{22}) + trace(A_1 Q_2 A_2 Q_3 A_3 I_3 d'_{32})$$

$$h_{213} = trace(A_1 A_2 Q_3 Q_3 A_3 I_3 d'_{32})$$

$$h_{221} = h_{212}$$

$$h_{231} = h_{213}$$

$$h_{222} = trace(A_1 Q_2 Q_2 A_2 I_2 d'_{22}) + trace(A_1 Q_2 A_2 Q_3 A_3 I_3 d'_{32})$$

$$h_{223} = trace(A_1 A_2 Q_3 Q_3 A_3 I_3 d'_{32})$$

$$h_{232} = h_{223}$$

$$h_{233} = trace(A_1 A_2 Q_3 Q_3 A_3 I_3 d'_{32})$$

$$H_2 = h_{211} \dot{\theta}_1 \dot{\theta}_1 + h_{212} \dot{\theta}_1 \dot{\theta}_2 + h_{213} \dot{\theta}_1 \dot{\theta}_3 + h_{221} \dot{\theta}_2 \dot{\theta}_1 + h_{222} \dot{\theta}_2 \dot{\theta}_2$$
$$+ h_{223} \dot{\theta}_2 \dot{\theta}_3 + h_{231} \dot{\theta}_3 \dot{\theta}_1 + h_{232} \dot{\theta}_3 \dot{\theta}_2 + h_{233} \dot{\theta}_3 \dot{\theta}_3$$

$$h_{311} = trace(A_0 Q_1 A_1 A_2 Q_3 A_3 I_3 d'_{33})$$

$$h_{312} = trace(A_1 Q_2 A_2 Q_3 A_3 I_3 d'_{33})$$

$$h_{313} = trace(A_1 A_2 Q_3 Q_3 A_3 I_3 d'_{33})$$

$$h_{321} = h_{312}$$

$$h_{331} = h_{313}$$

$$h_{322} = trace(A_1 Q_2 A_2 Q_3 A_3 I_3 d'_{33})$$

$$h_{323} = trace(A_1 A_2 Q_3 Q_3 I_3 d'_{33})$$

$$h_{332} = h_{323}$$

$$h_{333} = trace(A_1 A_2 Q_3 Q_3 A_3 I_3 d'_{33})$$

$$H_3 = h_{311}\dot{\theta}1\,\dot{\theta}1 + h_{312}\dot{\theta}1\,\dot{\theta}2 + h_{313}\dot{\theta}1\,\dot{\theta}3 + h_{321}\dot{\theta}2\,\dot{\theta}1 +$$
$$h_{322}\dot{\theta}2\,\dot{\theta}2 + h_{323}\dot{\theta}2\,\dot{\theta}3 + h_{331}\dot{\theta}3\,\dot{\theta}1 + h_{332}\dot{\theta}3\,\dot{\theta}2 + h_{333}\dot{\theta}3\,\dot{\theta}3$$

$$H = \begin{bmatrix} H_1 & H_2 & H_3 \end{bmatrix}$$

Calculation of stall torque

A =

$$\begin{bmatrix} \cos\theta_1\cos\theta_2\cos\theta_3 - \cos\theta_1\sin\theta_2\sin\theta_3 & -\cos\theta_1\cos\theta_2\sin\theta_3 - \cos\theta_1\cos\theta_3\sin\theta_2 & \sin\theta_1 & 13\cos\theta_1\cos\theta_2/50 - 77\cos\theta_1\sin\theta_2\sin\theta_3/200 + 77\cos\theta_1\cos\theta_2\cos\theta_3/200 \\ \cos\theta_2\cos\theta_3\sin\theta_1 - \sin\theta_1\sin\theta_2\sin\theta_3 & -\cos\theta_2\sin\theta_1\sin\theta_3 - \cos\theta_3\sin\theta_1\sin\theta_2 & -\cos\theta_1 & 13\cos\theta_2\sin\theta_1/50 - 77\sin\theta_1\sin\theta_2\sin\theta_3/200 + 77\cos\theta_2\cos\theta_3\sin\theta_1/200 \\ \cos\theta_2\sin\theta_3 + \cos\theta_3\sin\theta_2 & \cos\theta_2\cos\theta_3 - \sin\theta_2\sin\theta_3 & 0 & 13\sin\theta_2/50 + 77\cos\theta_2\sin\theta_3/200 + 77\cos\theta_3\sin\theta_2/200 + 9/50 \\ 0 & 0 & 0 & 1 \end{bmatrix}$$

J1 =

$$\begin{bmatrix} 77\sin\theta_1\sin\theta_2\sin\theta_3/200 - 13\cos\theta_2\sin\theta_1/50 - 77\cos\theta_2\cos\theta_3\sin\theta_1/200 \\ 13\cos\theta_1\cos\theta_2/50 - 77\cos\theta_1\sin\theta_2\sin\theta_3/200 + 77\cos\theta_1\cos\theta_2\cos\theta_3/200 \\ 0 \\ 0 \\ 0 \\ 1 \end{bmatrix}$$

J2 =

$$\begin{bmatrix} -\ 13\cos\theta_1\sin\theta_2/50\ -\ 77\cos\theta_1\cos\theta_2\sin\theta_3/200\ -\ 77\cos\theta_1\cos\theta_3\sin\theta_2/200 \\ -\ (13\sin\theta_1\sin\theta_2/50\ -\ (77\cos\theta_2\sin\theta_1\sin\theta_3/200\ -\ (77\cos\theta_3\sin\theta_1\sin\theta_2/200 \\ 13\cos\theta_2/50 + 77\cos\theta_2\cos\theta_3/200\ -\ 77\sin\theta_2\sin\theta_3/200 \\ \sin\theta_1 \\ -\cos\theta_1 \\ 0 \end{bmatrix}$$

J3 =

$$\begin{bmatrix} -\ 77\cos\theta_1\cos\theta_2\sin\theta_3/200\ -\ 77\cos\theta_1\cos\theta_3\sin\theta_2/200 \\ -\ (77\cos\theta_2\sin\theta_1\sin\theta_3/200\ -\ 77\cos\theta_3\sin\theta_1\sin\theta_2/200 \\ 77\cos\theta_2\cos\theta_3/200\ -\ 77\sin\theta_2\sin\theta_3/200 \\ \sin\theta_1 \\ -\cos\theta_1 \\ 0 \end{bmatrix}$$

$$F = \begin{bmatrix} f_x & f_y & f_z & 0 & 0 & 0 \end{bmatrix}$$

$\tau_{\text{static}} = J(q)^T \mathbf{F}$

T =

$$\begin{bmatrix} f_y(13\cos\theta_1\cos\theta_2/50\ -\ 77\cos\theta_1\sin\theta_2\sin\theta_3/200 + 77\cos\theta_1\cos\theta_2\cos\theta_3/200) - f_x(13\cos\theta_2\sin\theta_1/50\ -\ 77\sin\theta_1\sin\theta_2\sin\theta_3/200 + 77{*}\cos\theta_2\cos\theta_3\sin\theta_1/200) \\ f_z(13\cos\theta_2/50 + 77\cos\theta_2\cos\theta_3/200\ -\ 77\sin\theta_2\sin\theta_3/200) - f_y(13\sin\theta_1\sin\theta_2/50 + 77\cos\theta_2\sin\theta_1\sin\theta_3/200 + 77\cos\theta_3\sin\theta_1\sin\theta_2/200) - f_x(13\cos\theta_1\sin\theta_2/50 + 77\cos\theta_1\cos\theta_2\sin\theta_3/200 + 77\cos\theta_1\cos\theta_3\sin\theta_2/200) \\ f_z(77\cos\theta_2\cos\theta_3/200 - 77\sin\theta_2\sin\theta_3/200) - f_y(77\cos\theta_2\sin\theta_1\sin\theta_3/200 + 77\cos\theta_3\sin\theta_1\sin\theta_2/200) - f_x(77\cos\theta_1\cos\theta_2\sin\theta_3/200 + 77\cos\theta_1\cos\theta_3\sin\theta_2/200) \end{bmatrix}$$

θ_1 = [0   1.3090   2.6180]

θ_2 = [0   1.2217   2.4435]

θ_3 = [0   1.1345   2.2689]

$$\text{Static Torque} = \begin{bmatrix} 0 & 0 & 0 \\ 18.0600 & -5.1327 & -5.5768 \\ 10.7800 & -7.6226 & 0.0000 \end{bmatrix}$$

AKASH GUPTA

EDUCATION

2014-2016	M.Tech in Robotics Engineering, University of Petroleum & Energy Studies (UPES), Dehradun, India.
2010-2014	B.Tech in Mechanical Engineering, Visvesvaraya Technological University, Karnataka, India.

Ph.D. Publications

1. **Akash Gupta**, Anshuman Singh, Varnita Verma, Amit Kumar Mondal & Mukul Kumar Gupta (2020) "*Developments and clinical evaluations of robotic exoskeleton technology for human upper-limb rehabilitation*," Advanced Robotics, 34:15, 1023-1040, 10.1080/01691864.2020.1749926 **[SCI]**

2. **Akash Gupta**, Amit Kumar Mondal, and Mukul Kumar Gupta (2019). "*Kinematic, dynamic analysis and control of 3 DOF upper-limb robotic exoskeleton*," Journal Européen des Systèmes Automatisés, Vol. 52, No. 3, pp. 297-304. doi.org/10.18280/jesa.520311 **[SCOPUS]**

3. Varnita Verma, **Akash Gupta**, Mukul Kumar (2020) "*Performance Estimation of Computed Torque Control for Surgical Robot Application*," Journal of Mechanical Engineering and Sciences, *14*(3), 7017 - 7028. https://doi.org/10.15282/jmes.14.3.2020.04.0549 **[ESCI]**

4. Varnita Verma, **Akash Gupta**, Mukul Kumar Gupta (2020), *"CTC and Robust Control Based Stability Analysis and Trajectory Tracking of Robot Manipulator,"* International Journal of Mechatronics and Automation. **[SCOPUS]** (under review)

Other Publications

5. **Akash Gupta**, Anshuman Singh, Deepak Bharadwaj, Amit Kumar Mondal (2020), "*Humans and Robots: A mutually inclusive relationship in a contagious world,"* International Journal of Automation and Computing **[ESCI]** (Accepted)

6. Patel, Ravi Kumar, **Akash Gupta**, Vinay Chowdary, Vivek Kaundal, and Amit Kumar Mondal (2019). *"Wearable fitness band-based U-health monitoring."* In Sensors for Health Monitoring, *pp. 175-189. Academic Press, 2019* https://doi.org/10.1016/B978-0-12-819361-7.00009-9

DESIGN AND ANALYSIS OF ROBOTIC EXOSKELETON FOR HUMAN UPPER LIMB REHABILITATION

ORIGINALITY REPORT

10%	6%	8%	3%
SIMILARITY INDEX	INTERNET SOURCES	PUBLICATIONS	STUDENT PAPERS

PRIMARY SOURCES

1	urrg.eng.usm.my Internet Source	<1%
2	Submitted to Lebanese International University Student Paper	<1%
3	cyberleninka.org Internet Source	<1%
4	onlinelibrary.wiley.com Internet Source	<1%
5	robu.in Internet Source	<1%
6	Submitted to National Institute of Technology Karnataka Surathkal Student Paper	<1%
7	docplayer.net Internet Source	<1%
8	"Converging Clinical and Engineering Research on Neurorehabilitation II", Springer Science and Business Media LLC, 2017	<1%